

UC Davis

UC Davis Previously Published Works

Title

Stretchable One-Dimensional Conductors for Wearable Applications

Permalink

<https://escholarship.org/uc/item/6sp448q6>

Journal

ACS Nano, 16(12)

ISSN

1936-0851

Authors

Nie, Mingyu
Li, Boxiao
Hsieh, You-Lo
[et al.](#)

Publication Date

2022-12-27

DOI

10.1021/acsnano.2c08166

Peer reviewed

Stretchable One-Dimensional Conductors for Wearable Applications

Mingyu Nie,[#] Boxiao Li,[#] You-Lo Hsieh,^{*} Kun Kelvin Fu,^{*} and Jian Zhou^{*}



Cite This: *ACS Nano* 2022, 16, 19810–19839



Read Online

ACCESS |

Metrics & More

Article Recommendations

ABSTRACT: Continuous, one-dimensional (1D) stretchable conductors have attracted significant attention for the development of wearables and soft-matter electronics. Through the use of advanced spinning, printing, and textile technologies, 1D stretchable conductors in the forms of fibers, wires, and yarns can be designed and engineered to meet the demanding requirements for different wearable applications. Several crucial parameters, such as microarchitecture, conductivity, stretchability, and scalability, play essential roles in designing and developing wearable devices and intelligent textiles. Methodologies and fabrication processes have successfully realized 1D conductors that are highly conductive, strong, lightweight, stretchable, and conformable and can be readily integrated with common fabrics and soft matter. This review summarizes the latest advances in continuous, 1D stretchable conductors and emphasizes recent developments in materials, methodologies, fabrication processes, and strategies geared toward applications in electrical interconnects, mechanical sensors, actuators, and heaters. This review classifies 1D conductors into three categories on the basis of their electrical responses: (1) rigid 1D conductors, (2) piezoresistive 1D conductors, and (3) resistance-stable 1D conductors. This review also evaluates the present challenges in these areas and presents perspectives for improving the performance of stretchable 1D conductors for wearable textile and flexible electronic applications.

KEYWORDS: stretchable conductor, one dimension, conductivity, resistance stability, structural design, wearable electronics, fabrication technologies, wearable textiles



INTRODUCTION

With the fast-growing demand for wearable electronics, efforts are being made to develop ideal conductors with excellent electrical conductivity and stretchability.^{1–15} Wearable devices, whether attached to the human body or embedded within clothing materials, are subject to the strains of physical movement.^{16–22} Therefore, their constituent materials must have sufficient stretchability to meet the demands of wearability and mass production in the near future.^{23–29} Wearable products in stretchable electronics are expected to gain attraction in the market with the advancements of fundamental research in stretchable electronics and the development and adoption by key industry players. This alignment of industrial interest and adaptation with scientific research advancement is one of the major drivers for the growth of stretchable electronics in the marketplace.

Stretchable one-dimensional (1D) conductors are essential building blocks to realize textile-like wearable devices because of their small size, continuity, high surface area to volume ratio, high electrical conductivity, stretchability, and lightweight property. They can be used as an interconnection of various functional elements or as an electronic element in textile-based

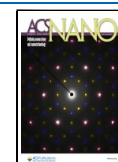
devices. In addition, they can be mass-produced and integrated by high-speed melt spinning or wet spinning into two-dimensional (2D) fabrics and three-dimensional (3D) products.

In recent years, progresses in various types of 1D conductors have been reviewed from different contexts. For instance, the preparations, properties, emerging applications, opportunities, and challenges of carbon nanomaterials, including carbon nanotube (CNT) and graphene-based fibers, have been thoroughly reviewed.^{30–35} These carbon-nanomaterial-based fibers are excellent material platforms for flexible fiber-type actuators, motors, multifunctional textiles, and energy storage devices.^{30–35} In addition, key conducting polymer materials and other promising candidates have also been extensively summarized in terms of fiber spinning methods, properties,

Received: August 15, 2022

Accepted: November 30, 2022

Published: December 8, 2022



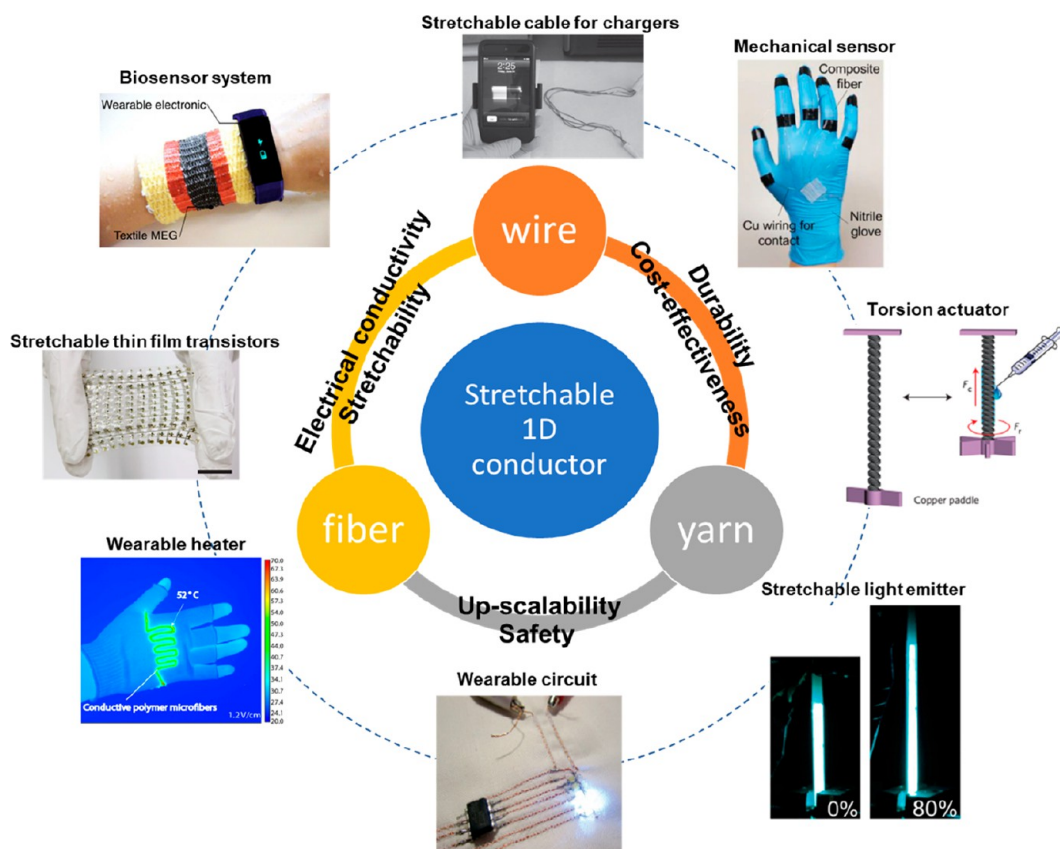


Figure 1. Characteristic properties and diverse applications of stretchable 1D conductors in wire, fiber, and yarn forms. Image “Stretchable cable for charges”: reprinted with permission from ref 48. Copyright 2013 John Wiley and Sons. Image “Mechanical sensor”: reprinted with permission from ref 49. Copyright 2015 John Wiley and Sons. Image “Torsion actuator”: reprinted with permission from ref 50. Copyright 2015 Springer Nature. Image “Stretchable light emitter”: reprinted with permission under a Creative Commons Attribution 4.0 International (CC BY 4.0) License from ref 51. Copyright 2018 The Authors. Image “Wearable circuit”: adopted from <http://www.kobakant.at/DIY/>. Image “Wearable heater”: reprinted with permission from ref 52. Copyright 2016 The Royal Society of Chemistry. Image “Stretchable thin-film transistors”: reprinted with permission under a Creative Commons CC BY License from ref 53. Copyright 2015 The Authors. Image “Biosensor system”: reprinted with permission under a Creative Commons CC BY License from ref 20. Copyright 2021 The Authors.

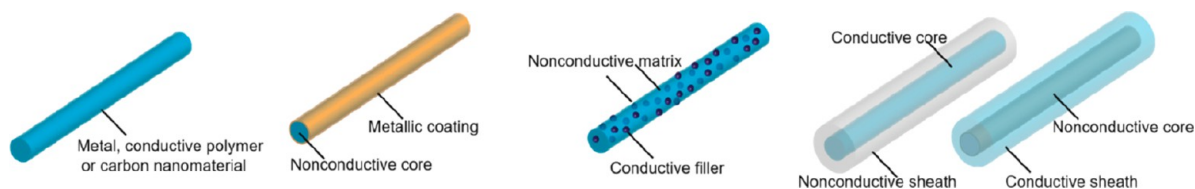


Figure 2. Schematic illustration of typical architectures of 1D fiber conductors: (left to right) intrinsic fiber conductor, metal-clad fiber conductor, composite fiber conductor, and coaxial fiber conductor.

and applications. In particular, their electrical conductivity and mechanical properties have improved to the level of carbon-based fibers for applications in sensors, actuators, neural recordings, and smart textiles.³⁶ At the same time, conductive polymer fibers have demonstrated more possibilities in yarns and textiles for electrochemical energy storage and tissue engineering.^{37–39} In addition, the assembly of the above-mentioned 1D conductors toward smart electronic textiles has been summarized to drive the development of wearable electronics.^{40–44}

Textiles typically consist of hierarchical structures at multiple scale levels of fibrils, fibers, yarns, fabrics, and their final products.^{45–47} The introduction of desired mechanical and electrical features at the fiber level is an efficient, yet overlooked, approach toward soft electronics. Therefore, this

review mainly focuses on the outstanding characteristics of stretchable 1D conductors at the fiber level. To date, “stretchable” and “1D” conductors have not been systematically evaluated, albeit because the classification of stretchable 1D conductors has not been clearly defined. This review fills these gaps by focusing on recent progress in continuous, 1D, and stretchable conductors to provide in-depth coverage of materials, synthesis methods, fabrication processes, performance and applications, and their potential impact. One emphasis is to summarize the strategies with structural engineering approaches (coaxial, crack-based, etc.) to confer superior stretchability to the 1D conductors. Furthermore, with excellent stretchability, more potentially promising contributions of 1D conductors to wearable electronics are highlighted.

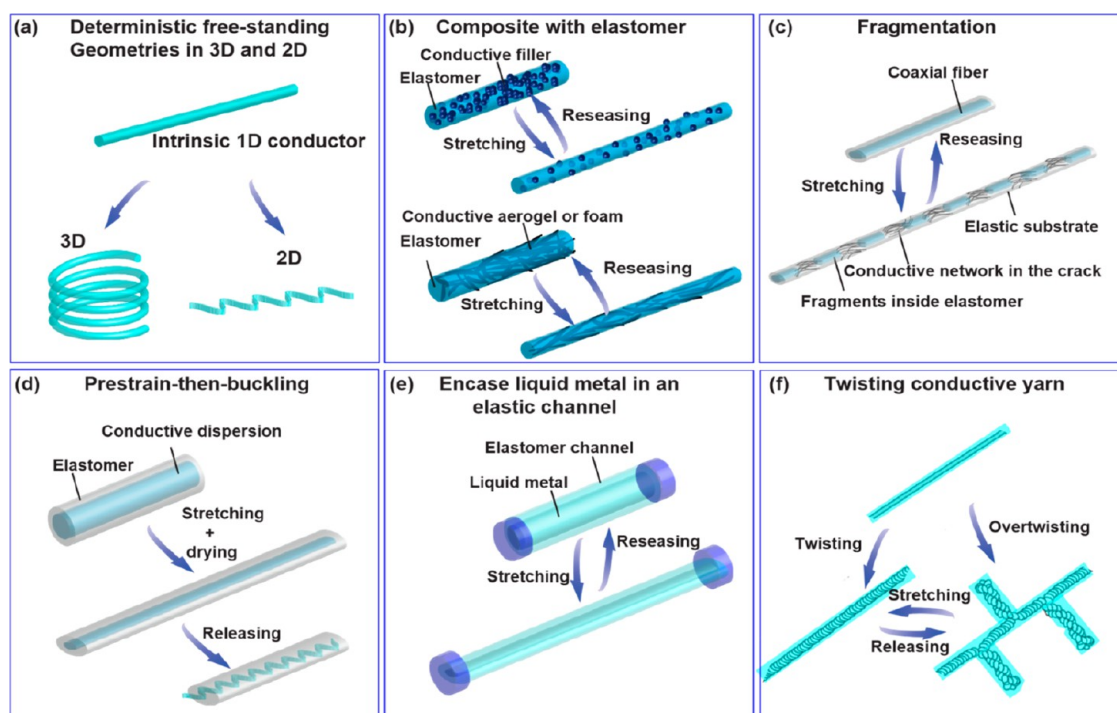


Figure 3. Strategies toward high stretchability. (a) Deterministic free-standing geometries in 3D and 2D. (b) Composite with elastomer. The stretchable composite fiber is prepared by (1) mixing conductive filler with elastomer and followed by spinning or (2) infusing conductive aerogel/foam with elastomer, which is then shaped into fibers. (c) Fragmentation. (d) Prestrain-then-buckling. (e) Encased liquid metal in an elastic channel. (f) Twisting of a conductive yarn.

Overall, from the perspective of the selection of materials for 1D conductors, this review focuses on conductive polymer fibers, carbon-nanomaterial-based (CNT and graphene) fibers, conductive coaxial fibers, and conductive composite fibers. From the perspective of device performance and fabrication, this review summarizes preparation strategies for stretchable electronics, including stretchable interconnects; deformable and wearable mechanical sensors; tensile and rotational actuators; and wearable heaters (Figure 1).

ESSENTIAL FEATURES OF THE 1D CONDUCTOR

Architecture. 1D conductors can be prepared in different architectures, dimensionalities, and compositions (Figure 2).

Intrinsic 1D Conductor. Intrinsic conductors are prepared from highly conductive species, such as metals, conductive polymers, and carbon nanomaterials. Different methodologies and processes can shape these electrically conductive materials into the 1D fiber, wire, and yarn conductors. However, these 1D conductors in their pure solid-state compositions are typically not stretchable or are very limited in stretchability. For example, metallic wires are the most conductive among all 1D conductors and excellent as electrical interconnects in civil engineering, but their nonstretchable nature and high density limit their use in stretchable electronics. Carbon fiber is a wonder 1D conductor, especially in high-modulus composite laminates, but is also not stretchable. The emergence of CNT and graphene-based fibers in the past decade is mainly ascribed to the need to develop wearable energy-storage applications. Although CNT fibers have significantly higher electrical conductivity than carbon fibers, their strength and modulus are 1 order of magnitude lower than carbon fibers. Some metal or carbon-based 1D conductors may be stretched reversibly at low strains (<3%), but most undergo brittle failure.

Metal-Clad 1D Conductor. Commercial metal-clad fibers contain a polymeric or metallic core within metallic coatings in different forms and are used in applications that range from textiles to aerospace wiring. Metal-clad polymer fibers can have the feel of flexible polymer fibers paired with the conductivity of copper wires. Although their production cost is low, these fibers can quickly lose electrical conductivity when stretched.

Composite 1D Conductor. Melt or wet spinning of conductive nanomaterials or nanofillers in an elastomer polymer matrix offers a way to prepare stretchable 1D conductors. Typical conductive nanomaterials are metal nanoparticles or nanowires, CNTs, graphene, and conductive polymers, which can be oriented along the fiber direction under an applied mechanical strain. High electrical conductivity can also be achieved with a high loading of conductive nanoparticles in the elastomer matrix.

Coaxial Structured 1D Conductor. The coaxial configuration makes it feasible to realize a stretchable 1D conductor with resistance stability under applied strain: a nonconductive sheath-wrapped conductive core or a conductive sheath-wrapped nonconductive core. The inner or outer parts structure could be engineered to realize high stretchability and resistance stability.

Strategies toward High Stretchability. Conductive materials can be rendered stretchable by six general strategies (Figure 3). Some categories are deterministic of the conducting materials, while others are aided with elastomers and a few with overlapping concepts.

Deterministic Free-Standing Geometries in 3D and 2D. The helical spring or coil structures have been used for centuries to form elongated structures on the basis of bending. The capability of this simple structure to develop a stretchable 1D conductor has continued to grow. Both hard (metallic

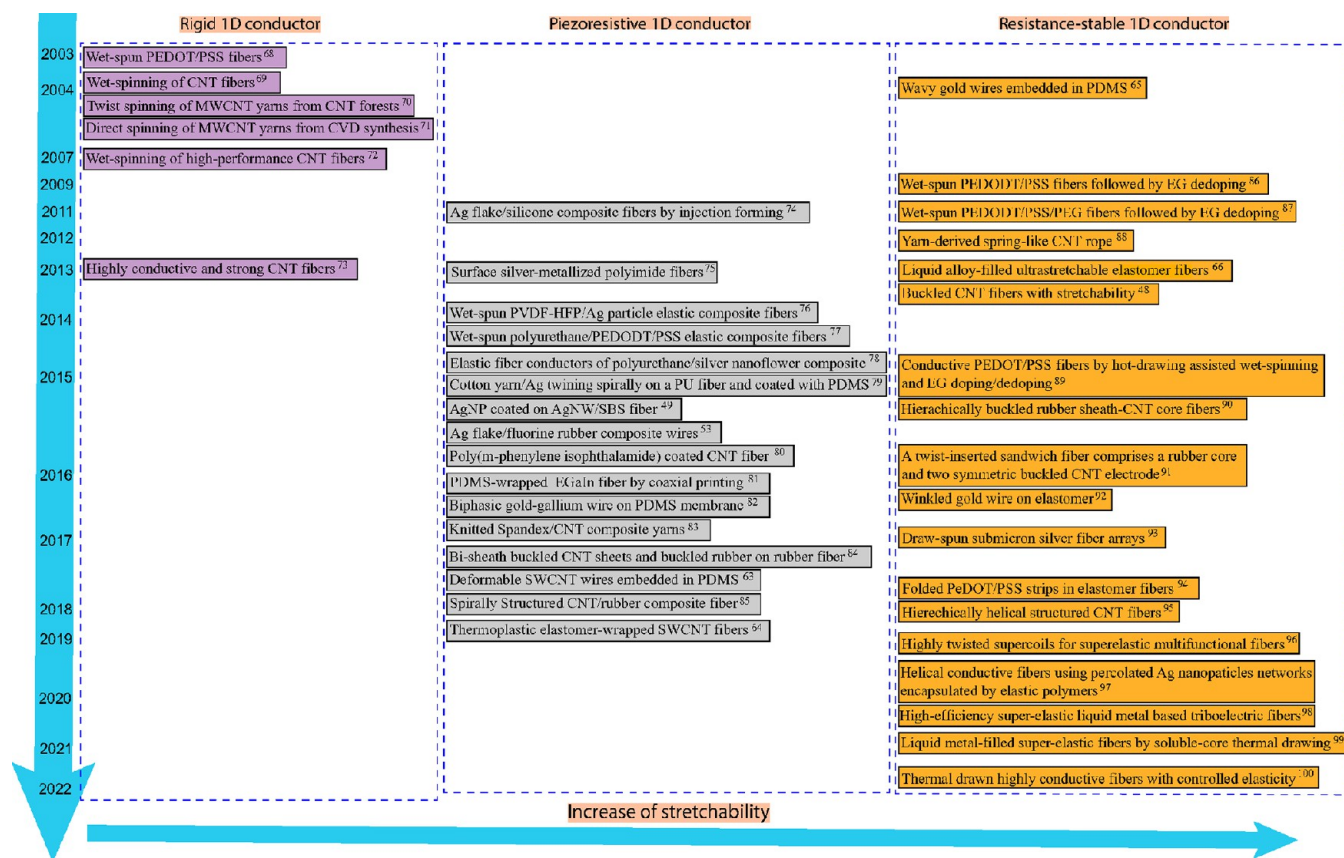


Figure 4. Timeline showing key developments of continuous 1D conductors in three categories: rigid 1D conductor, piezoresistive 1D conductor, and resistance-stable 1D conductor.

wire) and soft (conductive polymer) 1D conductors can be shaped into either 3D helical spirals or coils to enable material to elongate in response to stress without changing electrical conductivity (Figure 3a). Making 2D wavy structures, serpentine meshes, and intentionally fractal structures out of metal traces is generally compatible with conventional microfabrication techniques. However, the rigid nature of metals limits the ultimate strain before failure. These free-standing 2D stretchable structures are also incapable of recovering after reaching the ultimate elongation. Generally, 1D conductors based on 3D coiled structures are more stretchable than those with wavy or meandering structures because the 3D structure can restrain the local stresses formed in the 1D conductor upon stretching. In all cases, these 2D and 3D structural approaches take indirect paths and require more materials.

Elastomer Composites. Composite fibers are usually lower in conductivity than conductive nanomaterial fillers because of the presence of the nonconductive matrix. There are two general routes to produce a stretchable yet highly conductive 1D composite conductor (Figure 3b). One is to blend conductive nanomaterials with an elastic matrix, then melt or wet spin them into composite fibers. The choice and quantity of the conductive nanomaterials must be determined to match specific applications. The other is to infuse existing 3D conducting porous networks (conductive foams, aerogels, or porous fibers) with an elastomer precursor and then follow by curing. These composites can be cut into 1D conductors. This route can be extended to infuse porous fibers with elastomers. However, producing strong and continuous fibers with high

porosity remains challenging. Moreover, the performance of this kind of conductor is usually confined within a medium strain (e.g., 100%) to maintain the continuity of the conducting networks.

Fragmentation. Fragmentation refers to the multiplication of cracks^{54–58} that usually leads to damage to the materials in multilayer or laminated structures. Cracks are not necessarily detrimental to materials' overall mechanical and electrical properties when controlled and can be central to stretchable 1D conductors.^{59–62} Upon the stretching of a fragile 1D conductor embedded in an elastomer, a pseudoperiodical pattern of cracks develops perpendicular to the main loading direction. This fragmentation results in a quasi-random network of transverse cracks (Figure 3c). This is identical to the transverse cracking mechanism in laminated composites and the cracking mechanisms in thin coatings for which there are established micromechanical models in fracture mechanics. The stretchability of rigid materials like CNT wires within an elastomer is drastically improved by generating high-density cracks. These cracks generally propagate with contact loss in the conductive networks between crack tips.^{63,64} The prerequisite to applying fragmentation strategy for achieving high stretchability lies in that (1) the conductive materials need to be assembled into a fiber or wire and (2) the fiber or wire needs to be wrapped with an elastomer for achieving high stretchability.

Buckling from Prestrained Support. With prestrained elastomeric supports, rigid nonelastic conductive wires can become stretchable and, more importantly, recoverable. The execution of this strategy depends on the materials.^{65,66}

Table 1. Physical Properties of Piezoresistive 1D Stretchable Conductors

materials	preparation methods	initial electrical properties	$\Delta R/R_0$	maximum strain (ϵ_m)	disadvantage	applications	ref
Ag flake/silicone composite fiber	injection forming	$\sigma = 876 \text{ S cm}^{-1}$	3	13%	low stretchability	electrical interconnects	75
Ag nanoparticle/PVDF-co-HFP composite fiber	wet spinning and annealing	$\sigma = 17\,460 \text{ S cm}^{-1}$	10^5	300%	low stretchability	electrical interconnects, touch sensor	77
Ag nanoflowers/polyurethane composite fiber	wet spinning and annealing	$\sigma = 41\,245 \text{ S cm}^{-1}$	10^3	125%	low stretchability	electrical interconnects	79
Ag flake/fluorine rubber composite wire	Ag mix with fluorine rubber and surfactant	$\sigma = 738 \text{ S cm}^{-1}$	3	215%	low conductivity	electrical interconnects	53
AgNW/AgNP-embedded SBS composite fiber	AgNP coated on wet-spun AgNW/SBS fiber	$\sigma = 2450 \text{ S cm}^{-1}$	20	100%	low sensitivity	wearable sensors	49
PU/cotton yarn/AgNW/PDMS coaxial fiber	wrapping PU and dip coating by AgNW and PDMS	$\sigma = 4018 \text{ S cm}^{-1}$	3	500%	poor repeatability upon stretching	electrical interconnects	80
spirally structured CNT/rubber composite fiber	rolled up CNT-coated rubber film	$\sigma = 0.053 \text{ S cm}^{-1}$	7.5	300%	very low conductivity	electrical interconnects and strain sensors	103
PMIA/FWCNT coaxial fiber	dip coating	$\sigma = 167 \text{ S cm}^{-1}$	3.5	150%	low stretchability		81
bisheath coaxial fibers	buckled CNT film and rubber on a rubber fiber		1.6	600%	low conductivity, CNT exposed	sensors and actuators	85
TPE-wrapped CNT coaxial fiber	wet spinning and post-treatment	$R = 71.3 \text{ } \Omega \text{ cm}^{-1}$	325	100%		electrical interconnects and strain sensors	64

Despite highly limited stretchability (3%),⁶⁵ metals can bend if their cross sections are adequately small, thereby bringing the possibility to engineer stretchable structures through this strategy in four steps: (1) prestraining an elastic base layer. (2) depositing or printing the determined stretchable structure on the base layer, (3) encapsulating an elastic top layer, and (4) releasing the applied strain on the base layer to create a buckled wire inside the elastic substrate (Figure 3d). In one case with wet-spun CNT fibers, a thin layer coating of liquid polydimethylsiloxane (PDMS) enhanced the interfacial bonding with PDMS elastomer layers to form laterally buckled CNT fibers.⁶⁶ Another example couples this with the continuous coaxial fiber strategy by coaxially spinning a core conductive liquid dispersion with an elastic sheath, then stretching the as-spun fiber with the core still in the liquid phase before drying the core–sheath fiber. A buckled conductive wire inside an elastic sheath can be formed upon releasing the dried fiber.

Encased Liquid Metal Alloy with Elastomer. Liquid metals or their alloys are intrinsically conductive with a conductivity of $3.4 \times 10^4 \text{ S/cm}$.^{15,48} They do not store mechanical energy when deformed significantly but can be categorized as intrinsically stretchable 1D conductors encased within an elastomer channel (capillary, hollow fiber) that serves as a stretchable substrate to carry the liquid metals. Upon stretching, the liquid metal flows in the elastomer channel without losing significant electrical conductivity (Figure 3e), thus offering both superior conductivity and stretchability for 1D conductors. The drawback of such fibers is that the liquid metal can flow, and its resistance increases dramatically when pinched. Moreover, the risk of leaking is high when stretched beyond the maximum strain of the elastomer.

Twisting of Conductive Yarn. Twisting is a simple and classic practice to produce yarns, and thus, can be fully integrated with textile processing (Figure 3f). CNT yarns made by dry spinning from CNT forest or chemical vapor deposition (CVD) sources generally have low stretchability (less than 10%). A straight CNT yarn's excellent mechanical strength and flexibility allow it to be twisted into a helical structure.⁶⁷ Overtwisting the CNT yarn leads to an additional secondary hierarchically twisted entanglement structure that permits

stretching to much higher tensile strains (500%), with elastic strain recovery and linear change in yarn electrical resistance.⁶⁸

1D Conductor Categories by Strain Levels. The past decades have testified to the rapid advancement in the design and fabrication of 1D conductors in the form of fibers, wires, and yarns with varying architectures and dimensionalities through various preparation methods. The critical timeline of representative developments in 1D conductors reviewed in this article shows a trend from rigid 1D conductors toward stretchable 1D conductors (Figure 4).^{45,48,49,53,63–66,69–100}

Excellent stretchability and high conductivity are the key attributes of stretchable 1D conductors, but are often mutually exclusive and cannot be achieved simultaneously.⁶³ High stretchability requires large microstructure deformation, whereas high conductivity requires the preservation of microstructural integrity, i.e., the minimization of microstructural defects induced by stress concentration at high strains. Therefore, continuous 1D conductors are grouped by changing electrical responses to the external tensile strain into rigid, piezoresistive, and resistance-stable categories.

Rigid 1D Conductor. Intrinsically rigid 1D conductors generally have high tensile strengths and Young's moduli but are brittle and break at low strain (<5%). Pure metallic wires, metallic alloy wires, metal-clad fibers, carbon fibers, carbon-nanomaterial-based fibers, and some conductive polymer fibers fall into this category and have been extensively reviewed.^{30–35,101,102} With the advances in electronics, demands for these devices include their ability to be stretchable, twistable, and deformable into curvilinear shapes beyond what the current rigid 1D conductors can meet. The evolution of rigid 1D conductors into stretchable 1D conductors is critical for realizing these applications and falls into the following two categories.

Piezoresistive 1D Conductor. Piezoresistive 1D conductors exhibit a relatively big change in resistance or $\Delta R/R_0$ with relatively high strain, often >100% maximum strain, and the advances in this area are summarized in Table 1. Most intrinsically stretchable 1D conductors have been exploited by either (1) introducing conductive species into elastomers, which combines the electric properties of the conductive

Table 2. Summary of Physical Properties of Resistance-Stable 1D Stretchable Conductors

materials	preparation methods	initial electrical properties	$\Delta R/R_0$	maximum strain (ϵ_m)	disadvantage	applications	ref
wavy Au wires	lithography	$\sigma = 5.8 \times 10^5 \text{ S cm}^{-1}$	<0.01	2.7–54%	low stretchability	electrical interconnects	65
kinked CNT fiber	dry spinning and bulking	$\sigma = 475 \text{ S cm}^{-1}$	0.01	40%	low stretchability	electrical interconnects	66
overtwisted CNT yarn	dry spinning and twisting	$R = 210 \Omega$	0.6	500%	mechanical instability	strain sensors and rotational actuators	68
highly conductive PEDOT/PSS fiber	hot-drawing-assisted wet spinning/EG treatment	$\sigma = 2800 \text{ S cm}^{-1}$	0.1	21%	low stretchability	electrical interconnects, heaters and actuators	52, 90
folded PEDOT/PSS strips in elastomer fibers	wet spinning, stretching/drying/releasing	$\sigma = 500 \text{ S cm}^{-1}$	0.05	700%	low conductivity	stretchable interconnects and heaters	64
CNT/PU buckled coaxial fibers	PU prestraining, CNT wrapping, buckling	$\sigma = 0.1\text{--}3.6 \text{ S cm}^{-1}$	<0.05	1000%	low conductivity	sensors and actuators	104
twistable sandwiched CNT/rubber/CNT fiber	rubber sandwiched between buckled CNT layers	$R = 179 \Omega \text{ cm}^{-1}$	0.05	200%	SWCNT exposed	wearable sensors and supercapacitors	91

species and stretchability of the elastomer, or (2) fabricating fibers with coaxial configuration. The corresponding piezoresistivity mainly results from the disconnection between conductive fillers and the tunneling effect upon external loading.

Resistance-Stable 1D Conductor. Some soft, stretchable 1D conductors exhibit a relatively small change in resistance (<100%) when undergoing relatively large strains and are considered resistance-stable 1D conductors, as summarized in Table 2. The capability of stretchable conductors to maintain their electrical properties upon being stretched could be evaluated by either relative change in conductivity, i.e., $-\Delta\sigma/\sigma_0$, where, σ_0 , is the initial conductivity without deformation, and $-\Delta\sigma$ is the variation of conductivity at a strain of ϵ . The relative change in resistance, $\Delta R/R_0$, where, R_0 , is the initial resistance and ΔR , is the variation of resistance at a strain of ϵ . The essential features of this type of 1D conductor are that they are compliant and retain their electrical performance at high-strain deformation. In this review, $\Delta R/R_0 < 1$ is considered a resistance-stable 1D conductor.

Fabrication Technologies. Reliable manufacturing solutions are critical for developing scalable and batch-to-batch consistent fibers.²¹ Various fabrication strategies to obtain standalone functional fibers can be broadly classified into three categories: spinning, thermal drawing, and printing. Spinning can produce or functionalize continuous fibers, which has been realized for mass production.^{105,106} Fibers with different diameters and/or hierarchical structures are apt to be made from a single or multiple materials by tuning initial processing parameters. General spinning techniques such as wet spinning,¹⁰⁷ dry spinning,¹⁰⁸ melt spinning,¹⁰⁹ electrospinning¹¹⁰ and centrifugal spinning¹¹¹ have all been applied to fabricate fibers or yarns using various materials. In addition, thermal drawing is a facile and scalable approach to producing fibers and has been employed to fabricate smart textiles.^{112–119} This approach enables the targeted materials to be filled into a prepared “preform”¹²⁰ and allows simultaneous extrusion of various functional materials within a one-body design. It can assemble materials with different shapes and structures and integrate multiple functionalities to form complex fiber electronics. Furthermore, as thermal drawing can be miniaturized to the nanoscale,¹²¹ it is likely that the whole process of fiber fabrication may be optimized in the future. Furthermore, printing,¹²² including additive manufacturing, has also been used to either deposit inks onto textiles or directly extrude fibers in 3D structures. It has been

implemented at the industrial level, thereby demonstrating the potential for large-scale, autonomous, and low-cost processes.

In addition to the above techniques to fabricate standalone fibers, widely adopted coating methods, including dip coating,¹²³ spray coating,¹²⁴ and electrochemical coating,¹²⁵ can provide a low-cost and effective approach to modify and functionalize existing fibers and textiles. These coating processes may be exploited to transfer functional materials onto the surface of fibers or textiles to achieve desirable changes in the active layer by manipulating the thickness or the types of the coating materials.¹²⁶

RECENT ADVANCES IN THE STRETCHABLE 1D CONDUCTOR

Conductive Polymer Fibers. Conductive polymer fibers have been widely explored from both fundamental and application prospects to understand their electrical and mechanical performance.^{69,87,88,128,129} The main techniques for processing conductive polymers into fibers are dry spinning, wet spinning, and melt spinning. While both dry and melt spinning solidify respective polymer solutions and melts in the gaseous environment, wet spinning submerges the spun polymer solutions in coagulation baths to solidify the fibers.¹³⁰

Over the past 40 years, various types of conducting polymers have been developed.^{131–133} Among them, poly(3,4-ethylene dioxythiophene)/polystyrenesulfonate (PEDOT/PSS) is the conducting polymer that can be dispersed in water and various organic solvents to form dispersions.^{134,135} This gives PEDOT/PSS excellent processability that is better than other conducting polymers.^{136–140} Therefore, these most spinnable PEDOT/PSS dispersions have been successfully wet-spun into microfibers,^{87,88,129,141,142} and have been scaled up to industrial production.¹⁴³ In the past decade, the conductivity of PEDOT/PSS films and fibers has been improved by more than 2 orders of magnitude by doping and/or dedoping with various polar solvents, like ethylene glycol (EG),^{88,139,144–148} sulfuric acid (H_2SO_4),¹⁴⁹ hexafluoroacetone trihydrate (HFA),¹⁵⁰ dimethyl sulfoxide (DMSO),^{151,152} and anionic surfactant.¹⁴⁰ Doping PEDOT/PSS with a secondary high boiling point dopant (<6 wt %) changes its microstructure to a more conductive state (quinoid structure).^{153–155} Dedoping involves partial removal of the insulating and amorphous PSS by washing with polar solvents.^{153–155} Dedoping as-spun microfibers of various

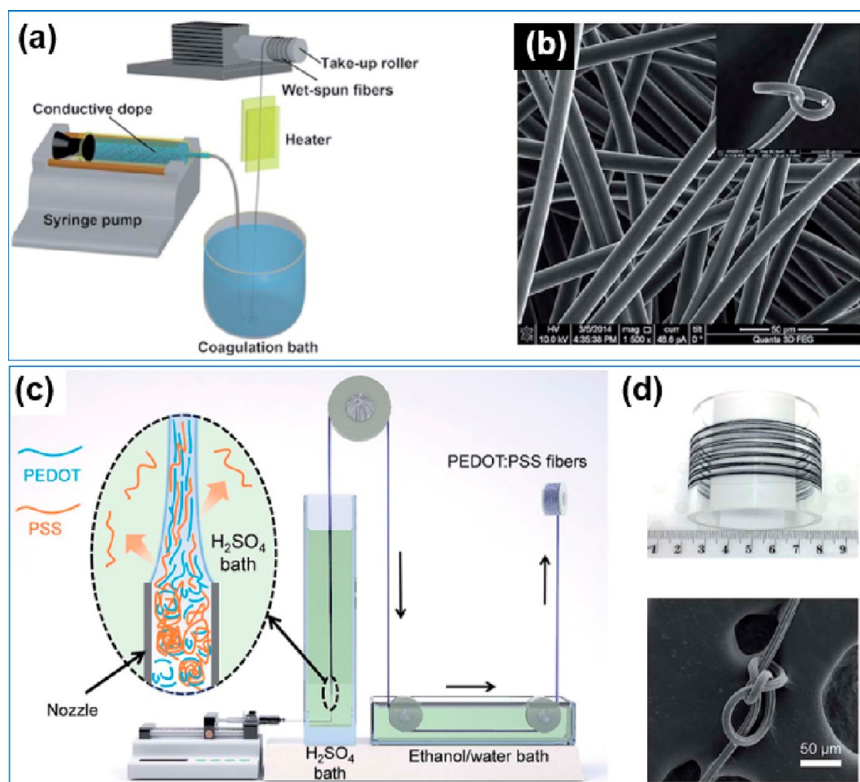


Figure 5. Highly conductive polymer fibers. (a) A schematic illustration of the wet spinning setup with the vertical hot-drawing. (b) SEM image of the as-spun PEDOT/PSS fibers. Reprinted with permission from ref 64. Copyright 2018 John Wiley and Sons. (c) Schematic drawing of the modified setup used in wet spinning PEDOT/PSS fibers using H₂SO₄ as the coagulant. Inset illustrates the alignment of PEDOT/PSS domains during fiber spinning and the diffusion of excess PSS to H₂SO₄ coagulant. (d) 100 m of continuous PEDOT/PSS fiber on a sample spool and SEM image of a PEDOT/PSS showing flexibility through tight knots. Reprinted with permission from ref 127. Copyright 2019 The Royal Society of Chemistry.

grade PEDOT/PSS (without dopant) with EG improved their low electrical conductivities (1 to 456 S cm⁻¹).^{87,88} A combination of both doping and dedoping with EG has shown to improve the electrical conductivity to 351 S cm⁻¹.⁸⁸ Spinning PEDOT/PSS with CNTs into composite fibers led to limited improvement in conductivity (400 S cm⁻¹).^{156,157} All fell short of the electrical conductivity needed for flexible interconnect electrodes, conductive textiles, and sensors and actuators. By hot drawing immediately following wet spinning and EG doping and dedoping, Zhou et al. reported conductive, strong, and stretchable PEDOT/PSS microfibers with 2804 S cm⁻¹ conductivity, 409.8 ± 13.6 MPa tensile strength, and 21.2 ± 1.4% elongation at break (Figure 5a,b).⁹⁰ This electrical conductivity of 2804 S cm⁻¹ is a 6-fold improvement over the previously reported best value for fibers (467 S cm⁻¹)⁸⁷ and double the best-reported value for EG doped PEDOT/PSS films (1418 S cm⁻¹).¹³⁸ The mechanical properties were extraordinarily superior to those previously reported PEDOT/PSS fibers with similar conductivities. The enhanced conductivity and strength are attributed to improved PEDOT alignment in the microstructure by hot drawing, partial removal of the insulating PSS by EG dedoping, and reduced electrostatic interaction of PEDOT and PSS by EG doping. The fibers also show high stiffness (8.3 GPa) with increased electrical conductivity (25%) at as high as 21% strain.⁹⁰

Zhang et al. have shown a facile production of PEDOT/PSS fibers using H₂SO₄ as the coagulant with a high electrical conductivity of 3828 S cm⁻¹, which is close to the highest value

reported for 100 nm thick PEDOT/PSS films.¹²⁷ The use of H₂SO₄ as a coagulant and modification of the wet spinning apparatus enabled the simultaneous removal of PSS within seconds and the alignment of PEDOT chains, which resulted in a tensile strength of 434.8 MPa and an elongation at break of 25.4%.¹²⁷ These results highlight the critical role of PEDOT alignment in conductivity and strength maximization of conductive polymer microfibers for potential use in textile-based stretchable devices.

Zhou et al. also showed the resistance stability of their fibers under applied strain. This behavior is needed for some electrical interconnects to maintain their electrical performance under strain. The relative change in resistance ($\Delta R/R_0$) upon incremental cyclic loading/unloading and extension at 21% strain was only 0.10, which indicated resistance stability. The intrinsic change in conductivity is determined by calculating the geometric factor and subtracting it from the measured resistance. The resistance, R , of a fiber with a round cross section is expressed by eq 1:

$$R = \frac{l}{\pi r^2 \sigma} \quad (1)$$

where σ is the electrical conductivity, and l and r are the fiber's length and radius, respectively. The relationship between the relative change in resistance, $\Delta R/R_0$, and the relative change in conductivity, $\Delta\sigma/\sigma$, is given by eq 2:

$$\frac{\Delta R}{R_0} = -\frac{\Delta\sigma}{\sigma} + \frac{\Delta l}{l} - 2\frac{\Delta r}{r} \quad (2)$$

With minor changes, $\Delta l/l = \varepsilon_f$ and $\Delta r/r = -\nu\varepsilon_f$, where ε_f is the strain in the fiber axis, and ν is the Poisson's ratio.⁹⁰ By substituting these values, the relative change in electrical conductivity, $\Delta\sigma/\sigma$, is expressed in eq 3:

$$\frac{\Delta\sigma}{\sigma} = \varepsilon_f(1 + 2\nu) - \frac{\Delta R}{R} \quad (3)$$

where $\varepsilon_f(1 + 2\nu)$ relates to the geometric change of the fiber cross section under the strain ε_f .⁹⁰ The $\Delta\sigma/\sigma$ reflects changes in the material's conductivity that depend on the strain. For example, the relative change in resistance $\Delta R/R_0$ is 0.23 at 13% strain for the as-spun PEDOT/PSS fibers. If it is assumed $\nu = 0.34$,¹⁵⁸ $\varepsilon_f(1 + 2\nu)$ is calculated to be 0.22, and $\Delta\sigma/\sigma \approx 0$. Therefore, the change in resistance is mostly related to the change in fiber geometry.

Composite 1D Conductor. Elastomer materials are stretchable and easy to process. The resulting structures offer design flexibility in form and function and are ideal building blocks for stretchable 1D conductors.^{65,77,159–162} The most used method for making a stretchable conductor is to incorporate the conducting fillers into a soft polymer matrix (an insulating elastomer) through melt compounding or solvent mixing. Then, the mixture is melt-spun or wet-spun into composite microfibers continuously. The electrical conduction in these composite fibers occurs through connected networks of metallic nanoparticles or nanowires, carbon nanomaterials, and conductive polymer nanoparticles. In the 3D percolation theory, the electrical conductivity of the conductive composite is calculated by the two equations below for the initial and the elongated states. The nanofiller volume mainly determines the nanocomposite conductivity fraction:^{163,164}

$$\sigma_{1, \text{ or } 2} = \sigma_0(V_{f_1, \text{ or } f_2} - V_c)^t \quad (4)$$

$$V_{f_1, \text{ or } f_2} = V_{\text{filler}}/V_{1, \text{ or } 2} \quad (5)$$

where indexes 1 and 2 describe the initial and elongated states, respectively; σ is the electrical conductivity in the axis direction of the 1D conductive composite; σ_0 is the scaling factor proportional to the intrinsic conductivity of the nanofiller; V_f and V_{filler} are the volume fraction and volume of conductive nanofillers, respectively; V_1 and V_2 are the volume of the conductive composites at the initial and elongated state, respectively; V_c is the percolation threshold, and t is the fitting exponent of the factor related to the dimensionality of the composite. The conductive species have to be highly conductive and with a high V_f in the elastomer to reach the ultimate goal of an electrical conductivity closer to that of a metal wire. Because of the network change under an elongated state, the σ_2 of the fiber may dramatically reduce, which is ascribed to the reduction of the local V_2 . Thus, the conductive fillers' initial conductivity, loading, and geometry must be considered.

These nanofillers can form a uniformly percolated network that grants conductive paths through a tunneling effect to the composite. However, the percolation threshold, V_c in eq 4, is primarily determined by the geometry of the nanofillers. According to microscopical morphologies, nanomaterials are grouped into three categories: 0D nanoparticles (NPs), 1D nanowires (NWs) and nanotubes (NTs), and 2D nanosheets.

If it is assumed that conductive NPs are homogeneously distributed among the flexible substrate, it is conceivable that the composite is divided into quantities of cubic elements. At a

free-standing state, the percolation threshold of the network (V_c) is determined by¹⁶⁵

$$V_c = \frac{\pi D^3}{6(D + D_{\text{IP}})^3} \quad (6)$$

where two key parameters are the diameter of the particle (D) and the interparticle distance (D_{IP}), respectively. Eq 6 indicates that V_c monotonically increases with increasing particle diameters. Additionally, the distance of adjacent particles has a considerable effect on the tunneling current,¹⁶⁶ i.e., the electrical conductivity of the 1D composite. Under applied stress, the smaller nanoscale NPs have a much greater degree of freedom to redistribute than their higher dimensional counterparts (NWs and nanosheets) to assemble and organize in a distinct configuration into a conductive band along the strain direction.¹⁶⁷ The strain-dependent threshold of the percolated network $V_c(\varepsilon)$ is described by¹⁶⁴

$$V_c(\varepsilon) = \frac{V_c^0}{1 + \alpha\sqrt{\varepsilon}} \quad (7)$$

where α presents the reorganizing capability of the NPs under stress, ε is the strain, and V_c^0 is the percolation threshold under the initial state. Those theoretical studies demonstrate the electrical properties of composites percolated with NPs and offer predictions to fabricate 1D conductive composites with both satisfactory electrical performances and mechanical tunability.

Because of the high aspect ratio, 1D NWs/NTs have a much lower V_c than the isotropic 0D NPs, which is illustrated in eq 8:^{164,165}

$$N_c L^2 = 5.71 \quad (8)$$

where N_c is the percolation threshold density, and L is the length of the 1D nanomaterials. The network conductivity (σ) can be defined by conductive filler density (N) as¹⁶⁴

$$\sigma \propto (N - N_c)^t \quad (9)$$

where t is the critical exponent in eq 4. Unlike 0D NPs, the highly persistent length of NWs/NTs can bridge multiple 1D structures to form a direct conductive path. Thus, junction conductivity plays a vital role in NW/NT-based composites. Intriguingly, some NWs exhibit intimate integration with a flexible substrate, which gives a feasible scheme for the construction of 1D conductive composites.

Because of the small contact space, 1D nanomaterials usually present large junction resistance when stretched to a large extent.¹⁶⁸ Thus, 2D nanosheets with large surface area and high charge carrier mobility have aroused tremendous interest to construct a broader and more stable conductive path in conductive composites. The 2D morphology can offer a much larger junction area than 1D NWs/NTs, which can increase the efficiency of interlayer electron tunneling and improve electrical performance. For instance, because of the high conductivity of 2D graphene even under large deformation, the intrasheet resistance is considerably small.¹⁶⁹ The overall resistance of graphene is governed by intersheet resistance, i.e., the contact resistance of nanosheets. When strain is applied, the intersheet resistance can be written as¹⁷⁰

$$R = ad_0(\varepsilon + 1) \times e^{bd(\varepsilon+1)} \quad (10)$$

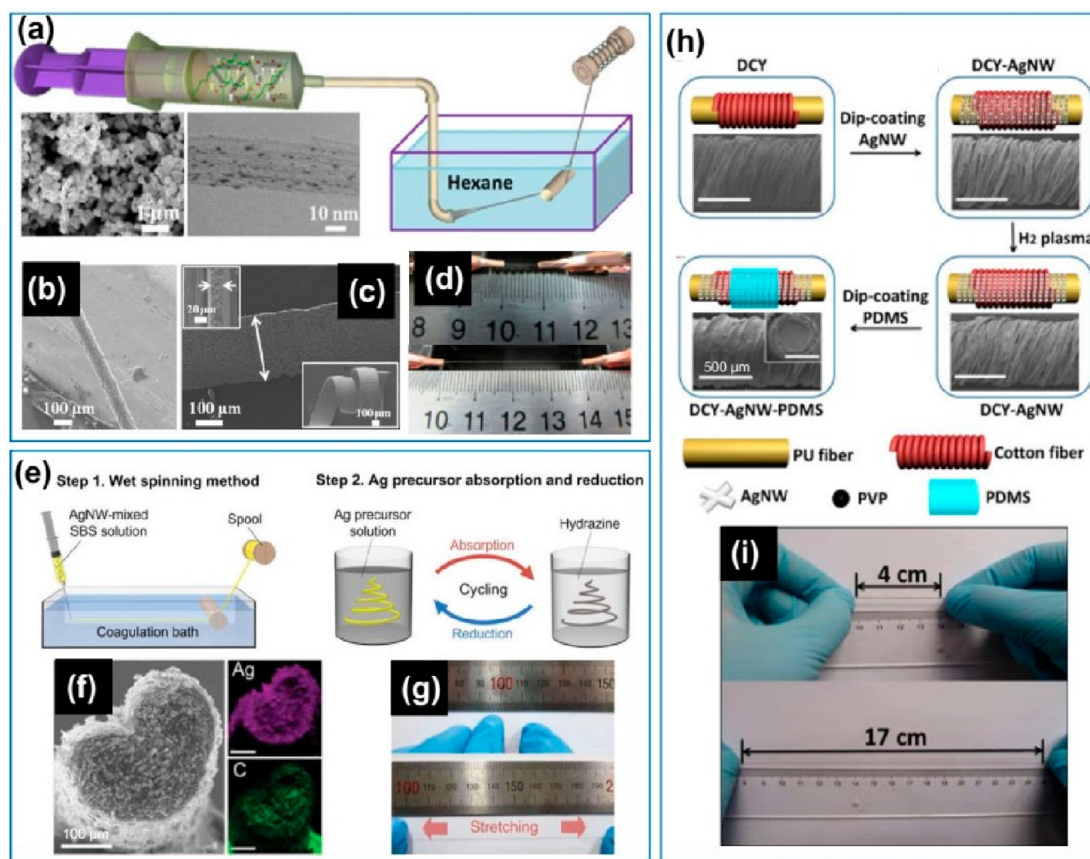


Figure 6. Silver nanomaterials-based composite fibers. (a–d) Wet-spun Ag-MWCNT-based stretchable fibers. (a) A schematic drawing of the wet spinning apparatus. An SEM image of Ag nanoparticles and an HRTEM image of nAg-MWNTs nanoparticles are shown. (b) SEM image of the spun fiber with a diameter of 100 μm . (c) SEM images of the hot-rolled fiber with width and thickness were 250 and 17 μm . (d) Optical images of the composite fiber (8.5 wt % of Ag) before and after stretching. Reprinted with permission from ref 77. Copyright 2014 American Chemical Society. (e–g) Wet-spun AgNW/AgNP/SBS composite fibers. (e) Schematic illustration of the preparation for the stretchable conductive fiber. (f) Cross-sectional SEM images and EDS mapping of Ag and C were obtained from the AgNW/AgNP-embedded composite fiber. Scale bar: 100 μm . (g) Optical images of pre- and 900%-strained composite fiber. Reprinted with permission from ref 49. Copyright 2015 John Wiley and Sons. (h,i) Cotton yarn/AgNW twining spirally on a PU fiber coated with PDMS. (h) Schematic illustration for preparing the composite fiber and corresponding SEM images. (i) A composite fiber of 4 cm was stretched to 17 cm length by hand. Reprinted with permission from ref 172. Copyright 2015 John Wiley and Sons.

where d_0 is the intersheet distance at the initial state without strain, and d is the intersheet distance under strain. Thus, the applied strain $\epsilon = (d - d_0)/d_0$. a and b are given by¹⁷¹

$$a = \frac{h^2}{Ae^2 \sqrt{2mE_B}} \quad \text{and} \quad b = \frac{4\pi}{h} \sqrt{2mE_B} \quad (11)$$

where A is the junction area, m is a constant related to the fractal structure, E_B is the height of the potential barrier between nanosheets, and h is Planck's constant. Therefore, the parameters such as the fracture structure of the nanosheets, nanosheet overlapping, etc. can be manipulated to design the blending system of 2D nanosheets-based stretchable conductors. Considering the interplay between the applied strain and intersheet separation, hypersensitive materials with high gauge factors can be practically used for wearable electronics.

Silver Nanomaterials-Based Stretchable 1D Conductors. Among conductive fillers, silver nanoparticles (AgNPs) or nanowires (AgNWs) have the highest electrical conductivity and, thus, are most desirable. Wakuda et al. reported a stretchable composite made of silicone-containing Ag microflakes (310 μm) by injection forming (into a hot oil bath).⁷⁵ Though the fibers have an initial conductivity of 876 S cm^{-1} ,

the conductivity dropped dramatically to 10 S cm^{-1} before failing at 14% tensile strain. The fiber's low stretchability was ascribed to the significant defects introduced by the microscale Ag flakes. Ma et al. reported a stretchable (nAg-MWNTs) composite fibers wet-spun from an ionic liquid containing 100–150 nm AgNPs and MWNTs decorated with 3–5 nm AgNPs (35 wt %) with flexible nitrile butadiene rubber or stretchable poly(vinylidene fluoride-hexafluoropropylene) (PVDF-HFP) elastomer into a hexane coagulation bath (Figure 6a).⁷⁷ The filament with a uniform 100 μm diameter (Figure 6b) and over 10 m length was cured at 135 $^\circ\text{C}$ or deformed into a helical shape through a hot rolling process (inset of Figure 6c). The initial fibers could reach a conductivity of 17 460 S cm^{-1} , which was attributed to the significantly improved agglomeration between microscale Ag particles and AgNPs preadsorbed on the CNT walls during curing. The rupture tensile strain was increased to 490% by decreasing the loading of the fillers to 8.5 wt % (Figure 6d), albeit at the expense of lowering the initial conductivity, which was reduced to 236 S cm^{-1} . In a follow-up study, Ma et al. wet-spun 39.5 vol % silver nanodisc-shaped petals (Ag nanoflowers) with polyurethane into Ag/PU composite fibers with a high conductivity of 41 245 S cm^{-1} , which is more than twice

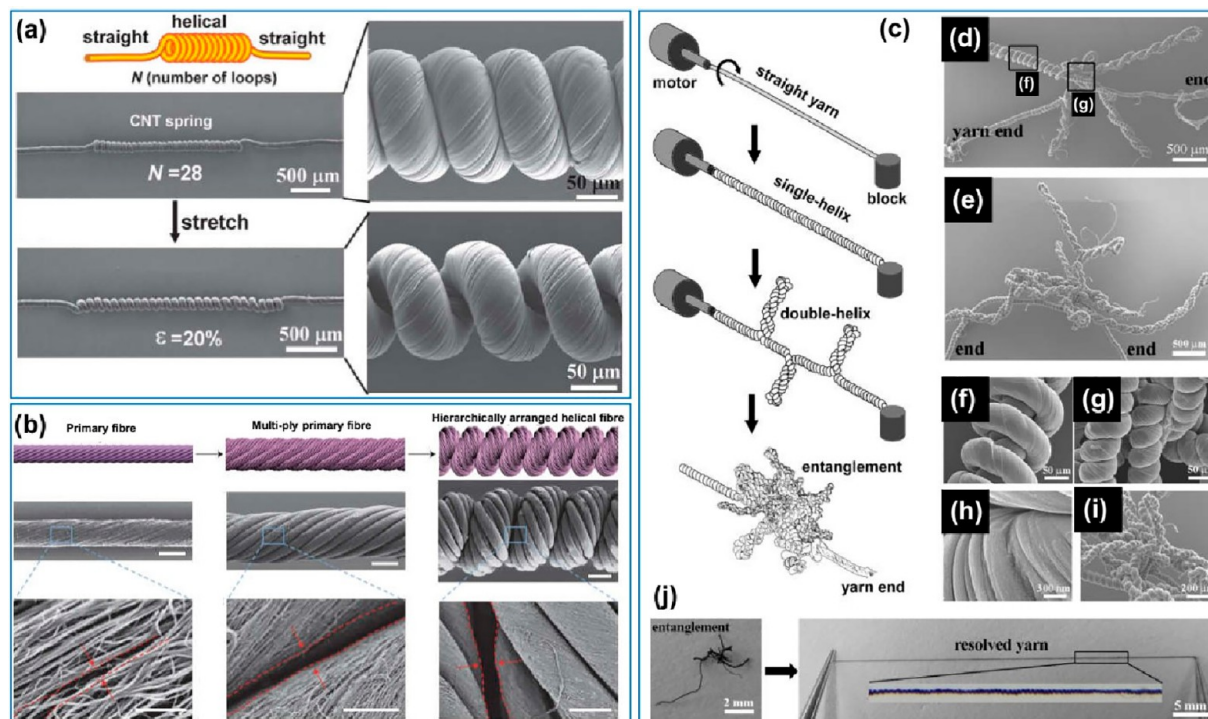


Figure 7. Stretchable CNT fibers. (a) SEM images of a CNT yarn with a helical structure containing twisted uniform loops were stretched to a strain of about 20%, thereby showing loop separations and illustrating the straight–helical–straight yarn structure. Reprinted with permission from ref 67. Copyright 2013 Royal Society of Chemistry. (b) Schematic illustration and SEM images of a hierarchical structured helical CNT fiber, prepared from multiple primary fibers through twisting. Reprinted with permission from ref 50. Copyright 2015 Springer Nature. (c) Schematic illustration of the spinning process: a straight yarn with two fixed ends was overtwisted into a helical shape and then an entanglement. (d,e) SEM images of two CNT entanglements with different morphologies. The entangled yarn can be stretched to resolve the entanglement. (f,g) Enlarged views of the entangled parts within the entanglement in (d). (h) Close view of the yarn surface. (i) Enlarged view of the entanglement in (e). (j) Photographs of a CNT entanglement and the resolved straight helix yarn. Reprinted with permission from ref 68. Copyright 2013 American Chemical Society.

that of the previous Ag microparticle-containing fibers and is ascribed to the enhanced coalescence of nanodisc-shaped petals (8 nm in thickness) from curing.⁷⁹ Again, a trade-off between electrical conductivity and stretchability was achieved to reach the maximum rupture strain at 776% by reducing Ag nanoflower loading from 39.5 vol % to 17.9 vol %. Since both fibers are piezoresistive, their electrical properties cannot be maintained under strain because the percolated network formed by the conductive fillers becomes disconnected with increasing strain.

Lee et al. preserved electrical conductivity under high strain by wet spinning a highly stretchable composite fiber composed of AgNWs and AgNPs embedded in a poly(styrene-*block*-butadiene-*block*-styrene) (SBS) elastomer (Figure 6e–g).⁴⁹ The AgNPs are formed on the surface and inside the AgNW/SBS fiber via repetitive silver precursor absorption and reduction cycles (Figure 6e) and in high density (Figure 6f). This AgNW/SBS fiber reached an impressive 900% maximum elongation at break with the highest conductivity of 2450 S cm⁻¹. During stretching, the embedded AgNWs act as conducting bridges and networks to connect AgNPs, which preserves 95.6% of the electrical conductivity at 100% strain.

Besides simple mixing and wet spinning for making composite fibers, Cheng et al. developed a “twining spring” architecture for a highly conductive and ultrastretchable composite fiber.¹⁷² The conductive composite fiber comprises a polyurethane fiber double-covered with cotton yarn (DCY) and AgNWs, which is then encapsulated in a strengthening and

protective layer of PDMS (Figure 6h). The initial conductivity of the composite fiber was 4018 S/cm and remained 688 S/cm at 500% strain, which presents a highly competitive Ag nanomaterial-based stretchable composite fiber conductor. The composite fiber also presented excellent cyclic performance, with a conductivity of 183 S/cm after 1000 stretching events of 200% strain. The gauge factor for the composite conducting fiber maintains a range from 0.166 to 0.251 when the strain changes from 100% to 500%, which suggests the superior stability of the electrical conductivity during deformation. When stretched, the elastic PU core fiber elongates while the spiral cotton yarns (CYs) twining around increase its winding angle, and the gaps between the CYs emerge and broaden with increasing strain. These microstructural changes allowed the DCY to undergo large strains without stretching the cotton fibers. Consequently, the conductive AgNW network confined on the cotton fiber surfaces experiences minor damage during stretching, thereby offering a stable conductive path along the cotton fibers. Among nearly all Ag-based composite fibers containing various forms of Ag, the resistance or conductivity is strain-dependent, and the extensibility is limited.

Carbon-Nanomaterial-Based Stretchable 1D Conductors. CNT yarns have been studied for potential applications in electrical wirings, sensors, actuators, and energy-storage devices.^{67,71,173–177} However, conventional CNT yarns are straight and lack the elasticity required for stretchable conductors. The resistance of the yarn can only be maintained

within a strain level below 1%, which is then increased dramatically because of sliding between CNTs that is irreversible to cause fracture and rapid degradation of electrical conductivity under even small strains (<10%).

Because CNT yarns are more flexible than wet-spun CNT fibers, they can be easily shaped into helical springs or coiled structures with traditional yarn twisting technology. Shang et al. converted an inelastic yarn into an elastic structure by spinning predefined helical loops along the yarn (Figure 7a).⁶⁷ The elastic and conductive yarns can be stretched to tensile strains up to 25% repeatedly for 1000 cycles with a very small $\Delta R/R_0$ (<0.012) without producing residual deformation. Similarly, Chen et al.⁵⁰ prepared primary fibers consisting of helical assemblies of MWCNTs, twisted them together to form the helical fiber bundles, then twisted multiple helical fiber bundles into multiply hierarchically twisted yarn (Figure 7b). Upon exposure to solvent vapors, these fibers contract up to 60% strain to form nanoscale gaps (between the nanotubes) and micrometer-scale gaps (among the primary fibers), in which both contribute to the rapid response and significant contraction in response to strain. These fibers are lightweight, flexible, and robust and suitable for various uses such as energy-harvesting generators, deformable sensors, and intelligent wearable electronics.

The high stretchability of CNT yarns can be achieved by the overtwisting method (Figure 7c) to enable a random entanglement of CNTs, which is analogous to a mingled and entangled rope (Figure 7d–i).⁶⁸ Such entangled CNT yarns have a higher structural hierarchy than simple straight or helical yarns. Moreover, the yarn entanglement can be completely released and stretched to a tensile strain of 500% (Figure 7j), with elastic recovery and a very low $\Delta R/R_0$ of 0.6.

Graphene, another form of carbon nanomaterials, has received significant attention as an outstanding material for fiber-type sensors and actuators, robots, photovoltaic cells, and supercapacitors.^{14,33–35} Although wet-spun graphene fibers exhibit a relatively high Young's modulus and tensile strength, their irregular cross sections along the fibers and wrinkled surfaces result in stress concentration under mechanical loadings, thus making them easy to break upon bending, twisting, or knotting, which is a severe disadvantage in applications. This issue has been solved by introducing stretchability via dry film scrolling and twisting,¹⁷⁸ in which graphene oxide (GO) films are made by bar coating aqueous GO dispersions, followed by ambient drying and scrolling into fibers. The resulting fibers have uniformly circular cross sections, smooth surfaces, high toughness, and outstanding ductility. When overtwisted, these fibers coil into a single yarn with a secondary coil and helical springlike structure to allow stretching up to 76% strain before failure. The maximum stretchability of the yarn is more than 1 order of magnitude higher than the reported values for graphene-based fibers.^{14,33–35}

Hydrogel-Based Stretchable 1D Conductors. A hydrogel, by definition, consists of water and a cross-linked polymer network, where water must make up at least 10% of the total weight (or volume) of the material. It exists in nature and can also be artificially synthesized. The water content of the synthesized hydrogels can even reach more than 90%.¹⁷⁹ Because of their cross-linked polymer network, hydrogels have great strain capacity. The presence of an ionic electrolyte makes it ionically conductive. In this case, many different charge carriers may be encountered, but the ionic mobility is

usually much smaller than the typical value for electrons,¹³⁵ which makes the conductivity of the most reported hydrogel less than 1 S/m. Many works report how to tune the physical properties or biocompatibility of hydrogels to fulfill the corresponding applications. For example, by adjusting the ratio of high-strength cross-linked chemical bonds to low-strength chemical bonds, the mechanical properties of hydrogels can be optimized in terms of stretchability and toughness.¹⁸⁰ For another example, hydrogels prepared from bacterial cellulose, because of their excellent biocompatibility, can be used in surgical sutures by enhancing their mechanical strength.¹⁸¹ Besides, much work has been devoted to improving the ionic conductivity of hydrogels to serve as solid-state electrolytes for electrochemical energy storage devices.¹⁸² Because this review focuses on stretchable 1D conductive materials, advances in conductive hydrogel fibers are expanded upon here.

Ionic polyimide hydrogel fibers were prepared by adding CaCl_2 to the coagulation bath during wet spinning. Because of the increased concentration of an ionic carrier, the electrical conductivity of the fibers was improved to 21 mS/cm. Furthermore, because of the ionic crosslinking between Ca^{2+} and the carboxyl (COO^-) group, the tensile strength was improved to 2.5 MPa with an elongation of 215%. In addition, the fibers obtained piezoresistive properties with a linear gauge factor of 0.76. On the basis of these properties, the fibers can be processed into textiles for detecting stress and strain caused by human motion.¹⁸³ In another example, a physically cross-linked poly(NAGA-co-AAm) (PNA) hydrogel was successfully prepared by wet spinning and UV curing, where the conductivity reached 0.69 S/m because of the addition of lithium chloride, and the gauge factor was increased from 0.44 to 0.94. In addition, the tensile strength of this hydrogel is 2.27 MPa and has self-healing properties (10 min of self-healing can reach 60% of the initial tensile strength). On the basis of these properties, the hydrogel fibers can be fabricated into smart textiles, such as wearable strain sensors.¹⁸⁴ Recently, scientists reported a strategy using a UV curing method combined with self-lubricating spinning to successfully fabricate poly(2-acrylamido-2-methylpropanesulfonic acid)/polyacrylamide (PAMPS/PAAm) hydrogel fibers. A part of PAMPS will carry water to the fiber surface during the spinning process and act as a lubricant. After the solvent exchange with triethylene glycol, which is believed to increase the intermolecular and intramolecular strength of the hydrogel (or it can be called an organohydrogel), the tensile strength of the hydrogel fibers prepared by this strategy was 5.6 MPa.¹⁰⁵ On the basis of this organohydrogel preparation strategy, 1D conductive poly(vinyl alcohol)-nanocellulose (bNF) antifreeze gel fibers have also been recently reported. They have a tensile stress of up to 2.1 MPa, tensile strain of up to 660%, and high electrical conductivity of 3.2 S m^{-1} at room temperature. In addition, since the gel is a coexistent phase of water and DMSO, it has an antifreezing effect (maintains the conductivity of 1.1 S/m at -70°C).¹⁸⁵

Conductive Coaxial Fibers. Continuous fibers with coaxial structures provide a versatile platform for engineering electrically conductive and mechanically stretchable 1D conductors. The high initial conductivity of the materials is one of the most essential characteristics for the performance of the fibers. These coaxial fibers may be piezoresistive or resistance-stable under external strains, depending on the microstructures of the materials.

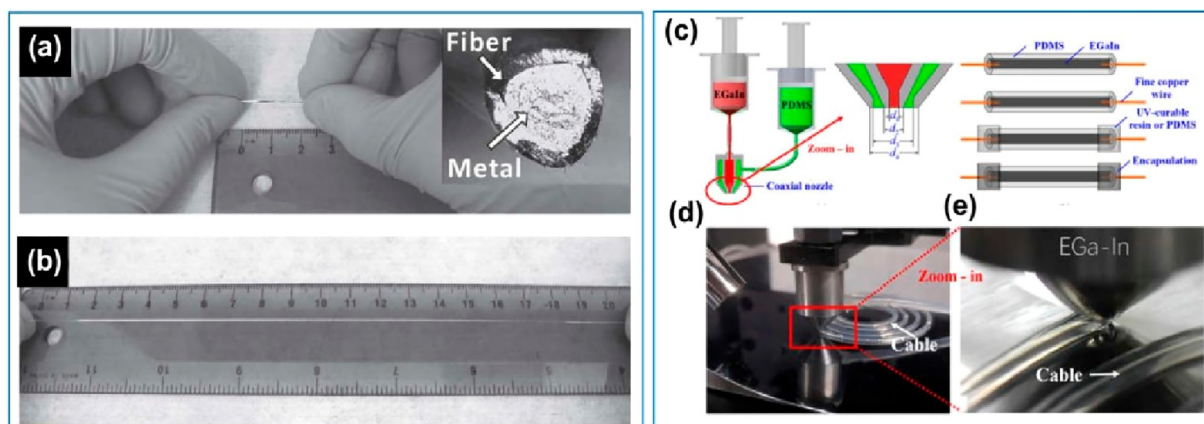


Figure 8. Liquid metal-based coaxial fibers. (a,b) Liquid metal alloy encased in poly[styrene-*b*-(ethylene-*co*-butylene)-*b*-styrene] (SEBS) fiber. (a) A relaxed and ultrastretchable conductive fiber. The core is a liquid metal alloy. (b) The fiber is stretched to a large extent, and the liquid metal appears to fill the stretched fiber uniformly. Reprinted with permission from ref 48. Copyright 2013 John Wiley and Sons. (c–e) PDMS-encased EGAIn fiber by coaxial writing. (c) Schematic of coaxial drawing of conductive cables of coaxial design with EGAIn as the core and PDMS as the shell. (d) The full direct drawing process. (e) Photographs of coaxial drawing details. Reprinted with permission from ref 82. Copyright 2016 AIP Publishing.

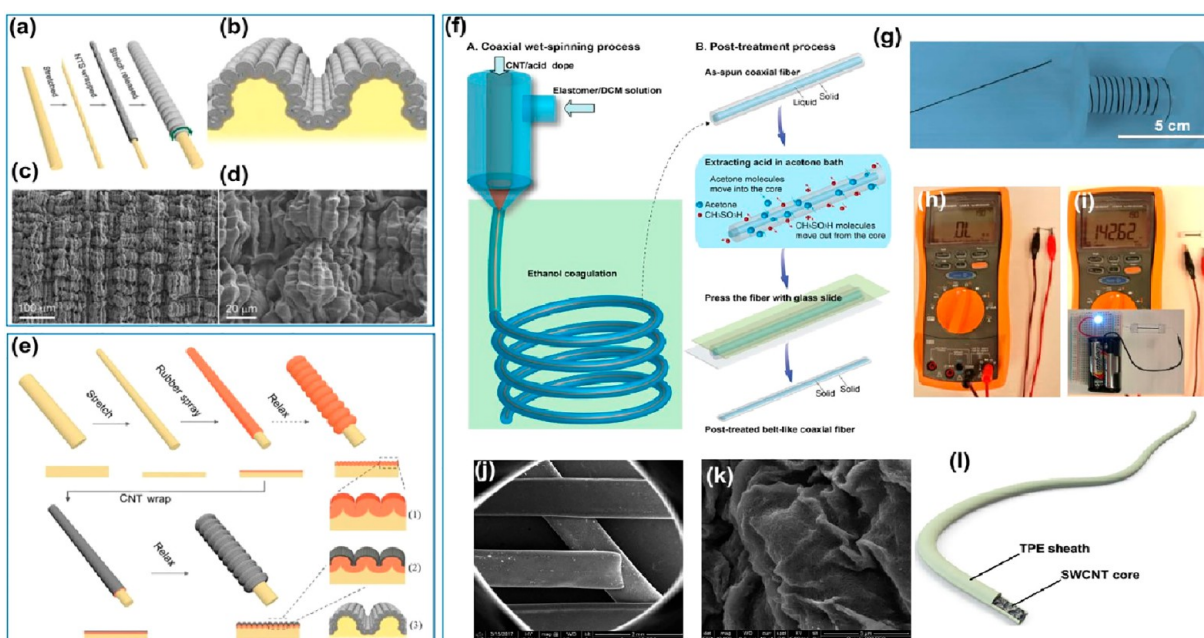


Figure 9. CNT-based coaxial fibers. (a–d) Steps in the fabrication of hierarchically buckled sheath–core fibers. SEM images show buckles for a sheath–core fiber at 100% applied strain. Reprinted with permission from ref 45. Copyright 2015 American Association for the Advancement of Science. (e) Fabrication of a bisheath–core fiber at different steps. Reprinted with permission from ref 85. Copyright 2017 John Wiley and Sons. (f–l) Coaxial thermoplastic elastomer-wrapped CNT fibers. (f) Schematic of the wet spinning and post-treatment process for the fibers. (g) After the post-treatment process, a single coaxial fiber was collected on a winding spool. (h,i) Initial electrical measurements were taken on the surface and in the core of the coaxial fiber. The inset in (i) shows an LED light by a coaxial fiber at 3 V. (j) SEM image of the coaxial fiber shows a belt structure and the cross section image of the fiber. (k) The SEM image shows randomly oriented networks of the SWCNT core after CH_2Cl_2 washed out the TPE sheath. (l) Schematic showing the coaxial structure of the fiber. Reprinted with permission from ref 64. Copyright 2018 John Wiley and Sons.

Liquid Metal-Based Coaxial Fiber. Liquid metals, as mentioned earlier, are intrinsically stretchable conductors that store mechanical energy. Liquid metals can theoretically be stretched with unlimited strain because of the nature of the liquid phase. The only limitation is the stretchability of the material it encapsulates. Therefore, reliable elastomer materials encasing or carrying liquid metals are crucial to this type of stretchable 1D conductor.

Liquid metal-based ultrastretchable coaxial fibers were fabricated by injecting liquid eutectic gallium–indium (EGaIn) into the hollow core of poly[styrene-*b*-(ethylene-*co*-butylene)-*b*-styrene] (SEBS) elastic fibers, which were prepared by melt spinning (Figure 8a,b).³³ The elastomeric sheaths are flexible insulating materials that support and maintain the liquid metal's high conductivity under high strain (over 700% depending on fiber diameter). In addition, deformation of these coaxial fibers by touching or squeezing

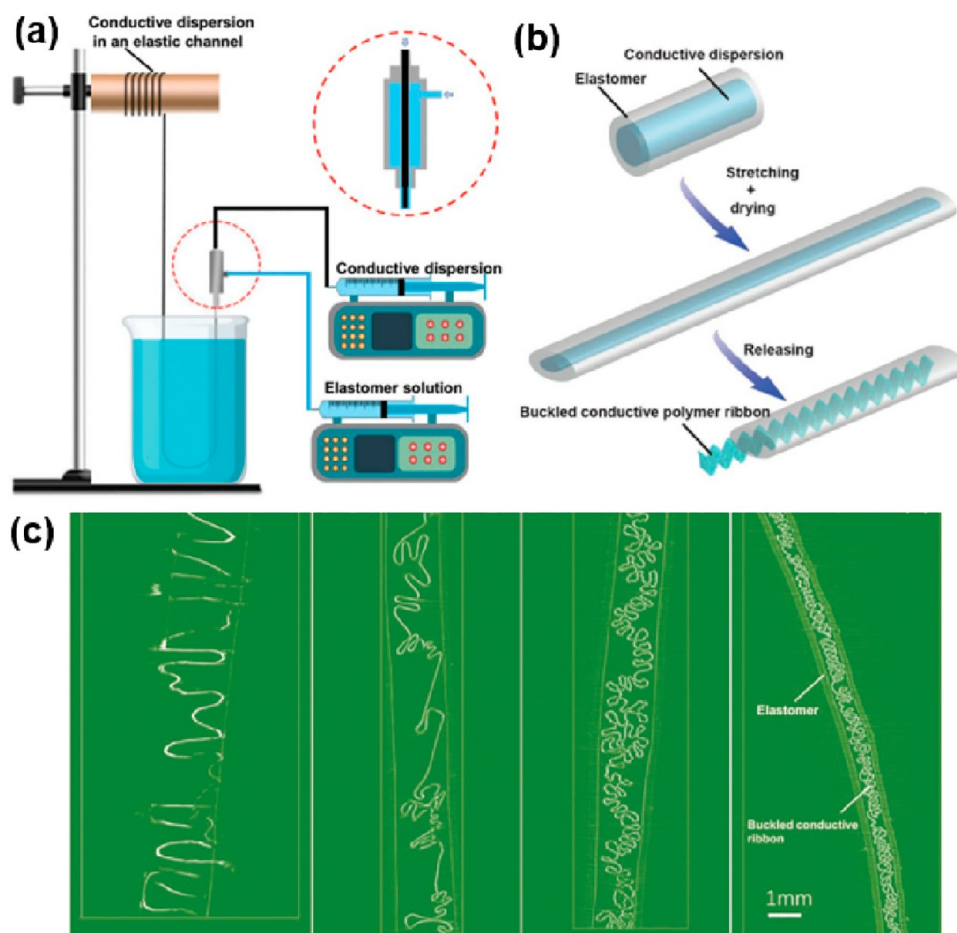


Figure 10. Conductive polymer-based coaxial fibers. (a) Schematic illustration presenting the coaxial wet spinning for encapsulating the conductive dispersion in a TPE channel. (b) Schematic showing how the prestrain-buckling strategy was able to achieve a folded ribbon structure in a TPE channel. (c) CT images of the buckled ribbons in the TPE channel with different prestrains (from left to right: 100%, 300%, 500%, and 700%). Reprinted with permission from ref 94. Copyright 2020 John Wiley and Sons.

can produce a piezoresistive signal. Yan et al. demonstrated a coextrusion method to produce liquid metal-based coaxial cables by applying a facile coaxial printing of the core and shell materials (Figure 8c–e).⁸² The core material is the EGaln alloy with 75.5% Ga and 24.5% In while the sheath material is a temperature- or UV-curable elastomer. This coaxial cable demonstrates well-posed performance under stretching for more than 350% with maintained metallic conductivity. Under compression, the coaxial cable also restores its original properties because of the high flowability of the liquid metal and the elasticity of the elastomeric shell. Zhang et al. presented the fabrication of stretchable coaxial fibers by spinning elastomeric filaments combined with a liquid metal coating.¹⁸⁶ The metallic conductivity of the fibers can be maintained at nearly 800% strain, which makes these fibers candidates for ultrastretchable conductors. The dimension and 2D configuration of the fibers can be manipulated by using the coaxial printing process. Although the combination of direct writing and dip-coating processes provides more freedom to fabricate interconnects that accommodate complex conditions, the potential exposure of liquid metal to air brings significant safety concerns in handling the coaxial fiber. In addition, thermal drawing is an inherently scalable manufacturing technique, which can be exploited in producing a wide range of functional fibers, despite its initial development for optical fibers. This technique successfully fabricates ultrastretchable

hollow fibers, which encapsulate liquid metal for superelastic and conductive coaxial fibers.^{113,114,187} This fabrication approach provides a promising way to achieve scalable fabrication of triboelectric nanogenerators (TENGs) fibers and textiles, thereby leaving more space to explore high-dimensional device integration.

CNT-Based Coaxial Fiber. Pure CNT fibers have been developed toward high-performance multifunctional fibers for a decade. CNT fibers can be produced by a solid-state process, in which CNTs are directly spun into a fiber from the reaction zone or drawn from the CNT forest.^{106,115–117} CNT fibers were initially produced by wet spinning CNTs dispersed in a liquid, which were extruded through a spinneret and then coagulated by extracting the dispersant.¹¹⁸ Behabtu et al. dispersed bulk-grown CNTs in chlorosulfonic acid to form a liquid crystalline phase, which allowed high-throughput wet spinning into CNTs fibers with perfect alignment. These CNT fibers combine the advantages of carbon nanomaterial (high specific strength, stiffness, and thermal conductivity) and metal materials (high specific electrical conductivity).⁷⁴ However, these pure CNT fibers are brittle and, thus, cannot be stretched.

A supporting substrate in the form of elastic filament is needed to introduce stretchability to these highly conductive and high-strength CNT fibers. CNT sheets were applied to wrap stretched rubber-fiber cores to form highly stretchable

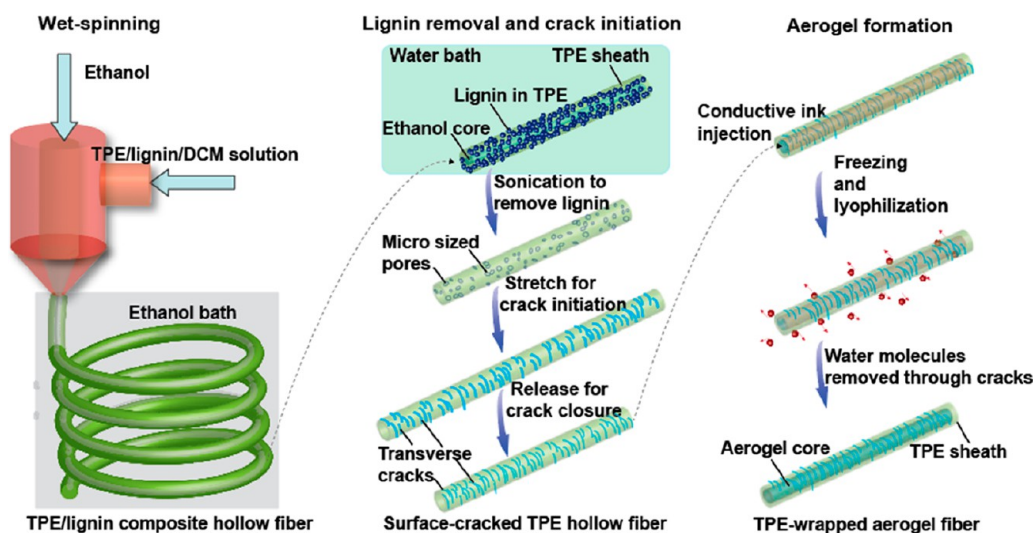


Figure 11. A proposed approach to construct conductive and stretchable aerogel fibers, including wet spinning of hollow fibers, lignin removal, crack initiation, and aerogel formation.

(up to 1320%) coaxial conducting fibers while maintaining electrical conductivity (Figure 9a).⁴⁵ The resulting coaxial fibers exhibited short- and long-period buckling in the sheath that occurred reversibly during the cyclic loading in the axial and belt directions, which resulted in a less than 5% relative change in resistance at 1000% strain (Figure 9b–d). In another study, a bisheath buckled structure was realized by inserting an additional buckled rubber layer between the rubber fiber and the CNT layer. This design made the relative change in resistance dependent on the degree of strain (Figure 9e).⁶³ The bisheath fiber can be reversibly stretched to 600%, thereby undergoing a linear resistance increase. This is because releasing the strain from the stretched state increases contact of the rubber interlayer by forming buckles, thus decreasing the resistance. In the studies mentioned above, the stretchability of CNT fibers is introduced by a prestrain postbuckling strategy. The relative change in resistance is strain-dependent when a buckled rubber layer between the rubber fiber and the CNT layer is inserted, but independent of strain when there is no additional buckled layer. Thus, the coaxial structure allows the design of both resistance-stable and piezoresistive fibers. However, several challenges still exist: (1) electrical conductivity is low (3.6 S/cm) because CNTs are aligned perpendicular to the fiber axial; (2) the critical prestrain-then-buckling strategy is a batch, not a continuous, process, and the fiber length is limited by the maximum width of the CNT sheets; and (3) the conductive CNT is on the fiber surface, thus prone to conductivity degradation with time or mechanical damage. Furthermore, there is a safety concern in wearable electronics if the CNT layer is not protected from skin contact.

Zhou et al. coaxially wet-spun thermoplastic elastomer and SWCNT/methanesulfonic acid dope as respective sheath and core to produce stretchable CNT-based fibers continuously (Figure 9f,g).^{64,146} The acetone post-treatment removes residual acid while simultaneously densifying the SWCNT core through pressing, which leads to a belt shape of cross-sectional coaxial fiber (Figure 9j–l). These coaxial fibers behave as an insulator when measured on their surface because of the insulating thermoplastic elastomer (TPE) sheath. When the 2 cm long sample was electrically connected through its

core, the fiber showed a low resistance of 142.6 Ω , which corresponds to the electrical conductivity of 6.5 S cm^{-1} to electrically connect a battery for powering an LED at 3 V (Figure 9h,i). This wet spinning and post-treatment process is simple and applicable to different conductive materials that cannot be wet-spun using previously reported methods. The electrically insulating and highly stretchable TPE sheath has enabled these stretchable CNT-based fibers to be used as safe stretchable interconnects.

In summary, the coaxial fiber structures were successfully fabricated using CNT assemblies as the core or sheath materials.^{50,63,120} For coaxial structure, high stretchability can be realized using an elastic filament to support the CNT assemblies. Although CNT-based coaxial fibers maintain the continuity of the CNTs in the fiber, the conductivity of the fiber is still very low. Furthermore, the methods to produce coaxial fibers require multiple steps, and sometimes the fiber length and, therefore, widespread appeal for constructing stretchable 1D conductors are limited by the CNT sheets.

Conductive Polymer-Based Coaxial Fiber. The continuous coaxial spinning process has provided a way to construct buckled conductive polymer ribbons inside thermoplastic elastomer channels. In this case, the thermoplastic elastomer solidifies rapidly in the coagulation bath, while the conductive polymer inside remains liquid⁹⁴ (Figure 10a). Then, the as-spun fiber is stretched with the core still in the liquid phase (Figure 10b). After release of the dried fiber (both elastomer sheath and inner core), a buckled conductive wire inside an elastic sheath can be formed. The buckled core in the axial direction was revealed by X-ray tomography (Figure 10c). By stretching the coaxial fibers, the resistance of the fiber remains very stable, with less than 4% variation under 680% applied strain.

The incorporation of 70 wt % polyethylene-*b*-poly(ethylene glycol) (PBP) in PEDOT/PSS/PBP composite allows the fiber to be easily stretched while maintaining a high conductivity; however, its Young's modulus decreases, and the core buckles at low-stress levels. A high loading of PBP replaces PEDOT/PSS, thereby reducing the material cost and making it an economically viable alternative. The elongation at break of the coaxial fibers can be manipulated by changing the prestrain

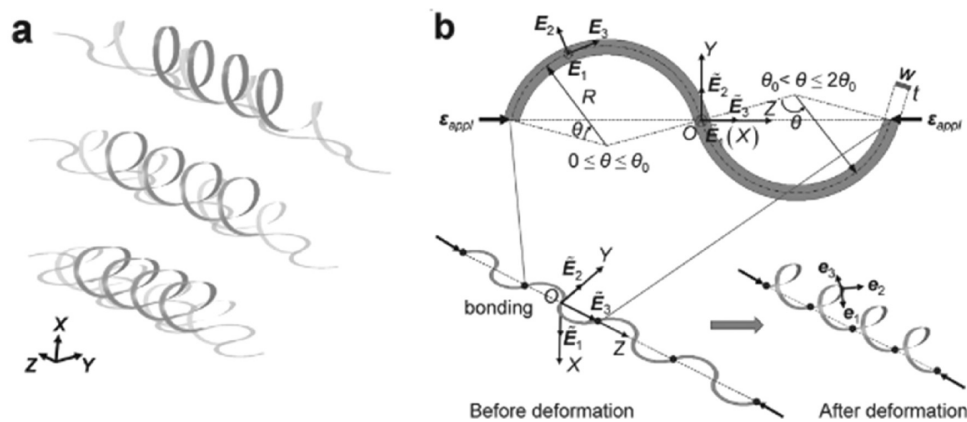


Figure 12. Illustration of 3D helical structures and parameters related to the mechanics model. (a) Schematic drawing of helical structures. (b) Illustration of the mechanics model in a Cartesian coordinate system. Reprinted with permission from ref 199. Copyright 2016 John Wiley and Sons.

applied to the fibers during the prestretching. These conductive coaxial fibers can be incorporated into various applications, including electrical interconnects and wearable heaters, that require large stretchability and stable electrical resistance.

Conductive Aerogel Fiber. Aerogels generally refer to highly porous materials with 3D structures that comprise more than 99% air, are supported by either a cellular or fibrous network, and exhibit many excellent features, like lightweight, high surface area, and superior thermal insulation performance.^{155,188–190} Conductive aerogel fibers, which combine the merits of aerogels and fibers, have aroused growing interest in the field of smart textiles and flexible electronic devices. Compared with bulk aerogels, aerogel-based fibers demonstrate high flexibility and weavability. Currently, aerogel fibers have been successfully fabricated from various materials, such as Kevlar,¹⁹¹ silica,¹⁹² graphenes,^{193,194} carbon nanotubes,¹⁹⁵ Mxene,¹⁹⁶ conductive polymers,¹⁹⁷ etc. Different from bulky aerogels based on a static sol–gel transition (SST) method, the preparation of aerogel fibers must ensure a continuous and stable gel fiber by a fast dynamic sol–gel transition (DST) method that obeys the following two rules: (i) the spinning dope should have a good spinnability, and (ii) the gelation process must be fast to maintain the shape of the fiber.¹⁹⁶

Compressive elasticity in different ranges has been achieved by a variety of aerogels. However, the achievement of reversible high stretchability of aerogels remains a grand challenge because of their brittle interconnections and fragile networks. A prestretch-freeze/lyophilization–release approach was demonstrated to achieve the stretchability of aerogel fibers by encasing the aerogel core with a thermoplastic elastomer (TPE) sheath functioning as a processable and stretchable surface layer to protect the aerogel structure from external forces.¹⁹⁸ First, a porous TPE hollow fiber was prepared by wet spinning TPE/lignin/DMAc dope into ethanol and followed by removing lignin in water. The hollow fiber was stretched and injected with conductive dispersions, then lyophilized to remove water from the core. Finally, the prestrain applied to the fiber was released, which led to highly stretchable and conductive TPE-wrapped aerogel fibers (Figure 11). The buckled structures of the aerogel core and the elastic nature of the TPE sheath collectively facilitated superb stretchability of up to 500% of the coaxial fiber with reversible stretching elasticity. These coaxial aerogel fibers could be evaluated as

high-performance thermal insulators and they have the potential to be used as deformable and wearable materials.

Twisted Conductive Yarns. The helical structure is commonly used in fabric-based wearable systems because it has a small binding force to the human skin and can effectively release the concentrated strain caused by body movement.²⁰⁰ As the stress is loaded, the helix acts like a spring that continuously releases the strain.²⁰¹ Therefore, when the helical electrode is embedded in the stretchable yarn, the desired elongation is achieved with a slight fluctuation in resistance. A theoretical model has been established to reveal the geometry-elastic and geometry-buckling relationships of the helical structure. Figure 12 shows the unit cell consists of two identical arcs with the thickness, t , and the width, w . Each arc has a radius, R , and a top angle, θ_0 (typically $0 < \theta_0 < 5\pi/4$). The whole strain energy in this serpentine unit cell primarily includes in-plane and out-of-plane bending energy, as well as twisting energy, which can be expressed in eq 12:¹⁹⁹

$$\begin{aligned} \Pi_{\text{total}} = & EI_1 \int_0^{\theta_0 R} \left(\hat{\kappa}_1 - \frac{1}{R} \right)^2 dS + EI_2 \int_0^{\theta_0 R} \hat{\kappa}_2^2 dS \\ & + GI_p \int_0^{\theta_0 R} \hat{\kappa}_3^2 dS \end{aligned} \quad (12)$$

where EI_1 , EI_2 , GI_p are the stiffness of in-plane bending, out-of-plane bending, and twisting, respectively; ν is the Poisson ratio; S is the arc length; and $\hat{\kappa}_1$, $\hat{\kappa}_2$, and $\hat{\kappa}_3$ are the curvatures of in-plane bending, out-of-plane bending, and twisting, respectively, among which the curvature of in-plane bending should be much smaller than the counterpart of out-of-plane bending and twisting for ultrathin serpentine structures. Two different strains mainly determine these curvatures: one is the displacement (U_1), and the other is the twisting (ϕ), as shown in eqs 13 and 14.

$$\hat{\kappa}_2 = U_1'' - \frac{R\phi - U_1}{R^2} \quad (13)$$

$$\hat{\kappa}_3 = \phi' \quad (14)$$

The solutions for displacement and twisting are shown in eqs 13 and 14, respectively, using the minimum energy approach.

$$\phi = (1.72 - 0.29\theta_0)\theta \sqrt{\varepsilon_{\text{appl}}} \quad (15)$$

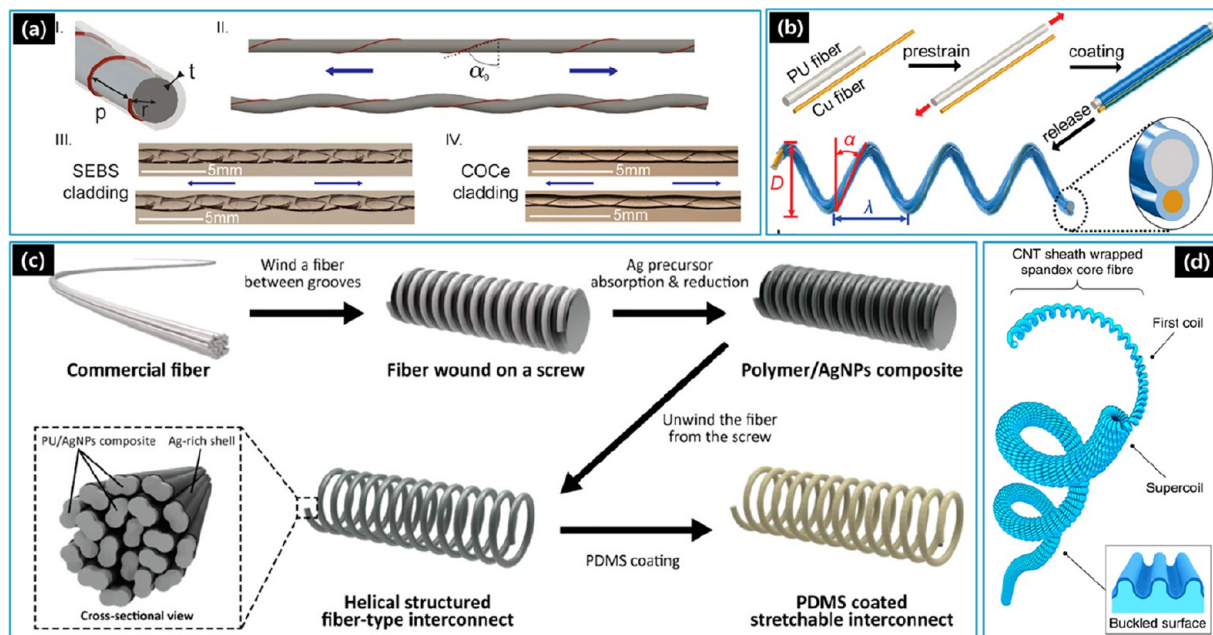


Figure 13. 3D helical fibers. (a) Geometric parameters of the helical structures and fibers with a helical auxetic yarn. Reprinted with permission from ref 100. Copyright 2022 John Wiley and Sons. (b) The preparation of the helical PU/Cu fiber with an illustration shows the inner structure. Reprinted with permission from ref 202. Copyright 2020 John Wiley and Sons. (c) Schematic drawing demonstrating the fabrication of the PDMS-coated helical fiber. Reprinted with permission from ref 97. Copyright 2020 John Wiley and Sons. (d) Schematic illustration of the supercoiled CNT-sheath-wrapped Spandex core fibers. Reprinted with permission under a Creative Commons CC BY License from ref 96. Copyright 2019 The Authors.

$$U_1 = R\theta_0(1.23 - 0.14\theta_0)\sin\left(\frac{\pi\theta}{2\theta_0}\right)\left(2 - \frac{\theta}{\theta_0}\right)^2\left(\frac{\theta}{\theta_0}\right)^2\sqrt{\varepsilon_{\text{appl}}} \quad (16)$$

These two formulas tell us the distribution of displacement and twisting along this arc when there is an applied strain. The insertion of eqs 15 and 16 into eqs 13 and 14 can resolve the out-of-plan bending curvature and twisting curvature, and thus, the mode ratio, ρ , (bending domination to twisting domination) can be obtained, accordingly, as shown in eq 17.

$$\rho = \frac{\int_0^{\theta_0 R} |\hat{\kappa}_2| dS}{\int_0^{\theta_0 R} |\hat{\kappa}_3| dS} \quad (17)$$

where $|\hat{\kappa}_2|$ and $|\hat{\kappa}_3|$ are the average curvatures of bending and twisting, respectively.

Apart from the mode ratio, the maximum strain in the helix can also be determined by eq 18, shown below,¹⁹⁹

$$\varepsilon_{\text{max}} = F_2(\theta_0)\frac{t}{R}\sqrt{\varepsilon_{\text{appl}}} \quad (18)$$

where $F_2(\theta_0)$ is a function of θ_0 . The equation suggests that the maximum strain of the helix is subject to the applied strain $\varepsilon_{\text{appl}}$, the arc angle θ_0 , and the normalized thickness t/R .¹⁹⁹

It is interesting to note that the 3D helical structures indicate negligible roles of material parameters, such as modulus and Poisson's ratio, and cross-sectional geometric parameters, with predominant roles of applied strain $\varepsilon_{\text{appl}}$ and arc angle θ_0 for the distribution and type of the strain.

Experimental and analytical methods also elucidated how the helical structures affect the fiber's elasticity and Young's modulus. Marion et al. gained an insight into this by presenting a helical auxetic yarn (HAY) model that probed how the

geometric parameters influenced the mechanical properties.¹⁰⁰ The fiber could be considered a helix wrapped around an elastomeric core (Figure 13a). It was found that the initial wrapping angle α_0 is a key geometric parameter in the helix and it could be defined by eq 13:¹⁰⁰

$$\alpha_0 = \tan^{-1}\left(\frac{p}{2\pi r}\right) \quad (19)$$

where p is pitch, and r is the initial radius of the helix. Furthermore, for the same helical wire, two types of elastomers, SEBS and CoCe, were used to investigate the effects of α_0 on the tensile properties of the fiber. Linear regression in Figure 13a gave:¹⁰⁰

$$E_{\text{fiber}} = 57\,400 \times \tan(\alpha_0) \times \frac{A_{\text{wire}}}{A_{\text{fiber}}} + 48.7 \text{ MPa} \quad (20)$$

where A_{wire} and A_{fiber} are the cross-sectional areas of the helical wire and the whole fiber, respectively. The intrinsic Young's modulus of the elastomer is up to 48.7 MPa, which shows that α_0 and the cladding material, together, dictate the mechanical properties of the stretchable fiber-embedded helical electrodes.

A polydimethylsiloxane (PDMS)-coated multifilament polyurethane (PU)-based helical conductive fiber was developed by Woo et al. The fiber benefitted from the helical structures and exhibited outstanding resistance stability and mechanical durability even after experiencing 10 000 stretching cycles of 100% strain and 1000 cycles of vertical loadings, respectively (Figure 13c).⁹⁷ Similarly, highly stretchable and electrically conductive fibers in a 3D helical shape were obtained by relaxing the stress of prestretched elastic PU and conductive copper wires. The electrical performance of this fiber showed a minor resistance change $\approx 0.07\%$ at 200% deformation strain (Figure 13b).²⁰² Fibers with supercoil structures were prepared

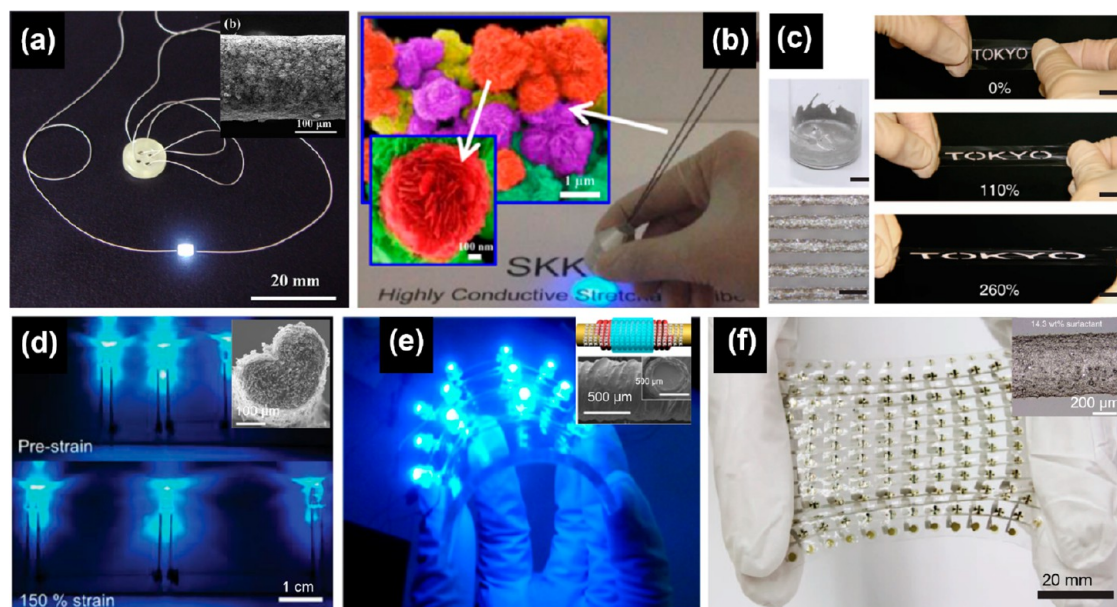


Figure 14. Stretchable Ag-based composite fibers for electrical interconnects. (a) AgNP/elastomer composite fiber prepared by injection forming. The fiber connected to an LED can be stretched to 14% strain. Reprinted with permission from ref 203. Copyright 2011 AIP Publishing. (b) The LED is connected to two conductive ropes made from Ag nanoflower/PU composite fibers. Ag nanoflower images are shown as false-colored inset images. Reprinted with permission from ref 79. Copyright 2015 American Chemical Society. (c) Printed elastic conductor from elastic conductor ink and demonstration of the stretchability. Reprinted with permission under a Creative Commons CC BY License from ref 53. Copyright 2015 The Authors. (d) Images of blue LEDs connected by AgNW/AgNP-based composite fibers at 0% and 150% strains with 0.1 mA current. Reprinted with permission from ref 49. Copyright 2015 John Wiley and Sons. (e) Bendable and stretchable LED arrays using cotton yarn-AgNW/PDMS composite fibers as electrical interconnects in the circuit. The LED arrays were kept operational with no obvious weakening of the light intensity during the cyclic bending test. Reprinted with permission from ref 80. Copyright 2015 American Chemical Society. (f) A stretchable organic thin-film-transistor active matrix using Ag elastic wire as electrical interconnects. The active matrix is stretched to about 60%. Reprinted with permission under a Creative Commons CC BY License from ref 53. Copyright 2015 The Authors.

by inserting a twist into Spandex-core fibers wrapped in a sheath of CNTs. Compared with single helical fibers and other first coil fibers, these supercoil fibers exhibited superior tensile properties, with a resistance increase of only 4.2% at 1000% tensile strain (Figure 13d).⁹⁶

Highly stretchable and conductive interconnects have always been a vital building link for electronic textiles. These results may provide a promising approach for manipulating 3D helical fibers to obtain high-performance, elastic conductors. The fibers can be readily integrated into functional components of complex wearable devices. This strategy offers excellent potential for the application of functional devices, such as stretchable heaters, woven optical antennas, etc.

DEVICE APPLICATIONS

Stretchable electronic devices demand simultaneous developments in stretchable 1D conductor materials and integration with other device-related manufacturing technologies. This section presents some examples of electronic devices based on stretchable 1D conductors ranging from single 1D devices to multiple 1D-level components with a detailed investigation into their electrical stability under different mechanical deformations, such as extension bending and twisting modes. The range of electronic devices based on stretchable 1D conductors includes transistors, antennas, energy converters, energy-storage devices, electric connectors, sensors and actuators, and heaters.²³ Of these, an emphasis on wearable electronics, stretchable interconnects/wirings, deformable and

wearable mechanical sensors, tensile and rotational actuators, and electrical heaters are outlined in this section.

Stretchable Interconnects/Wirings. The development of stretchable electronics has placed stretchability as a requirement on a variety of materials and sections, and interconnects (used to transmit electrical signals between different modules) are no exception. The current electrical interconnects in the market are mainly metallic wires. In the lab, wirelike macroscopic assemblies of CNT can also serve as electrical interconnects.^{32,101} Both types of wires can be flexible when their cross sections are thin enough but they lack stretchability. Among the examples of electrical interconnects made from stretchable 1D composite conductors (Figure 14), a stretchable Ag flake/silicone composite fiber was prepared through injection forming in a high-temperature silicone oil bath to obtain a uniform diameter of ca. 230 μm (Figure 14a).⁷⁵ The fiber exhibits high flexibility and possesses high electrical conductivity ($470 \pm 23 \text{ S cm}^{-1}$). Excellent insulating performance was provided by coating Ag flower-PU composite fibers with insulating PDMS.⁵⁹ Then, an LED was suspended by Ag flower-PU composite ropes with a 1.8 V power supply. The elastic composite fibers enabled selective illumination of the desired area. The LED could return to its original position after the illumination. The fibers maintained brightness during the stretching/relaxation (Figure 14b).⁷⁹ Figure 14c presents the conductive ink made by adding Ag flakes to a fluorine copolymer. It can be readily patterned with conventional printing techniques for highly stretchable wirings logos.³⁸ Lee et al. constructed a simple circuit of three blue-

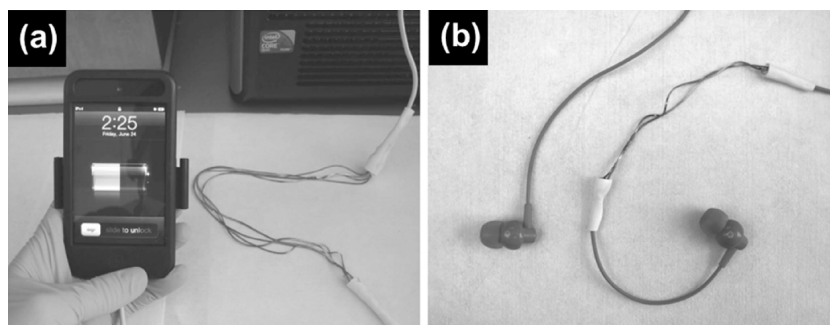


Figure 15. Stretchable liquid metal-based fibers for electrical interconnects. (a) A photograph shows a stretchable charger for an iPod. (b) A photograph shows a stretchable cable for earphones. The fiber in (a) and (b) was made by injection of a liquid metal alloy into a hollow elastic fiber. Reprinted with permission from ref 48. Copyright 2013 John Wiley and Sons.

colored LEDs connected with AgNW–AgNP reinforced composite fibers and visually confirmed the preservation of the electrical property of the fibers under high strain (Figure 14d). All LEDs showed stable illumination when the fibers were stretched to 150% strain.⁴⁹ Cheng et al. demonstrated stretchable electrical interconnects in large-area stretchable electronics by integrating commercial electronic components (LED) onto a transparent and stretchable substrate by taking advantage of stretchable composite fibers.⁸⁰ Figure 14e shows the LED arrays on a stretchable substrate with integrated LED arrays connected by cotton yarn–AgNW–PDMS composite fiber. Lit up at 3 V, the LED arrays shine with stable illumination during cyclic bending and stretching at 30% strain. In another example, Matsuhisa et al. constructed a stretchable organic thin-film-transistor active matrix using the printed Ag elastic wires (Figure 14f). These devices are more mechanically robust than Si and serpentine Au interconnects.³ The transistors are embedded in PDMS where wirings and interconnections are formed by printing elastic conductors. The resulting device is soft and resilient to large deformations up to 60% strain.⁵³

Zhu et al. demonstrated the application of liquid metal-based fibers as electrical interconnects by utilizing the elastomer-encased liquid metal fibers as stretchable wires for a charger and earphones for an iPod.⁴⁸ A portion of an iPod charger line was replaced with stretchable fibers (Figure 15a). The iPod began charging through the stretchable charger and continued charging while the fibers were cyclically stretched and relaxed. Moreover, the presented charger replenished the battery at around the same rate as the commercial one. The stretchable fibers were also used to replace a portion of the wires for the earphones (Figure 15b) and to play music continuously without obvious degradation to volume or sound quality. This is ascribed to the lower resistance per unit length of the stretchable fibers than commercial wires, which showed no degradation in performance because the liquid metal can maintain its metallic conductivity when stretched. Zhang et al. used liquid metal-coated elastomer fibers to bridge rigid LEDs. No apparent change in LED light intensity was observed when the circuit was stretched to 85% and 210%, which indicated the minimal resistance change under tensile strain.¹⁸⁶

Deformable and Wearable Mechanical Sensors. Stretchable 1D conductors are not only crucial components of electrical interconnects but also important building blocks for deformable mechanical sensors. Conventional gauges made from metallic foils or semiconductors for strain detection can only tolerate small deformations of less than 5%^{204–206} and are

easily destroyed when removed from target samples. Piezoresistive stretchable 1D conductors are promising candidates for future deformable mechanical sensors. They can be adapted to deformable or expandable surfaces or integrated with wearable textiles.^{23,45,48,72,172,207–209}

This section focuses mainly on the advances in strain sensors on the basis of stretchable 1D conductors. The key parameters for the performance of strain sensors include sensitivity, stretchability, and linearity. The sensitivity is usually defined by the gauge factor (GF) and expressed by the relative change in resistance ($\Delta R/R_0$) with external strain.^{104,210–212} A high sensitivity of the materials is ensured by the initial resistance, R_0 , which has to be low enough by using highly conductive materials, while the ΔR needs to be enlarged. The stretchability is the ultimate uniaxial tensile strain before the elongation at break, which determines the sensing strain range.²⁰⁵ The linearity determines how constant the GF is over the strain range. High linearity and a single linear region across the entire measurement range make the calibration process more accessible and ensure accurate measurements throughout applied strain ranges.^{63,64,104,213} Recently, stretchable 1D conductors have been developed toward high stretchability and sensitivity to be used in applications like deformable or expandable surfaces, e-skins, and health monitoring systems.^{23,212,214–217} These piezoresistive 1D conductors are generally in the form of composites or coaxial fibers. Upon stretching, the $\Delta R/R_0$ increases dramatically because of the disconnection of the conductive networks.

Wet spinning has been well established to produce continuous polymer fibers for decades. It is also a robust route using a single, coaxial, or multinozzle system to engineer conductive fibers for strain sensors.^{23,52,64,72,90,143,218} Previously, an AgNP/TPE mixture was wet-spun to create fiber-based strain sensors, but it was hard to maintain continuous conductive paths and a homogeneous distribution of the AgNP fillers.⁴⁹ A conductive polymer/TPE composite fiber was also fabricated by wet spinning for stretchable sensors, but it was challenging to maintain both stretchability and sensitivity.^{159,160} PEDOT/PSS polymer fibers fabricated via hot-drawing-assisted wet spinning were also demonstrated as strain sensors. However, the maximum stretchability was limited to 20%, and the GF was only 1.8 at 13% strain because of the brittle nature of PEDOT/PSS.⁹⁰ We can see that developing a strain sensor with high sensitivity, stretchability, and linearity has been challenging for years. Sensitivity and stretchability, especially, are two seemingly contradictory targets to be achieved simultaneously.

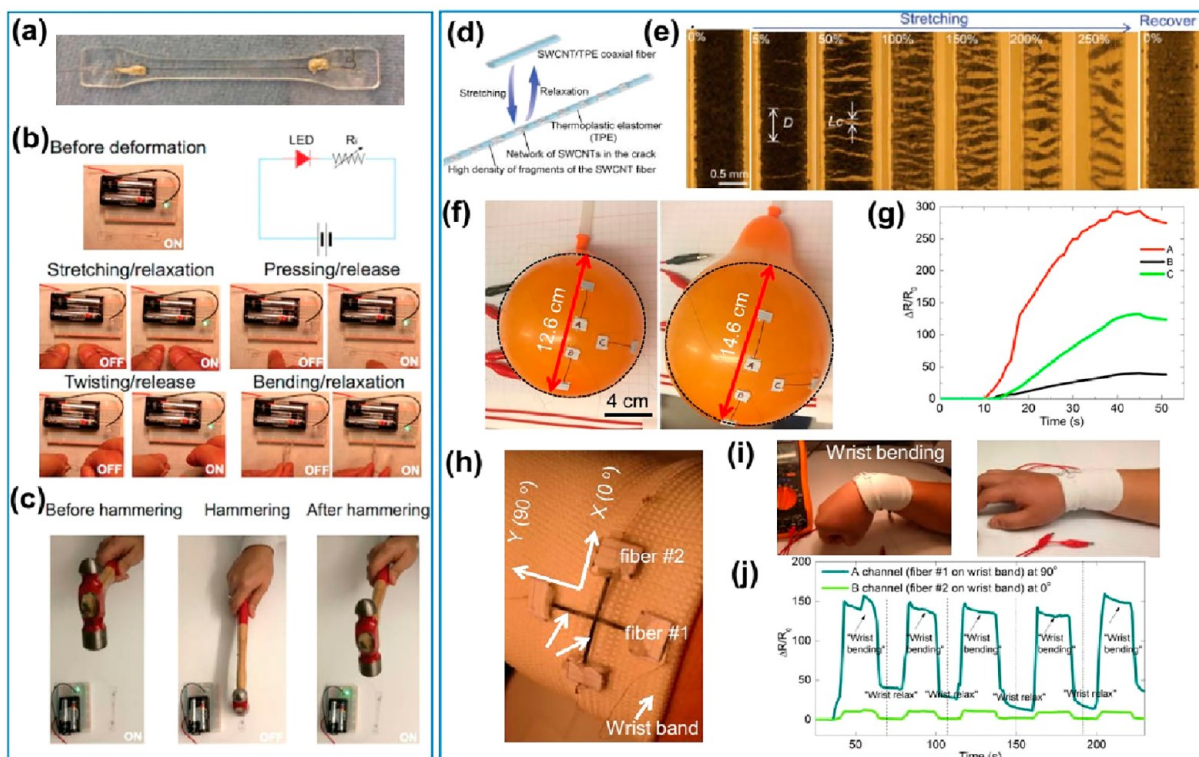


Figure 16. Elastomer-encased CNT wires for deformable mechanical sensors. (a–c) The CNT wire/PDMS mechanical sensor responds to large mechanical deformations and motion detection applications. (a) An SWCNT wire is embedded in the PDMS substrate. (b) An electrical circuit connected to an LED presents resistance recovery at different mechanical deformations. (c) An electrical circuit connected to an LED showed resistance recovery after the hammering. Reprinted with permission from ref 63. Copyright 2016 The Royal Society of Chemistry. (d) Schematic drawing presenting the fragmentation mechanism of the coaxial fiber. (e) Images of a coaxial fiber when stretched from 0 to 25% strain and relaxation. D and L_c are the average spacing between the cracks and the average crack opening displacement, respectively. (f) A balloon's initial and inflated state with three coaxial fiber sensors. (g) Relative change in resistance of the fibers under continuous balloon inflation. (h) A photograph presents the coaxial fibers attached to a wristband. (i) A photograph shows the bending and relaxation of the wrist. (j) Relative change in resistance during wrist bending and relaxing. Reprinted with permission from ref 64. Copyright 2018 John Wiley and Sons.

Zhou et al. created a mechanical sensor by embedding wet-spun CNT wires in PDMS (Figure 16a).⁶³ Through the application of various mechanical stimuli, the wire becomes fragmented, and its resistance increases drastically from 360 Ω to infinity in a recoverable manner, even after the electrical disconnection. The sensor is sensitive enough to present a GF of 10^5 at 15% uniaxial strain. The sensors' sensing performance and resistance recoverability were demonstrated by wiring an LED with the sensor. The SWCNT wire resistance was low enough to light the LED at 3 V (Figure 16b). The sensor also exhibited resistance recoverability after mechanical deformation, such as stretching, pressing, twisting, and bending, thereby presenting that the light intensity of the LED degrades negligibly from these deformations. Upon extreme impact from a hammer, the LED went out but readily came back instantly when the sample was removed from the hammer (Figure 16c). These results suggest that these sensors are distinguished from conventional sensors, which cannot restore their sensing functions after electrical disconnection. However, the stretchability is limited to 15%, which is insufficient for a human wearable device that needs to accommodate a strain larger than 55%.

A significant deformation of the microstructure is required to obtain high sensitivity (high GF). Minimization of the effect of microstructure defects so that the microstructure integrity is preserved at large deformation achieves high stretchability.

Thus, both characteristics could not be obtained synchronously in the simple design of 1D structures. In a follow-up study, Zhou et al. showed that this paradox could be overcome by the fragmentation of conductive CNT wires with high crack density (17 mm^{-1}) in an elastomer fiber (Figure 16d,e).⁶⁴ The high crack density is key to increasing the stretchability and linearity response of the fibers during deformation. The performance of the fragmented fibers was successfully demonstrated to sense motions during the expansion of a balloon (Figure 16f,g). They can differentiate the strain changes at different locations, which shows that they can be used as strain gauges for detecting strains on expandable structures. Moreover, these coaxial fibers were integrated with textiles as wearable electronics for sensor/human interface interactions, thereby showing that the sensor could detect motions at different locations on the wrist (Figure 16h,f,j). Thus, the fragmented coaxial fibers can be used as deformable and wearable strain sensors.

Tensile and Rotational Actuators. Actuators, also called artificial muscles, change volume/shape or generate force responsive to applied external stimuli,^{13,219} including electrical current, temperature, pH, chemical agent, solvent vapor, relative humidity, etc.,^{50,52,143,145,220} Flexible actuators, which can behave like natural muscles, have been widely used in wearable electronics.^{221,222} However, 1D actuators in the shape of wires, fibers, and yarns are rarely reported. This section

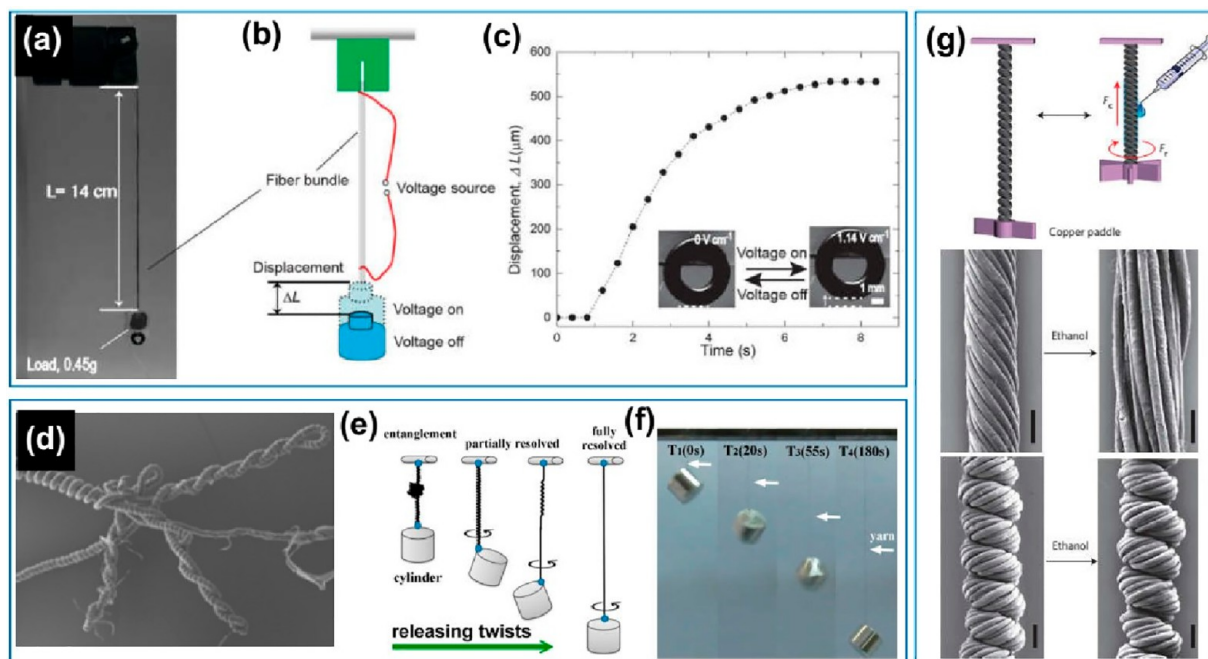


Figure 17. Stretchable conductive polymer fibers and CNT fibers as actuators. (a) Photograph of a 3 mg PEDOT/PSS fiber bundle carrying a 0.45 g load. (b) A setup illustration shows the actuator's motion by turning on and off the voltage. (c) The change of displacement with time at 1.14 V cm^{-1} . Reprinted with permission from ref 52. Copyright 2016 The Royal Society of Chemistry. (d) SEM images show an overtwisted CNT yarn with entanglements. (e) An illustration of the setup shows an entanglement was fixed to a horizontal rod and attached by a metal cylinder. (f) Snapshots of the rotating cylinder were recorded during actuation with white arrows pointing to the CNT yarn. Reprinted with permission from ref 68. Copyright 2013 American Chemical Society. (g) Schematic illustration of contractive and rotary actuators on the basis of a hierarchical helical CNT yarn. Reprinted with permission from ref 50. Copyright 2015 Springer Nature.

shows examples of fiber-based tensile and rotational actuators with different external stimuli.

A conductive polymer (PEDOT/PSS) fiber bundle displayed linear electromechanical motion under an applied external voltage. The actuation performance of a 118 conductive polymer fiber bundle in 14 cm length under isotonic conditions is shown in Figure 17a–c. When the voltage was applied, the 3 mg fiber bundle lifted 150 times (0.45 g) the fiber bundle weight. The fiber bundle actuator took about 6 s to reach a maximum displacement (530 mm) with a first-order response of 2 s (Figure 17c).⁵²

The actuation mechanism in the air is well established for PEDOT/PSS-based actuators. When PEDOT/PSS film or fiber is subjected to a voltage or an electrical current, Joule heating induces water desorption in PSS, which results in volume shrinkage. Actuation in PEDOT/PSS results from an electro–thermal–mechanical multiphysics coupling that responds to various actuation stimuli, including electrical current, temperature, and relative humidity.^{143,145,149,150,223}

Besides linear actuators, Li et al. reported that an overtwisted carbon nanofiber yarn with entanglement could be fully resolved and stretched to extensive tensile strains (Figure 17d). Moreover, the twists can be released under predefined tensile loads to rotate an object for many cycles with a high-output energy density (Figure 17e,f). After entanglement has been fully resolved, one can twist it and use it repeatedly after the entanglement has been fully resolved. These results present a twist-induced yarn structure and its potential use as a rotational actuator.⁶⁸ Chen et al. developed solvent-driven actuators on the basis of CNT fibers (Figure 17g). Their fibers responded to solvent and vapor through the hierarchical and helical structure of aligned CNTs. The primary fibers

containing helical assemblies of MWCNTs were twisted together to form the helical fibers (Figure 7b). Single-ply and hierarchically arranged helical fibers can produce contractive and rotary actuation in response to polar solvents. The solvents and vapors diffuse through the gaps and then transport through the nanoscale gaps, which results in a rapid response and large stroke of the actuating fibers.⁵⁰

An electrical field can also drive rotational actuators with specific designs. Liu et al. demonstrated hierarchically buckled sheath–core CNT fibers for rotational actuators operating reversibly by a tension-to-torsion actuation mechanism.¹⁰⁴ In detail, a rubber core fiber was stretched to 1400% strain during the wrapping of CNT aerogel sheets (denoted as NTS_m@fibers, where “m” represents the number of layers of CNT on the rubber core). Then, to the outer surface, a rubber layer was deposited on an NTS_m@fiber that was not stretched, followed by wrapping the fiber with additional CNT layers when the rubber core was stretched (denoted as NTS_n@rubber@NTS_m@fibers, where “n” represents the number of layers of CNT on the thick rubber coating). A high-stroke rotational actuator was achieved by inserting a twist into the sheath–core NTS_n@rubber@NTS_m@fibers and maintaining a constant fiber length. This actuator operated isobarically so that it provided both tensile and rotational actuation. The maximum electric field applied to the fiber was between 10.3 and 11.7 MV/m. For an NTS₁₀@rubber@NTS₂₀@fiber actuator, the rotational stroke reached a maximum value of $21.8^\circ \text{ cm}^{-1}$ for the 0.9 mm diameter fiber.¹⁰⁴

Wearable Heaters. Electroactive materials capable of converting electrical to thermal energy demonstrate tremendous potential for heating components in wearable textiles.²²⁴

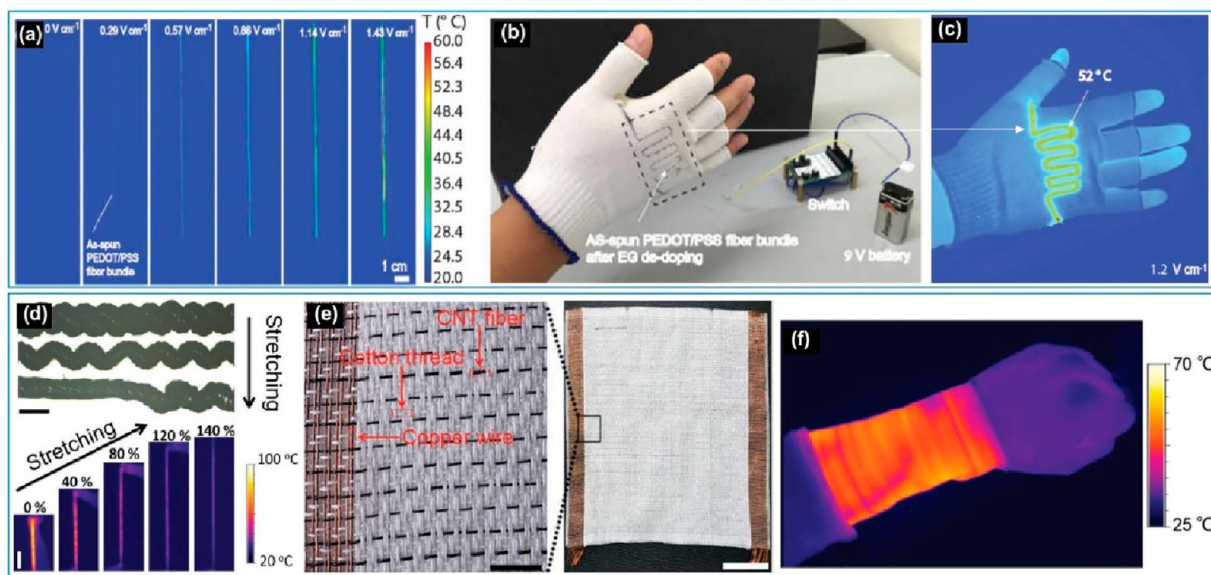


Figure 18. Stretchable conductive polymer fibers and CNT fibers as electrical heaters. (a) The thermal photographs of the PEDOT/PSS fiber bundle at different voltages. (b) A picture of the circuit with a heatable glove. (c) A thermal image shows a temperature distribution of the conductive fiber bundle on a textile glove at 1.2 V cm^{-1} . Reprinted with permission from ref 52. Copyright 2016 The Royal Society of Chemistry. (d) Optical and infrared images of hierarchically and helical CNT yarn during deformation. (e) Photograph of the heating textile using stretchable CNT yarns. (f) Infrared image of the heating textile wrapped on the wrist. Reprinted with permission from ref 95. Copyright 2018 John Wiley and Sons.

They are helpful for wearable applications, such as thermal therapy, when affixed to the human body.

Among electroactive materials, PEDOT/PSS conductive polymer fibers are very promising for these applications because of their tunable electrical conductivity. They can be easily used as low-voltage driven heaters. Zhou et al. demonstrated the fast electrothermal heating process of PEDOT/PSS conductive fibers made through a hot-drawing-assisted wet spinning and solvent post-treatment.^{52,90,218} The first-order response time of a 2 cm long single PEDOT/PSS fiber (3136.6 S cm^{-1}) was 1.2 s by applying 7 V cm^{-1} for 25 s. The heating rate was estimated to be $63.1 \text{ }^\circ\text{C s}^{-1}$, which is a faster response rate than other heaters.⁵² Figure 18a shows the temperature of a fiber bundle increased with voltages, which indicates the Joule heating effect of the conductive polymer fibers. Figure 18b,c demonstrates the use of PEDOT/PSS fiber bundles as a wearable heater. A heating glove was fabricated by knitting a PEDOT/PSS fiber bundle onto the textile glove. These conducting fibers show excellent stretchability (16 to 21%), compared with metallic wires or CNT fibers (1 to 8%), to avoid damage from knitting or repetitive tensile and bending strains. The steady-state thermal image at 1.2 V cm^{-1} shows a temperature map of the PEDOT/PSS fiber bundle, with a predominately homogeneous temperature distribution of the coiled fiber bundle. Moreover, the fiber bundle produces heat along the conductive paths where the bundle extends and into the spaces between adjacent areas.⁵²

By designing a hierarchically helical structure, both Liu et al. and Chen et al. created a CNT fiber with good mechanical and thermal behaviors in their works.^{14,50} This structure allowed the aligned CNT fibers to present high stretchability without reducing the electrical conductivity and extended the distinguished performances of CNT that were crucial for heaters to the microfiber. Moreover, these fibers also present toughness, softness, fast thermal response, and low-operation voltage. At a steady voltage, the temperatures of the helical

fiber dropped by $35 \text{ }^\circ\text{C}$ within 40% strain and only $15 \text{ }^\circ\text{C}$ within the rest strain up to 140% (Figure 18d). These CNT fibers can be woven with copper wires and cotton threads into textiles for wearable heaters (Figure 18e). The heating textiles exhibit stable performance under distortion, which makes them practical for wearable uses, such as wound healing and drug delivery when attached to a wrist (Figure 18f).¹⁴

Large-Area Multifunctional Smart Display System.

Smart textiles, which consist of versatile electronic devices on the basis of fiber substrates, have led to breakthroughs in material and process developments.^{227–230} Unlike flexible electronics in which digital devices are printed or deposited on flexible substrates, fiber or textile electronics exhibit far fewer constraints in terms of the size of fabrication methods and flexibility because of fiber structures and weaving processes. Therefore, it provides more degree of freedom for structural design. With the development of textile technology, the system architecture of fabric integrated with electronic devices will no longer be an illusion. Textiles with multiple functions are emerging, and forward-looking functions are being explored.

This promise to revolutionize the way we interact with electronic devices is one of the goals of wearable technology. Despite the great strides in smart textiles for display/lighting applications, scalable approaches for integrating multifunctional smart display systems are rarely reported. Large-scale systematic integration of discrete fiber devices into textiles will face serious challenges, including (i) structural design and compatibility between fibers and digital devices, (ii) non-destructive weaving patterns, (iii) applications in textiles platform interconnection methods, and (iv) real-time signal processing/coding.²²⁶

For instance, Shi et al. have prepared a long and wide display that contains 5×10^5 electroluminescent units by weaving conductive and luminescent fibers with cotton yarns to form luminescent units in a textile, thereby demonstrating touch

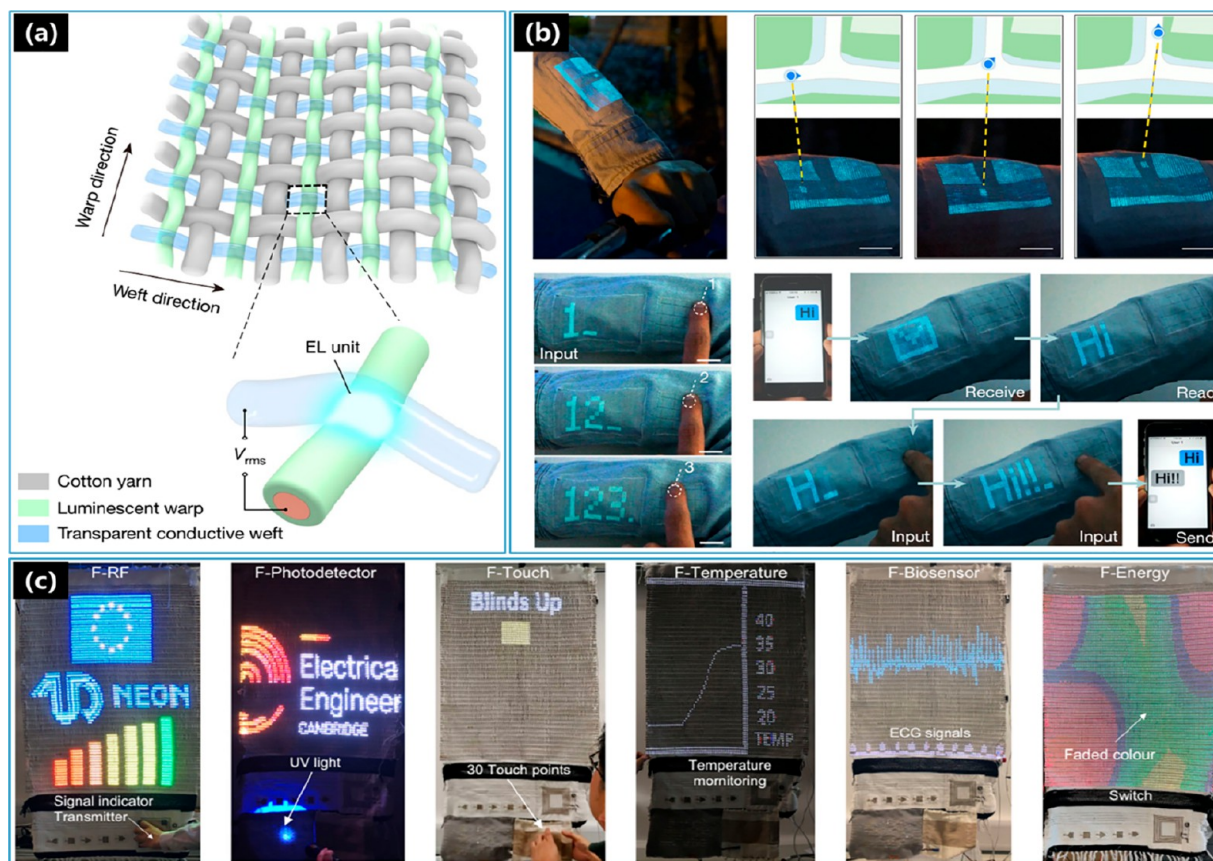


Figure 19. Structure and application of stretchable fiber-based display textiles. (a) Schematic drawing of the woven textile display. The electroluminescent unit is formed by contacting luminescent warp and transparent conductive weft. (b) The real-time patterns are displayed on a sleeve and synchronized with the location map on a smartphone. Reprinted with permission from ref 225. Copyright 2021 Springer Nature. (c) List of real-time operation photos of devices integrated into the smart textile. Reprinted with permission under a Creative Commons CC BY License from ref 226. Copyright 2022 The Authors.

sensing and biosignal detection capabilities (Figure 19a,b).²²⁵ The intensity for a vast proportion of units can maintain stability after 1000 cycles of stretching. This method is simple and can readily form multifunctional integrated smart textiles for various applications. Choi et al. demonstrated the smart textile display system by coupling multifunctional fiber devices.²²⁶ The one-fiber LED output and six input devices are compatible with both symmetric and asymmetric weaving patterns and have been integrated into a single smart textile display system. These design prototypes exhibit tremendous prospects for realizing applications in healthcare, smart home furniture, electronic communications, etc.

CHALLENGES AND OUTLOOK

Despite the encouraging advances in 1D conductors and their applications, stretchable 1D conductors or device prototypes are still in the early stages of growth and development. Scientific, engineering, and safety challenges must be overcome before they can be mass-produced and fully integrated into actual devices. It is a necessity to present the current challenges and explore directions for stretchable 1D conductors. This demands metal-level conductivity, structural or functional consistency under large deformation, durability over time, integration with textile technology, comfort, scalability, safety, and cost-effectivity.

Safety. Safety, among all aspects, is the priority to be considered in the practical application of the 1D stretchable

conductors. Many conductive materials bring safety concerns over their preparation process or when they come into contact with a human. For example, the handling of a strong acid like chlorosulfonic acid, which has been used to disperse CNTs (2 to 6 wt %) to achieve spinnable liquid crystal dope, brings enormous risks to personnel and the environment.^{231,232} Although, CNT fibers or yarns demonstrate high strength and good electrical conductivity, there is always concern about the risk of cancer through exposure and inhalation.⁴⁵ As a result, it is preferred to encapsulate CNT-based products for their use near the human body. Gallium-based liquid metals, with a lower vapor pressure at room temperature, have become materials of interest for fabricating stretchable 1D conductors and are now encased in elastic channels to replace liquid mercury. Their ability to store mechanical energy gives them the advantage of stretching without losing high conductivity. Although gallium-based liquid metals were suggested to have low toxicity, leakage of the liquid metal during the encasing process still poses risks, and their impact on the human body is unclear.^{48,51} Moreover, if the elastomer-encased liquid-metal fiber is stretched beyond its maximum strain, the liquid-metal splash can quickly contact or even enter the human body.¹⁵ Therefore, stretchable 1D conductors should be fabricated from safe and highly biocompatible materials, and when materials in question have no alternative, effective encapsulation strategies should be employed to ensure safe handling and nontoxic exposure.

High Conductivity and Stretchability. The electrical conductivity of current stretchable 1D conductors is more than 1 order of magnitude lower than that of commercially available copper wires. Each strategy to achieve stretchability is limited to specific material or structure, and no universal strategy currently exists. Furthermore, only structural engineering strategies can introduce stretchability to a 1D conductor, such as CNT fibers and metal wires, because of their intrinsically rigid nature. These limitations impose device fabrication and system integration challenges and have become the focus of electronic system development research.

Prototype Devices. In terms of developments and applications of prototype devices, some of them are still in the very early stages, and the involved demonstration (under certain experimental conditions) does not necessarily reflect their practical performance. The use of stretchable 1D conductors for electrical interconnects is not apparent. For example, the conductor's ampacity (current density) is an important criterion but barely reported.¹²⁸ The washability of the conductor is also a practical concern for use in wearable electronics. Although the demonstrated prototypes show good prospects, they are still far below the requirements of large-scale applications.

Large-Scale Production. Scalable, continuous production of stretchable 1D conductors is critical. The top-down approaches, like melt and wet spinning techniques, have seen great success for continuous filaments because of their compatibility with large batch fabrication. However, additional steps are required to introduce stretchability to the materials and sometimes add complexity to the manufacturing process. For instance, the "pre-strain induced buckling" approach presently limited to CNT-based materials can only reach tens of centimeters in length.⁶⁵

Textile Mill Manufacture Compatibility. Many complicated fabrication steps make it difficult to produce on a large scale. For example, a fiber needs to be densified for application, and the CNT core must be fragmented to serve as a high-performance strain sensor.⁶⁴ Presently, it remains impossible to assess if the current lab-scale synthesis and bottom-up assembly methods can achieve the same level of precision and uniformity when scaled up.

Integration and Multifunction. It is still challenging to achieve the monolithic integration of multiple functionalities into a single fiber. The size of the functional materials needs to be scaled down while maintaining their functionalities to increase device density on a single fiber.¹²⁰ Thus, nanomaterials, such as nanoparticles, nanowires, and nanoplates, with ideal rheological properties, can retain their functionalities at lower dimensions and become a good candidate to be integrated into multifunctional and high-performance fibers. It seems almost inevitable that with the emergence of multifunctional fiber conductors with sophisticated nanostructures and fiber architectures, quantities of electronic functionalities will be scaling in capabilities.

Structural Design. The fundamental theory of the formation of nanostructures, as well as the interplay between structures and properties, are still poorly understood. Mechanical models and theoretical simulations are strongly desirable to guide the structural design of fibers, which would enhance comprehensive performances, unveil numerous applications, and enable the practical implementation of fiber conductors.

Environmental Stability and Mechanical Durability. To date, the electrical properties of most stretchable 1D conductors deteriorate with repetitive stretching and release cycles. The long period of chemical and physical stability, or conductivity stability, of conductive surfaces needs further investigation before practical use. For materials and/or devices used on the human body or in the natural environment, ambient (humidity, solar radiation, and atmosphere)-stable materials are preferred. In addition, encapsulation strategies need to be developed to protect unstable materials or parts. Moreover, reliable electric interconnects among each conductive element must be established to ensure that the entire system is robust. For hydrogel-based fibers, loss of water may occur to dramatically decrease their stretchability. In addition, while the electrical conductivity of hydrogel fibers can satisfy applications such as sensors, the low mobility of ions in solution limits the electrical conductivity of fibers. There is also a risk of redox reactions (water electrolysis) when the voltage is greater than 1 V. For example, even a 3 mm diameter LED bulb requires an operating voltage of around 2 V, which is beyond the capabilities of normal hydrogels.

Other Challenges. For wearable materials, stretchable 1D conductors must be integrated with textile materials. Therefore, it should withstand exposure to a cleaning environment and the shear force induced by washing to perform consistently over time. More effort is needed to verify if a protective layer is needed. Attention must also be extended to challenges like durability under extended and repeated use, cost-effectiveness, and integration between 1D stretchable conductors and other required components, including electrical circuits and mechanical sensors.

The development and existing challenges in stretchable 1D conductors also lead us to think about future directions. Material innovation is critical to the design and development of breakthrough technologies to address these challenges. Of course, suitable and safe materials and newly designed manufacturing technology for wearable electronics are imminently needed to achieve better performance than the current stretchable 1D conductors, as well as the scalability of the 1D stretchable conductors. Interdisciplinary collaboration is crucial, particularly in materials chemistry, materials engineering, electrical engineering, and mechanical engineering.

CONCLUSIONS

This work presents a critical review of the advances in the architecture and fabrication strategies of continuous, stretchable 1D conductors in the forms of wires, fibers, and yarns. The 1D conductors are grouped into three major categories: rigid 1D conductor, piezoresistive 1D conductor, and resistance-stable 1D conductor. This review focuses on the latter two in terms of critical developments with their timeline. This review also summarizes how the structure of the materials can be manipulated by selected fabrication strategies to optimize the properties of stretchable 1D conductors. For example, piezoresistive 1D conductors require significant resistance changes upon deformation, while a resistance-stable 1D conductor requires both low and steady resistance when being deformed. Such features could be realized using specific material synthetic and preparation methodologies. Recent advances in representative stretchable 1D conductors are reviewed to focus on conductive polymer fibers, composite 1D conductors, carbon nanomaterials-based 1D conductors,

conductive coaxial fibers, etc. The applications of stretchable 1D conductors as stretchable interconnects, deformable mechanical sensors, actuators, and stretchable heaters are presented. Although the demonstrated prototypes of various stretchable 1D conductors show good prospects, they are still far below the performance required by commercial electronics.

AUTHOR INFORMATION

Corresponding Authors

You-Lo Hsieh – *Biological and Agricultural Engineering, University of California at Davis, California 95616, United States*; orcid.org/0000-0003-4795-260X; Email: ylhsieh@ucdavis.edu

Kun Kelvin Fu – *Department of Mechanical Engineering, University of Delaware, Newark, Delaware 19716, United States*; orcid.org/0000-0003-4963-615X; Email: kfu@udel.edu

Jian Zhou – *School of Material Science and Engineering Key Laboratory for Polymeric Composite & Functional Materials of Ministry of Education Guangzhou Key Laboratory of Flexible Electronic Materials and Wearable Devices, Sun Yat-sen University Guangzhou, Guangdong 510275, China*; orcid.org/0000-0003-0144-5901; Email: zhouj296@mail.sysu.edu.cn

Authors

Mingyu Nie – *School of Material Science and Engineering Key Laboratory for Polymeric Composite & Functional Materials of Ministry of Education Guangzhou Key Laboratory of Flexible Electronic Materials and Wearable Devices, Sun Yat-sen University Guangzhou, Guangdong 510275, China*; orcid.org/0000-0003-0361-1010

Boxiao Li – *School of Material Science and Engineering Key Laboratory for Polymeric Composite & Functional Materials of Ministry of Education Guangzhou Key Laboratory of Flexible Electronic Materials and Wearable Devices, Sun Yat-sen University Guangzhou, Guangdong 510275, China*; orcid.org/0000-0002-5858-7161

Complete contact information is available at: <https://pubs.acs.org/10.1021/acsnano.2c08166>

Author Contributions

[#]M.N. and B.L. contributed equally to the manuscript. The manuscript was written through contributions of all authors. All authors have approved the final version of the manuscript.

Notes

The authors declare no competing financial interest.

ACKNOWLEDGMENTS

The authors appreciate the funding support from the California Rice Research Board. The Natural Science Foundation of Guangdong Province (2019A1515011812), the 100 Top Talents Program-Sun Yat-sen University (29000-18841225), Central University Basic Research Fund of China (20lgy12), and the Guangzhou Key Laboratory of Flexible Electronic Materials and Wearable Devices are gratefully acknowledged.

VOCABULARY

1D conductor, conductive materials in the forms of fibers, wires, or yarns; wearable electronics, wearable products with implemented electronic and smart devices to achieve daily

functionalities; electronic textile, textiles capable of embedding electronics, such as batteries, lights, sensors, and micro-controllers; stretchability, the ability of a material to be stretched while maintaining its functions normally; resistance stability, the performance that the relative change in resistance of the 1D conductor is less than 100% when applied a certain strain; structural design, the design of the architecture and morphology in different dimensions to realize high stretchability and resistance stability

REFERENCES

- (1) Sekitani, T.; Noguchi, Y.; Hata, K.; Fukushima, T.; Aida, T.; Someya, T. A Rubberlike Stretchable Active Matrix Using Elastic Conductors. *Science* **2008**, *321* (5895), 1468–1472.
- (2) Savagatrup, S.; Printz, A. D.; O'Connor, T. F.; Zaretski, A. V.; Lipomi, D. J. Molecularly Stretchable Electronics. *Chem. Mater.* **2014**, *26* (10), 3028–3041.
- (3) Kim, D. H.; Lu, N.; Ma, R.; Kim, Y. S.; Kim, R. H.; Wang, S.; Wu, J.; Won, S. M.; Tao, H.; Islam, A.; Yu, K. J.; Kim, T. I.; Chowdhury, R.; Ying, M.; Xu, L.; Li, M.; Chung, H. J.; Keum, H.; McCormick, M.; Liu, P.; et al. Epidermal Electronics. *Science* **2011**, *333* (6044), 838–843.
- (4) Yao, S.; Zhu, Y. Nanomaterial-Enabled Stretchable Conductors: Strategies, Materials and Devices. *Adv. Mater.* **2015**, *27* (9), 1480–1511.
- (5) Zhao, S.; Li, J.; Cao, D.; Zhang, G.; Li, J.; Li, K.; Yang, Y.; Wang, W.; Jin, Y.; Sun, R.; Wong, C. P. Recent Advancements in Flexible and Stretchable Electrodes for Electromechanical Sensors: Strategies, Materials, and Features. *ACS Appl. Mater. Interfaces* **2017**, *9* (14), 12147–12164.
- (6) Trung, T. Q.; Lee, N. E. Recent Progress on Stretchable Electronic Devices with Intrinsically Stretchable Components. *Adv. Mater.* **2017**, *29* (3), 1603167–1603195.
- (7) Someya, T.; Bao, Z.; Malliaras, G. G. The Rise of Plastic Bioelectronics. *Nature* **2016**, *540* (7633), 379–385.
- (8) McCoul, D.; Hu, W. L.; Gao, M. M.; Mehta, V.; Pei, Q. B. Recent Advances in Stretchable and Transparent Electronic Materials. *Adv. Electron Mater.* **2016**, *2* (5), 1500407–1500525.
- (9) Wu, H.; Huang, Y.; Xu, F.; Duan, Y.; Yin, Z. Energy Harvesters for Wearable and Stretchable Electronics: From Flexibility to Stretchability. *Adv. Mater.* **2016**, *28* (45), 9881–9919.
- (10) Kim, J.; Kumar, R.; Bandodkar, A. J.; Wang, J. Advanced Materials for Printed Wearable Electrochemical Devices: A Review. *Adv. Electron Mater.* **2017**, *3* (1), 1600260–1600302.
- (11) Gong, S.; Cheng, W. One-Dimensional Nanomaterials for Soft Electronics. *Adv. Electron Mater.* **2017**, *3* (3), 1600314–1600343.
- (12) Gong, S.; Cheng, W. L. Toward Soft Skin-Like Wearable and Implantable Energy Devices. *Adv. Energy Mater.* **2017**, *7* (23), 1700648–1700681.
- (13) Chen, D.; Pei, Q. Electronic Muscles and Skins: A Review of Soft Sensors and Actuators. *Chem. Rev.* **2017**, *117* (17), 11239–11268.
- (14) Liu, Y.; Pharr, M.; Salvatore, G. A. Lab-on-Skin: A Review of Flexible and Stretchable Electronics for Wearable Health Monitoring. *ACS Nano* **2017**, *11* (10), 9614–9635.
- (15) Dickey, M. D. Stretchable and Soft Electronics Using Liquid Metals. *Adv. Mater.* **2017**, *29* (27), 1606425–1606444.
- (16) Chen, G.; Li, Y.; Bick, M.; Chen, J. Smart Textiles for Electricity Generation. *Chem. Rev.* **2020**, *120* (8), 3668–3720.
- (17) Chen, G.; Xiao, X.; Zhao, X.; Tat, T.; Bick, M.; Chen, J. Electronic Textiles for Wearable Point-of-Care Systems. *Chem. Rev.* **2022**, *122* (3), 3259–3291.
- (18) Deng, W.; Zhou, Y.; Libanori, A.; Chen, G.; Yang, W.; Chen, J. Piezoelectric Nanogenerators for Personalized Healthcare. *Chem. Soc. Rev.* **2022**, *51* (9), 3380–3435.
- (19) Chen, G.; Zhao, X.; Andalib, S.; Xu, J.; Zhou, Y.; Tat, T.; Lin, K.; Chen, J. Discovering Giant Magnetoelasticity in Soft Matter for Electronic Textiles. *Matter* **2021**, *4* (11), 3725–3740.

- (20) Zhao, X.; Zhou, Y.; Xu, J.; Chen, G.; Fang, Y.; Tat, T.; Xiao, X.; Song, Y.; Li, S.; Chen, J. Soft Fibers with Magnetoelasticity for Wearable Electronics. *Nat. Commun.* **2021**, *12* (1), 6755–6765.
- (21) Libanori, A.; Chen, G. R.; Zhao, X.; Zhou, Y. H.; Chen, J. Smart Textiles for Personalized Healthcare. *Nat. Electron.* **2022**, *5* (3), 142–156.
- (22) Meng, K.; Xiao, X.; Wei, W.; Chen, G.; Nashalian, A.; Shen, S.; Xiao, X.; Chen, J. Wearable Pressure Sensors for Pulse Wave Monitoring. *Adv. Mater.* **2022**, *34* (21), 2109357–2109379.
- (23) Zeng, W.; Shu, L.; Li, Q.; Chen, S.; Wang, F.; Tao, X. M. Fiber-Based Wearable Electronics: A Review of Materials, Fabrication, Devices, and Applications. *Adv. Mater.* **2014**, *26* (31), 5310–5336.
- (24) Stoppa, M.; Chiolerio, A. Wearable Electronics and Smart Textiles: A Critical Review. *Sensors (Basel)* **2014**, *14* (7), 11957–11992.
- (25) Hammock, M. L.; Chortos, A.; Tee, B. C.; Tok, J. B.; Bao, Z. 25th Anniversary Article: The Evolution of Electronic Skin (E-Skin): A Brief History, Design Considerations, and Recent Progress. *Adv. Mater.* **2013**, *25* (42), 5997–6038.
- (26) Zhang, Y.; Zhao, Y.; Ren, J.; Weng, W.; Peng, H. Advances in Wearable Fiber-Shaped Lithium-Ion Batteries. *Adv. Mater.* **2016**, *28* (22), 4524–4531.
- (27) Weng, W.; Chen, P.; He, S.; Sun, X.; Peng, H. Smart Electronic Textiles. *Angew. Chem., Int. Ed. Engl.* **2016**, *55* (21), 6140–6169.
- (28) Ghosh, T. Stretchable Electronics. Stretch, Wrap, and Relax to Smartness. *Science* **2015**, *349* (6246), 382–383.
- (29) Wang, C.; Li, X.; Gao, E.; Jian, M.; Xia, K.; Wang, Q.; Xu, Z.; Ren, T.; Zhang, Y. Carbonized Silk Fabric for Ulstretchable, Highly Sensitive, and Wearable Strain Sensors. *Adv. Mater.* **2016**, *28* (31), 6640–6648.
- (30) Lu, W.; Zu, M.; Byun, J. H.; Kim, B. S.; Chou, T. W. State of the Art of Carbon Nanotube Fibers: Opportunities and Challenges. *Adv. Mater.* **2012**, *24* (14), 1805–1833.
- (31) Di, J.; Zhang, X.; Yong, Z.; Zhang, Y.; Li, D.; Li, R.; Li, Q. Carbon-Nanotube Fibers for Wearable Devices and Smart Textiles. *Adv. Mater.* **2016**, *28* (47), 10529–10538.
- (32) Lekawa-Raus, A.; Patmore, J.; Kurzepa, L.; Bulmer, J.; Koziol, K. Electrical Properties of Carbon Nanotube Based Fibers and Their Future Use in Electrical Wiring. *Adv. Funct. Mater.* **2014**, *24* (24), 3661–3682.
- (33) Meng, F.; Lu, W.; Li, Q.; Byun, J. H.; Oh, Y.; Chou, T. W. Graphene-Based Fibers: A Review. *Adv. Mater.* **2015**, *27* (35), 5113–5131.
- (34) Cheng, H. H.; Hu, C. G.; Zhao, Y.; Qu, L. T. Graphene Fiber: A New Material Platform for Unique Applications. *Npg Asia Materials* **2014**, *6* (7), 113–125.
- (35) Xu, Z.; Gao, C. Graphene Fiber: A New Trend in Carbon Fibers. *Mater. Today* **2015**, *18* (9), 480–492.
- (36) Mirabedini, A.; Foroughi, J.; Farajikhah, S.; Wallace, G. G. Correction: Developments in Conducting Polymer Fibres: From Established Spinning Methods toward Advanced Applications. *RSC Adv.* **2016**, *6* (110), 108152–108152.
- (37) Raji, R. K.; Miao, X. H.; Boakye, A. Electrical Conductivity in Textile Fibers and Yarns-Review. *Aatcc Journal of Research* **2017**, *4* (3), 8–21.
- (38) Akbari, M.; Tamayol, A.; Bagherifard, S.; Serex, L.; Mostafalu, P.; Faramarzi, N.; Mohammadi, M. H.; Khademhosseini, A. Textile Technologies and Tissue Engineering: A Path toward Organ Weaving. *Adv. Healthc Mater.* **2016**, *5* (7), 751–766.
- (39) Huang, Q. Y.; Wang, D. R.; Zheng, Z. J. Textile-Based Electrochemical Energy Storage Devices. *Adv. Energy Mater.* **2016**, *6* (22), 1600783–1600810.
- (40) Yetisen, A. K.; Qu, H.; Manbachi, A.; Butt, H.; Dokmeci, M. R.; Hinestroza, J. P.; Skorobogatiy, M.; Khademhosseini, A.; Yun, S. H. Nanotechnology in Textiles. *ACS Nano* **2016**, *10* (3), 3042–3068.
- (41) Hosne Asif, A. K. M. A.; Hasan, M. Z. Application of Nanotechnology in Modern Textiles: A Review. *International Journal of Current Engineering and Technology* **2018**, *8* (02), 227–231.
- (42) Fang, Y.; Chen, G.; Bick, M.; Chen, J. Smart Textiles for Personalized Thermoregulation. *Chem. Soc. Rev.* **2021**, *50* (17), 9357–9374.
- (43) Wang, H.; Zhang, Y.; Liang, X.; Zhang, Y. Smart Fibers and Textiles for Personal Health Management. *ACS Nano* **2021**, *15*, 12497–12508.
- (44) Shah, M. A.; Pirzada, B. M.; Price, G.; Shibiru, A. L.; Qurashi, A. Applications of Nanotechnology in Smart Textile Industry: A Critical Review. *J. Adv. Res.* **2022**, *38*, 55–75.
- (45) Liu, Z. F.; Fang, S.; Moura, F. A.; Ding, J. N.; Jiang, N.; Di, J.; Zhang, M.; Lepro, X.; Galvao, D. S.; Haines, C. S.; Yuan, N. Y.; Yin, S. G.; Lee, D. W.; Wang, R.; Wang, H. Y.; Lv, W.; Dong, C.; Zhang, R. C.; Chen, M. J.; Yin, Q.; et al. Hierarchically Buckled Sheath-Core Fibers for Superelastic Electronics, Sensors, and Muscles. *Science* **2015**, *349* (6246), 400–404.
- (46) Xie, K.; Wei, B. Materials and Structures for Stretchable Energy Storage and Conversion Devices. *Adv. Mater.* **2014**, *26* (22), 3592–3617.
- (47) Jost, K.; Dion, G.; Gogotsi, Y. Textile Energy Storage in Perspective. *J. Mater. Chem. A* **2014**, *2* (28), 10776–10787.
- (48) Zhu, S.; So, J. H.; Mays, R.; Desai, S.; Barnes, W. R.; Pourdeyhimi, B.; Dickey, M. D. Ulstretchable Fibers with Metallic Conductivity Using a Liquid Metal Alloy Core. *Adv. Funct. Mater.* **2013**, *23* (18), 2308–2314.
- (49) Lee, S.; Shin, S.; Lee, S.; Seo, J.; Lee, J.; Son, S.; Cho, H. J.; Algadi, H.; Al-Sayari, S.; Kim, D. E.; Lee, T. Stretchable Electronics: Ag Nanowire Reinforced Highly Stretchable Conductive Fibers for Wearable Electronics. *Adv. Funct. Mater.* **2015**, *25* (21), 3114–3121.
- (50) Chen, P.; Xu, Y.; He, S.; Sun, X.; Pan, S.; Deng, J.; Chen, D.; Peng, H. Hierarchically Arranged Helical Fibre Actuators Driven by Solvents and Vapours. *Nat. Nanotechnol* **2015**, *10* (12), 1077–1083.
- (51) Hu, D.; Xu, X.; Miao, J.; Gidron, O.; Meng, H. A Stretchable Alternating Current Electroluminescent Fiber. *Materials (Basel)* **2018**, *11* (2), 184–193.
- (52) Zhou, J.; Mülle, M.; Zhang, Y. B.; Xu, X. Z.; Li, E. Q.; Han, F.; Thoroddsen, S. T.; Lubineau, G. High-Ampacity Conductive Polymer Microfibers as Fast Response Wearable Heaters and Electro-mechanical Actuators. *J. Mater. Chem. C* **2016**, *4* (6), 1238–1249.
- (53) Matsuhisa, N.; Kaltenbrunner, M.; Yokota, T.; Jinno, H.; Kuribara, K.; Sekitani, T.; Someya, T. Printable Elastic Conductors with a High Conductivity for Electronic Textile Applications. *Nat. Commun.* **2015**, *6*, 7461–7471.
- (54) Arreiro, A.; Catalanotti, G.; Melro, A. R.; Linde, P.; Camanho, P. P. Micro-Mechanical Analysis of the In Situ Effect in Polymer Composite Laminates. *Compos. Struct.* **2014**, *116*, 827–840.
- (55) Arreiro, A.; Catalanotti, G.; Melro, A. R.; Linde, P.; Camanho, P. P. Micro-Mechanical Analysis of the Effect of Ply Thickness on the Transverse Compressive Strength of Polymer Composites. *Composites Part a-Applied Science and Manufacturing* **2015**, *79*, 127–137.
- (56) Nasr Saleh, M.; Lubineau, G. Understanding the Mechanisms That Change the Conductivity of Damaged Ito-Coated Polymeric Films: A Micro-Mechanical Investigation. *Sol. Energy Mater. Sol. Cells* **2014**, *130*, 199–207.
- (57) Yang, T. T.; Li, X. M.; Jiang, X.; Lin, S. Y.; Lao, J. C.; Shi, J. D.; Zhen, Z.; Li, Z. H.; Zhu, H. W. Structural Engineering of Gold Thin Films with Channel Cracks for Ultrasensitive Strain Sensing. *Mater. Horiz* **2016**, *3* (3), 248–255.
- (58) Wang, X. H.; Zhang, B. M.; Du, S. Y.; Wu, Y. F.; Sun, X. Y. Numerical Simulation of the Fiber Fragmentation Process in Single-Fiber Composites. *Mater. Des* **2010**, *31* (5), 2464–2470.
- (59) Lipomi, D. J. Stretchable Figures of Merit in Deformable Electronics. *Adv. Mater.* **2016**, *28* (22), 4180–4183.
- (60) Amjadi, M.; Turan, M.; Clementson, C. P.; Sitti, M. Parallel Microcracks-Based Ultrasensitive and Highly Stretchable Strain Sensors. *ACS Appl. Mater. Interfaces* **2016**, *8* (8), 5618–5626.
- (61) Zeng, S.; Zhang, D.; Huang, W.; Wang, Z.; Freire, S. G.; Yu, X.; Smith, A. T.; Huang, E. Y.; Nguon, H.; Sun, L. Bio-Inspired Sensitive and Reversible Mechanochromisms Via Strain-Dependent Cracks and Folds. *Nat. Commun.* **2016**, *7*, 11802.

- (62) Zhou, J.; Yu, H.; Xu, X.; Han, F.; Lubineau, G. Ultrasensitive, Stretchable Strain Sensors Based on Fragmented Carbon Nanotube Papers. *ACS Appl. Mater. Interfaces* **2017**, *9* (5), 4835–4842.
- (63) Zhou, J.; Xu, X.; Yu, H.; Lubineau, G. Deformable and Wearable Carbon Nanotube Microwire-Based Sensors for Ultrasensitive Monitoring of Strain, Pressure and Torsion. *Nanoscale* **2017**, *9* (2), 604–612.
- (64) Zhou, J.; Xu, X. Z.; Xin, Y. Y.; Lubineau, G. Coaxial Thermoplastic Elastomer-Wrapped Carbon Nanotube Fibers for Deformable and Wearable Strain Sensors. *Adv. Funct. Mater.* **2018**, *28* (16), 1705591–1705598.
- (65) Gray, D. S.; Tien, J.; Chen, C. S. High Conductivity Elastomeric Electronics. *Adv. Mater.* **2004**, *16*, 393–397.
- (66) Zu, M.; Li, Q. W.; Wang, G. J.; Byun, J. H.; Chou, T. W. Carbon Nanotube Fiber Based Stretchable Conductor. *Adv. Funct. Mater.* **2013**, *23* (7), 789–793.
- (67) Shang, Y.; Li, Y.; He, X.; Zhang, L.; Li, Z.; Li, P.; Shi, E.; Wu, S.; Cao, A. Elastic Carbon Nanotube Straight Yarns Embedded with Helical Loops. *Nanoscale* **2013**, *5* (6), 2403–2410.
- (68) Li, Y.; Shang, Y.; He, X.; Peng, Q.; Du, S.; Shi, E.; Wu, S.; Li, Z.; Li, P.; Cao, A. Overtwisted, Resolvable Carbon Nanotube Yarn Entanglement as Strain Sensors and Rotational Actuators. *ACS Nano* **2013**, *7* (9), 8128–8135.
- (69) Okuzaki, H.; Ishihara, M. Spinning and Characterization of Conducting Microfibers. *Macromol. Rapid Commun.* **2003**, *24* (3), 261–264.
- (70) Ericson, L. M.; Fan, H.; Peng, H.; Davis, V. A.; Zhou, W.; Sulpizio, J.; Wang, Y.; Booker, R.; Vavro, J.; Guthy, C.; Parra-Vasquez, A. N.; Kim, M. J.; Ramesh, S.; Saini, R. K.; Kittrell, C.; Lavin, G.; Schmidt, H.; Adams, W. W.; Billups, W. E.; Pasquali, M.; et al. Macroscopic, Neat, Single-Walled Carbon Nanotube Fibers. *Science* **2004**, *305* (5689), 1447–1450.
- (71) Zhang, M.; Atkinson, K. R.; Baughman, R. H. Multifunctional Carbon Nanotube Yarns by Downsizing an Ancient Technology. *Science* **2004**, *306* (5700), 1358–1361.
- (72) Kou, L.; Huang, T.; Zheng, B.; Han, Y.; Zhao, X.; Gopalsamy, K.; Sun, H.; Gao, C. Coaxial Wet-Spun Yarn Supercapacitors for High-Energy Density and Safe Wearable Electronics. *Nat. Commun.* **2014**, *5*, 3754–3763.
- (73) Koziol, K.; Vilatela, J.; Moissala, A.; Motta, M.; Cunniff, P.; Sennett, M.; Windle, A. High-Performance Carbon Nanotube Fiber. *Science* **2007**, *318* (5858), 1892–1895.
- (74) Behabtu, N.; Young, C. C.; Tsentelovich, D. E.; Kleinerman, O.; Wang, X.; Ma, A. W.; Bengio, E. A.; ter Waarbeek, R. F.; de Jong, J. J.; Hoogerwerf, R. E.; Fairchild, S. B.; Ferguson, J. B.; Maruyama, B.; Kono, J.; Talmon, Y.; Cohen, Y.; Otto, M. J.; Pasquali, M. Strong, Light, Multifunctional Fibers of Carbon Nanotubes with Ultrahigh Conductivity. *Science* **2013**, *339* (6116), 182–186.
- (75) Wakuda, D.; Suganuma, K. Stretchable Fine Fiber with High Conductivity Fabricated by Injection Forming. *Appl. Phys. Lett.* **2011**, *98* (7), 073304–073306.
- (76) Han, E.; Wang, Y.; Chen, X.; Shang, G.; Yu, W.; Niu, H.; Qi, S.; Wu, D.; Jin, R. Consecutive Large-Scale Fabrication of Surface-Silvered Polyimide Fibers Via an Integrated Direct Ion-Exchange Self-Metallization Strategy. *ACS Appl. Mater. Interfaces* **2013**, *5* (10), 4293–4301.
- (77) Ma, R.; Lee, J.; Choi, D.; Moon, H.; Baik, S. Knitted Fabrics Made from Highly Conductive Stretchable Fibers. *Nano Lett.* **2014**, *14* (4), 1944–1951.
- (78) Seyedin, M. Z.; Razal, J. M.; Innis, P. C.; Wallace, G. G. Strain-Responsive Polyurethane/PEDOT:PSS Elastomeric Composite Fibers with High Electrical Conductivity. *Adv. Funct. Mater.* **2014**, *24* (20), 2957–2966.
- (79) Ma, R.; Kang, B.; Cho, S.; Choi, M.; Baik, S. Extraordinarily High Conductivity of Stretchable Fibers of Polyurethane and Silver Nanoflowers. *ACS Nano* **2015**, *9* (11), 10876–10886.
- (80) Cheng, Y.; Wang, R.; Sun, J.; Gao, L. Highly Conductive and Ulstretchable Electric Circuits from Covered Yarns and Silver Nanowires. *ACS Nano* **2015**, *9* (4), 3887–3895.
- (81) Jiang, S.; Zhang, H.; Song, S.; Ma, Y.; Li, J.; Lee, G. H.; Han, Q.; Liu, J. Highly Stretchable Conductive Fibers from Few-Walled Carbon Nanotubes Coated on Poly(M-Phenylene Isophthalamide) Polymer Core/Shell Structures. *ACS Nano* **2015**, *9* (10), 10252–10257.
- (82) Yan, H. L.; Chen, Y. Q.; Deng, Y. Q.; Zhang, L. L.; Hong, X.; Lau, W. M.; Mei, J.; Hui, D.; Yan, H.; Liu, Y. Coaxial Printing Method for Directly Writing Stretchable Cable as Strain Sensor. *Appl. Phys. Lett.* **2016**, *109* (8), 083502–083505.
- (83) Hirsch, A.; Michaud, H. O.; Gerratt, A. P.; de Mulatier, S.; Lacour, S. P. Intrinsically Stretchable Biphasic (Solid-Liquid) Thin Metal Films. *Adv. Mater.* **2016**, *28* (22), 4507–4512.
- (84) Foroughi, J.; Spinks, G. M.; Aziz, S.; Mirabedini, A.; Jeiranikhameneh, A.; Wallace, G. G.; Kozlov, M. E.; Baughman, R. H. Knitted Carbon-Nanotube-Sheath/Spandex-Core Elastomeric Yarns for Artificial Muscles and Strain Sensing. *ACS Nano* **2016**, *10* (10), 9129–9135.
- (85) Wang, R.; Jiang, N.; Su, J.; Yin, Q.; Zhang, Y.; Liu, Z. S.; Lin, H. B.; Moura, F. A.; Yuan, N. Y.; Roth, S.; Rome, R. S.; Ovalle-Robles, R.; Inoue, K.; Yin, S. G.; Fang, S. L.; Wang, W. C.; Ding, J. N.; Shi, L. Q.; Baughman, R. H.; Liu, Z. F. A Bi-Sheath Fiber Sensor for Giant Tensile and Torsional Displacements. *Adv. Funct. Mater.* **2017**, *27* (35), 1702134–1702146.
- (86) Wu, X.; Han, Y.; Zhang, X.; Lu, C. Spirally Structured Conductive Composites for Highly Stretchable, Robust Conductors and Sensors. *ACS Appl. Mater. Interfaces* **2017**, *9* (27), 23007–23016.
- (87) Okuzaki, H.; Harashina, Y.; Yan, H. Highly Conductive PEDOT/PSS Microfibers Fabricated by Wet-Spinning and Dip-Treatment in Ethylene Glycol. *Eur. Polym. J.* **2009**, *45* (1), 256–261.
- (88) Jalili, R.; Razal, J. M.; Innis, P. C.; Wallace, G. G. One-Step Wet-Spinning Process of Poly(3,4-Ethylenedioxythiophene):Poly(styrenesulfonate) Fibers and the Origin of Higher Electrical Conductivity. *Adv. Funct. Mater.* **2011**, *21* (17), 3363–3370.
- (89) Shang, Y.; He, X.; Li, Y.; Zhang, L.; Li, Z.; Ji, C.; Shi, E.; Li, P.; Zhu, K.; Peng, Q.; Wang, C.; Zhang, X.; Wang, R.; Wei, J.; Wang, K.; Zhu, H.; Wu, D.; Cao, A. Super-Stretchable Spring-Like Carbon Nanotube Ropes. *Adv. Mater.* **2012**, *24* (21), 2896–2900.
- (90) Zhou, J.; Li, E. Q.; Li, R. P.; Xu, X. Z.; Ventura, I. A.; Moussawi, A.; Anjum, D. H.; Hedhili, M. N.; Smilgies, D. M.; Lubineau, G.; Thoroddsen, S. T. Semi-Metallic, Strong and Stretchable Wet-Spun Conjugated Polymer Microfibers. *J. Mater. Chem. C* **2015**, *3* (11), 2528–2538.
- (91) Choi, C.; Lee, J. M.; Kim, S. H.; Kim, S. J.; Di, J.; Baughman, R. H. Twistable and Stretchable Sandwich Structured Fiber for Wearable Sensors and Supercapacitors. *Nano Lett.* **2016**, *16* (12), 7677–7684.
- (92) Kim, J.; Park, S. J.; Nguyen, T.; Chu, M.; Pegan, J. D.; Khine, M. Highly Stretchable Wrinkled Gold Thin Film Wires. *Appl. Phys. Lett.* **2016**, *108* (6), 061901–061905.
- (93) Bai, X.; Liao, S.; Huang, Y.; Song, J.; Liu, Z.; Fang, M.; Xu, C.; Cui, Y.; Wu, H. Continuous Draw Spinning of Extra-Long Silver Submicron Fibers with Micrometer Patterning Capability. *Nano Lett.* **2017**, *17* (3), 1883–1891.
- (94) Zhou, J.; Tian, G. Q.; Jin, G.; Xin, Y. Y.; Tao, R.; Lubineau, G. Buckled Conductive Polymer Ribbons in Elastomer Channels as Stretchable Fiber Conductor. *Adv. Funct. Mater.* **2020**, *30* (5), 1907316–1907324.
- (95) Liu, P.; Li, Y.; Xu, Y.; Bao, L.; Wang, L.; Pan, J.; Zhang, Z.; Sun, X.; Peng, H. Stretchable and Energy-Efficient Heating Carbon Nanotube Fiber by Designing a Hierarchically Helical Structure. *Small* **2018**, *14* (4), 1702926–1702931.
- (96) Son, W.; Chun, S.; Lee, J. M.; Lee, Y.; Park, J.; Suh, D.; Lee, D. W.; Jung, H.; Kim, Y. J.; Kim, Y.; Jeong, S. M.; Lim, S. K.; Choi, C. Highly Twisted Supercoils for Superelastic Multi-Functional Fibres. *Nat. Commun.* **2019**, *10* (1), 426.
- (97) Woo, J.; Lee, H.; Yi, C.; Lee, J.; Won, C.; Oh, S.; Jekal, J.; Kwon, C.; Lee, S.; Song, J.; Choi, B.; Jang, K. I.; Lee, T. Ulstretchable Helical Conductive Fibers Using Percolated Ag Nanoparticle Networks Encapsulated by Elastic Polymers with High

Durability in Omnidirectional Deformations for Wearable Electronics. *Adv. Funct. Mater.* **2020**, *30* (29), 1910026–1910036.

(98) Dong, C.; Leber, A.; Das Gupta, T.; Chandran, R.; Volpi, M.; Qu, Y.; Nguyen-Dang, T.; Bartolomei, N.; Yan, W.; Sorin, F. High-Efficiency Super-Elastic Liquid Metal Based Triboelectric Fibers and Textiles. *Nat. Commun.* **2020**, *11* (1), 3537.

(99) Chen, M.; Wang, Z.; Zhang, Q.; Wang, Z.; Liu, W.; Chen, M.; Wei, L. Self-Powered Multifunctional Sensing Based on Super-Elastic Fibers by Soluble-Core Thermal Drawing. *Nat. Commun.* **2021**, *12* (1), 1416.

(100) Marion, J. S.; Gupta, N.; Cheung, H.; Monir, K.; Anikeeva, P.; Fink, Y. Thermally Drawn Highly Conductive Fibers with Controlled Elasticity. *Adv. Mater.* **2022**, *34* (19), 2201081–2201090.

(101) Lekawa-Raus, A.; Kurzepa, L.; Peng, X. Y.; Koziol, K. Towards the Development of Carbon Nanotube Based Wires. *Carbon* **2014**, *68*, 597–609.

(102) Agcayazi, T.; Chatterjee, K.; Bozkurt, A.; Ghosh, T. K. Flexible Interconnects for Electronic Textiles. *Adv. Mater. Technol.* **2018**, *3* (10), 1700277–1700308.

(103) Wu, X.; Han, Y.; Zhang, X.; Lu, C. Highly Sensitive, Stretchable, and Wash-Durable Strain Sensor Based on Ultrathin Conductive Layer@Polyurethane Yarn for Tiny Motion Monitoring. *ACS Appl. Mater. Interfaces* **2016**, *8* (15), 9936–9945.

(104) Liu, Z.; Qi, D.; Guo, P.; Liu, Y.; Zhu, B.; Yang, H.; Liu, Y.; Li, B.; Zhang, C.; Yu, J.; Liedberg, B.; Chen, X. Thickness-Gradient Films for High Gauge Factor Stretchable Strain Sensors. *Adv. Mater.* **2015**, *27* (40), 6230–6237.

(105) Duan, X.; Yu, J.; Zhu, Y.; Zheng, Z.; Liao, Q.; Xiao, Y.; Li, Y.; He, Z.; Zhao, Y.; Wang, H.; Qu, L. Large-Scale Spinning Approach to Engineering Knittable Hydrogel Fiber for Soft Robots. *ACS Nano* **2020**, *14* (11), 14929–14938.

(106) Huang, Y.; Bai, X.; Zhou, M.; Liao, S.; Yu, Z.; Wang, Y.; Wu, H. Large-Scale Spinning of Silver Nanofibers as Flexible and Reliable Conductors. *Nano Lett.* **2016**, *16* (9), 5846–5851.

(107) Tang, Z.; Jia, S.; Wang, F.; Bian, C.; Chen, Y.; Wang, Y.; Li, B. Highly Stretchable Core-Sheath Fibers Via Wet-Spinning for Wearable Strain Sensors. *ACS Appl. Mater. Interfaces* **2018**, *10* (7), 6624–6635.

(108) Zhao, Y. M.; Dong, D. S.; Gong, S.; Brassart, L.; Wang, Y.; An, T.; Cheng, W. L. A Moss-Inspired Electroless Gold-Coating Strategy toward Stretchable Fiber Conductors by Dry Spinning. *Adv. Electron Mater.* **2019**, *5* (1), 1800462–1800469.

(109) Wang, Q. Q.; Ma, W. J.; Yin, E. Q.; Yu, S. L.; Wang, S. C.; Xiang, H. X.; Li, D. X.; Zhu, M. F. Melt Spinning of Low-Cost Activated Carbon Fiber with a Tunable Pore Structure for High-Performance Flexible Supercapacitors. *ACS Appl. Energy Mater.* **2020**, *3* (9), 9360–9368.

(110) Nayeem, M. O. G.; Lee, S.; Jin, H.; Matsuhisa, N.; Jinno, H.; Miyamoto, A.; Yokota, T.; Someya, T. All-Nanofiber-Based, Ultra-sensitive, Gas-Permeable Mechanoacoustic Sensors for Continuous Long-Term Heart Monitoring. *Proc. Natl. Acad. Sci. U. S. A.* **2020**, *117* (13), 7063–7070.

(111) Zhang, X.; Tang, S.; Wu, Z.; Chen, Y.; Li, Z.; Wang, Z.; Zhou, J. Centrifugal Spinning Enables the Formation of Silver Microfibers with Nanostructures. *Nanomaterials (Basel)* **2022**, *12* (13), 2145–2157.

(112) Yan, W.; Dong, C. Q.; Xiang, Y. Z.; Jiang, S.; Leber, A.; Loke, G.; Xu, W. X.; Hou, C.; Zhou, S. F.; Chen, M.; Hu, R.; Shum, P. P.; Wei, L.; Jia, X. T.; Sorin, F.; Tao, X. M.; Tao, G. M. Thermally Drawn Advanced Functional Fibers: New Frontier of Flexible Electronics. *Mater. Today* **2020**, *35*, 168–194.

(113) Khudiyev, T.; Hou, C.; Stolyarov, A. M.; Fink, Y. Sub-Micrometer Surface-Patterned Ribbon Fibers and Textiles. *Adv. Mater.* **2017**, *29* (22), 1605868–1605873.

(114) Chocat, N.; Lestoquoy, G.; Wang, Z.; Rodgers, D. M.; Joannopoulos, J. D.; Fink, Y. Piezoelectric Fibers for Conformal Acoustics. *Adv. Mater.* **2012**, *24* (39), 5327–5332.

(115) Yuan, R.; Nagarajan, M. B.; Lee, J.; Voldman, J.; Doyle, P. S.; Fink, Y. Designable 3D Microshapes Fabricated at the Intersection of

Structured Flow and Optical Fields. *Small* **2018**, *14* (50), 1803585–1803592.

(116) Maayani, S.; Foy, C.; Englund, D.; Fink, Y. Distributed Quantum Fiber Magnetometry. *Laser Photonics Rev.* **2019**, *13* (7), 1900075–1900081.

(117) Shahriari, D.; Loke, G.; Tafel, I.; Park, S.; Chiang, P. H.; Fink, Y.; Anikeeva, P. Scalable Fabrication of Porous Microchannel Nerve Guidance Scaffolds with Complex Geometries. *Adv. Mater.* **2019**, *31* (30), 1902021–1902028.

(118) Khudiyev, T.; Lee, J. T.; Cox, J. R.; Argentieri, E.; Loke, G.; Yuan, R.; Noel, G. H.; Tataru, R.; Yu, Y.; Logan, F.; Joannopoulos, J.; Shao-Horn, Y.; Fink, Y. 100 M Long Thermally Drawn Supercapacitor Fibers with Applications to 3D Printing and Textiles. *Adv. Mater.* **2020**, *32* (49), 2004971–2004979.

(119) Park, J.; Zeng, J. S.; Sahasrabudhe, A.; Jin, K.; Fink, Y.; Manthiram, K.; Anikeeva, P. Electrochemical Modulation of Carbon Monoxide-Mediated Cell Signaling. *Angew. Chem., Int. Ed. Engl.* **2021**, *60* (37), 20325–20330.

(120) Loke, G.; Yan, W.; Khudiyev, T.; Noel, G.; Fink, Y. Recent Progress and Perspectives of Thermally Drawn Multimaterial Fiber Electronics. *Adv. Mater.* **2020**, *32* (1), 1904911–1904940.

(121) Wang, Z.; Wu, T.; Wang, Z.; Zhang, T.; Chen, M.; Zhang, J.; Liu, L.; Qi, M.; Zhang, Q.; Yang, J.; Liu, W.; Chen, H.; Luo, Y.; Wei, L. Designer Patterned Functional Fibers Via Direct Imprinting in Thermal Drawing. *Nat. Commun.* **2020**, *11* (1), 3842.

(122) Zhang, M. C.; Zhao, M. Y.; Jian, M. Q.; Wang, C. Y.; Yu, A. F.; Yin, Z.; Liang, X. P.; Wang, H. M.; Xia, K. L.; Liang, X.; Zhai, J. Y.; Zhang, Y. Y. Printable Smart Pattern for Multifunctional Energy-Management E-Textile. *Matter* **2019**, *1* (1), 168–179.

(123) Zheng, C. L.; Sun, Y. P.; Cui, Y. W.; Yang, W. J.; Lu, Z.; Shen, S. T.; Xia, Y. Z.; Xiong, Z. Superhydrophobic and Flame-Retardant Alginate Fabrics Prepared through a One-Step Dip-Coating Surface-Treatment. *Cellulose* **2021**, *28* (9), 5973–5984.

(124) Samanta, A.; Bordes, R. Conductive Textiles Prepared by Spray Coating of Water-Based Graphene Dispersions. *RSC Adv.* **2020**, *10* (4), 2396–2403.

(125) Park, Y.; Park, M. J.; Lee, J. S. Reduced Graphene Oxide-Based Artificial Synapse Yarns for Wearable Textile Device Applications. *Adv. Funct. Mater.* **2018**, *28* (42), 1804123–1804129.

(126) Allison, L.; Hoxie, S.; Andrew, T. L. Towards Seamlessly-Integrated Textile Electronics: Methods to Coat Fabrics and Fibers with Conducting Polymers for Electronic Applications. *Chem. Commun. (Camb)* **2017**, *53* (53), 7182–7193.

(127) Zhang, J. Z.; Seyedin, S.; Qin, S.; Lynch, P. A.; Wang, Z. Y.; Yang, W. R.; Wang, X. G.; Razal, J. M. Fast and Scalable Wet-Spinning of Highly Conductive PEDOT:PSS Fibers Enables Versatile Applications. *J. Mater. Chem. A* **2019**, *7* (11), 6401–6410.

(128) Fanous, J.; Schweizer, M.; Schwallier, D.; Buchmeiser, M. R. Crystalline and Conductive Poly(3-Hexylthiophene) Fibers. *Macromol. Mater. Eng.* **2012**, *297* (2), 123–127.

(129) Foroughi, J.; Spinks, G. M.; Wallace, G. G. A Reactive Wet Spinning Approach to Polypyrrole Fibres. *J. Mater. Chem.* **2011**, *21* (17), 6421–6426.

(130) Adams, W. W.; Eby, R. K. High-Performance Polymer Fibers. *MRS Bull.* **1987**, *12* (8), 22–26.

(131) Tang, H.; Liang, Y.; Liu, C.; Hu, Z.; Deng, Y.; Guo, H.; Yu, Z.; Song, A.; Zhao, H.; Zhao, D.; Zhang, Y.; Guo, X.; Pei, J.; Ma, Y.; Cao, Y.; Huang, F. A Solution-Processed N-Type Conducting Polymer with Ultrahigh Conductivity. *Nature* **2022**, *611*, 271.

(132) Yang, C. Y.; Stoeckel, M. A.; Ruoko, T. P.; Wu, H. Y.; Liu, X.; Kolhe, N. B.; Wu, Z.; Puttison, Y.; Musumeci, C.; Masetti, M.; Sun, H.; Xu, K.; Tu, D.; Chen, W. M.; Woo, H. Y.; Fahlman, M.; Jenekhe, S. A.; Berggren, M.; Fabiano, S. A High-Conductivity N-Type Polymeric Ink for Printed Electronics. *Nat. Commun.* **2021**, *12* (1), 2354.

(133) Riaz, U.; Singh, N.; Banoo, S. Theoretical Studies of Conducting Polymers: A Mini Review. *New J. Chem.* **2022**, *46* (11), 4954–4973.

- (134) Wang, Y.; Zhu, C.; Pfattner, R.; Yan, H.; Jin, L.; Chen, S.; Molina-Lopez, F.; Lissel, F.; Liu, J.; Rabiha, N. I.; Chen, Z.; Chung, J. W.; Linder, C.; Toney, M. F.; Murmann, B.; Bao, Z. A Highly Stretchable, Transparent, and Conductive Polymer. *Sci. Adv.* **2017**, *3* (3), 1602076.
- (135) Owen, J. Ionic Conductivity. In *Comprehensive Polymer Science and Supplements*; Allen, G., Bevington, J. C., Eds.; Pergamon, 1989; pp 669–686.
- (136) Alemu, D.; Wei, H. Y.; Ho, K. C.; Chu, C. W. Highly Conductive PEDOT:PSS Electrode by Simple Film Treatment with Methanol for Ito-Free Polymer Solar Cells. *Energy Environ. Sci.* **2012**, *5* (11), 9662–9671.
- (137) Kim, N.; Kee, S.; Lee, S. H.; Lee, B. H.; Kahng, Y. H.; Jo, Y. R.; Kim, B. J.; Lee, K. Highly Conductive PEDOT:PSS Nanofibrils Induced by Solution-Processed Crystallization. *Adv. Mater.* **2014**, *26* (14), 2268–2272.
- (138) Kim, Y. H.; Sachse, C.; Machala, M. L.; May, C.; Muller-Meskamp, L.; Leo, K. Highly Conductive PEDOT:PSS Electrode with Optimized Solvent and Thermal Post-Treatment for Ito-Free Organic Solar Cells. *Adv. Funct. Mater.* **2011**, *21* (6), 1076–1081.
- (139) Ouyang, J.; Xu, Q. F.; Chu, C. W.; Yang, Y.; Li, G.; Shinar, J. On the Mechanism of Conductivity Enhancement in Poly(3,4-Ethylenedioxythiophene): Poly(Styrene Sulfonate) Film through Solvent Treatment. *Polymer* **2004**, *45* (25), 8443–8450.
- (140) Fan, B. H.; Mei, X. G.; Ouyang, J. Y. Significant Conductivity Enhancement of Conductive Poly(3,4-Ethylenedioxythiophene): Poly(Styrenesulfonate) Films by Adding Anionic Surfactants into Polymer Solution. *Macromolecules* **2008**, *41* (16), 5971–5973.
- (141) Pomfret, S. J.; Adams, P. N.; Comfort, N. P.; Monkman, A. P. Electrical and Mechanical Properties of Polyaniline Fibres Produced by a One-Step Wet Spinning Process. *Polymer* **2000**, *41* (6), 2265–2269.
- (142) Zhang, J.; Seyedin, S.; Qin, S.; Wang, Z.; Moradi, S.; Yang, F.; Lynch, P. A.; Yang, W.; Liu, J.; Wang, X.; Razal, J. M. Highly Conductive $Ti_3C_2t_x$ Mxene Hybrid Fibers for Flexible and Elastic Fiber-Shaped Supercapacitors. *Small* **2019**, *15* (8), 1804732–1804740.
- (143) Miura, H.; Fukuyama, Y.; Sunda, T.; Lin, B. J.; Zhou, J.; Takizawa, J.; Ohmori, A.; Kimura, M. Foldable Textile Electronic Devices Using All-Organic Conductive Fibers. *Adv. Eng. Mater.* **2014**, *16* (5), 550–555.
- (144) Zhou, J.; Lubineau, G. Improving Electrical Conductivity in Polycarbonate Nanocomposites Using Highly Conductive PEDOT/PSS Coated Mwcnts. *ACS Appl. Mater. Interfaces* **2013**, *5* (13), 6189–6200.
- (145) Zhou, J. A.; Fukawa, T.; Shirai, H.; Kimura, M. Anisotropic Motion of Electroactive Papers Coated with PEDOT/PSS. *Macromol. Mater. Eng.* **2010**, *295* (7), 671–675.
- (146) Zhou, J.; Anjum, D. H.; Lubineau, G.; Li, E. Q.; Thoroddsen, S. T. Unraveling the Order and Disorder in Poly(3,4-Ethylenedioxythiophene)/Poly(Styrenesulfonate) Nanofilms. *Macromolecules* **2015**, *48* (16), 5688–5696.
- (147) Zhou, J.; Fukawa, T.; Kimura, M. Directional Electro-mechanical Properties of PEDOT/PSS Films Containing Aligned Electrospun Nanofibers. *Polym. J.* **2011**, *43* (10), 849–854.
- (148) Zhou, J.; Kimura, M. Electromechanical Actuation of Highly Conductive PEDOT/PSS-Coated Cellulose Papers. *Sen-I Gakkaishi* **2011**, *67* (6), 125–131.
- (149) Xia, Y.; Sun, K.; Ouyang, J. Solution-Processed Metallic Conducting Polymer Films as Transparent Electrode of Optoelectronic Devices. *Adv. Mater.* **2012**, *24* (18), 2436–2440.
- (150) Xia, Y.; Ouyang, J. Significant Different Conductivities of the Two Grades of Poly(3,4-Ethylenedioxythiophene): Poly(Styrenesulfonate), Clevios P and Clevios Ph1000, Arising from Different Molecular Weights. *ACS Appl. Mater. Interfaces* **2012**, *4* (8), 4131–4140.
- (151) Na, S. I.; Kim, S. S.; Jo, J.; Kim, D. Y. Efficient and Flexible Ito-Free Organic Solar Cells Using Highly Conductive Polymer Anodes. *Adv. Mater.* **2008**, *20* (21), 4061–4067.
- (152) Na, S. I.; Wang, G.; Kim, S. S.; Kim, T. W.; Oh, S. H.; Yu, B. K.; Lee, T.; Kim, D. Y. Evolution of Nanomorphology and Anisotropic Conductivity in Solvent-Modified PEDOT:PSS Films for Polymeric Anodes of Polymer Solar Cells. *J. Mater. Chem.* **2009**, *19* (47), 9045–9053.
- (153) Li, B. X.; Ni, D. K.; Fan, J. C.; Zhou, J. Vapor Phase Polymerized High-Performance Poly(3,4-Ethylenedioxythiophene) Using Polyethyleneimine (PEI) as the Base Inhibitor and Grafting Agent for Electrochromic Medical Face Shields. *Chem. Eng. J.* **2022**, *445*, 136818–136826.
- (154) Li, B. X.; Li, J.; Ni, D. K.; Tang, S. S.; Fan, J. C.; Shi, K. Y.; Li, Z.; Zhou, J. Spontaneously Spread Polymer Thin Films on the Miscible Liquid Substrates. *Chem. Eng. J.* **2022**, *437*, 135443–135453.
- (155) Tang, S. S.; Zhang, X. J.; Fan, J. C.; Li, B. X.; Li, Z.; Wang, C.; Li, H.; Zhang, P.; Zhou, J. Fibrillation of Well-Formed Conductive Aerogel for Soft Conductors. *Applied Materials Today* **2022**, *26*, 101399–101409.
- (156) Jalili, R.; Razal, J. M.; Wallace, G. G. Exploiting High Quality PEDOT:PSS-Swnt Composite Formulations for Wet-Spinning Multifunctional Fibers. *J. Mater. Chem.* **2012**, *22* (48), 25174–25182.
- (157) Jalili, R.; Razal, J. M.; Wallace, G. G. Wet-Spinning of PEDOT:PSS/Functionalized-SWNTs Composite: A Facile Route toward Production of Strong and Highly Conducting Multifunctional Fibers. *Sci. Rep.* **2013**, *3*, 3438.
- (158) Lang, U.; Naujoks, N.; Dual, J. Mechanical Characterization of PEDOT:PSS Thin Films. *Synth. Met.* **2009**, *159* (5–6), 473–479.
- (159) Granero, A. J.; Wagner, P.; Wagner, K.; Razal, J. M.; Wallace, G. G.; Panhuis, M. I. H. Highly Stretchable Conducting Sibs-P3ht Fibers. *Adv. Funct. Mater.* **2011**, *21* (5), 955–962.
- (160) Seyedin, S.; Razal, J. M.; Innis, P. C.; Jeiranikhameneh, A.; Beirne, S.; Wallace, G. G. Knitted Strain Sensor Textiles of Highly Conductive All-Polymeric Fibers. *ACS Appl. Mater. Interfaces* **2015**, *7* (38), 21150–21158.
- (161) Grigoryev, A.; Sa, V.; Gopishetty, V.; Tokarev, I.; Kornev, K. G.; Minko, S. Wet-Spun Stimuli-Responsive Composite Fibers with Tunable Electrical Conductivity. *Adv. Funct. Mater.* **2013**, *23* (47), 5903–5909.
- (162) Zhao, Y.; Dong, D.; Gong, S.; Brassart, L.; Wang, Y.; An, T.; Cheng, W. A Moss-Inspired Electroless Gold-Coating Strategy toward Stretchable Fiber Conductors by Dry Spinning. *Adv. Electron Mater.* **2019**, *5* (1), 1800462–1800469.
- (163) Kim, S.; Choi, S.; Oh, E.; Byun, J.; Kim, H.; Lee, B.; Lee, S.; Hong, Y. Revisit to Three-Dimensional Percolation Theory: Accurate Analysis for Highly Stretchable Conductive Composite Materials. *Sci. Rep.* **2016**, *6*, 34632–34641.
- (164) Wang, C.; Wang, C.; Huang, Z.; Xu, S. Materials and Structures toward Soft Electronics. *Adv. Mater.* **2018**, *30* (50), 1801368–1801416.
- (165) Liang, J.; Li, L.; Niu, X.; Yu, Z.; Pei, Q. Elastomeric Polymer Light-Emitting Devices and Displays. *Nat. Photonics* **2013**, *7* (10), 817–824.
- (166) Park, M.; Park, J.; Jeong, U. Design of Conductive Composite Elastomers for Stretchable Electronics. *Nano Today* **2014**, *9*, 244–260.
- (167) Matsuhisa, N.; Inoue, D.; Zalar, P.; Jin, H.; Matsuba, Y.; Itoh, A.; Yokota, T.; Hashizume, D.; Someya, T. Printable Elastic Conductors by In Situ Formation of Silver Nanoparticles from Silver Flakes. *Nat. Mater.* **2017**, *16* (8), 834–840.
- (168) Kim, J.; Lee, M.; Shim, H. J.; Ghaffari, R.; Cho, H. R.; Son, D.; Jung, Y. H.; Soh, M.; Choi, C.; Jung, S.; Chu, K.; Jeon, D.; Lee, S. T.; Kim, J. H.; Choi, S. H.; Hyeon, T.; Kim, D. H. Stretchable Silicon Nanoribbon Electronics for Skin Prosthesis. *Nat. Commun.* **2014**, *5*, 5747–5757.
- (169) Gómez-Navarro, C.; Burghard, M.; Kern, K. Elastic Properties of Chemically Derived Single Graphene Sheets. *Nano Lett.* **2008**, *8* (7), 2045–2049.
- (170) Zhu, S. E.; Ghatkesar, M. K.; Zhang, C.; Janssen, G. C. A. M. Graphene Based Piezoresistive Pressure Sensor. *Appl. Phys. Lett.* **2013**, *102* (16), 161904–161906.

- (171) Boland, C. S.; Khan, U.; Ryan, G.; Barwich, S.; Charifou, R.; Harvey, A.; Backes, C.; Li, Z.; Ferreira, M. S.; Möbius, M. E.; Young, R. J.; Coleman, J. N. Sensitive Electromechanical Sensors Using Viscoelastic Graphene-Polymer Nanocomposites. *Science* **2016**, *354* (6317), 1257–1260.
- (172) Cheng, Y.; Wang, R.; Sun, J.; Gao, L. A Stretchable and Highly Sensitive Graphene-Based Fiber for Sensing Tensile Strain, Bending, and Torsion. *Adv. Mater.* **2015**, *27* (45), 7365–7371.
- (173) Zhao, H.; Zhang, Y.; Bradford, P. D.; Zhou, Q.; Jia, Q.; Yuan, F. G.; Zhu, Y. Carbon Nanotube Yarn Strain Sensors. *Nanotechnology* **2010**, *21* (30), 305502–305507.
- (174) Hong, T.; Jeong, S. M.; Choi, Y. K.; Lim, T.; Ju, S. Superhydrophobic, Elastic, and Conducting Polyurethane-Carbon Nanotube-Silane-Aerogel Composite Microfiber. *Polymers (Basel)* **2020**, *12* (8), 1772–1782.
- (175) Probst, H.; Katzer, K.; Nocke, A.; Hickmann, R.; Zimmermann, M.; Cherif, C. Melt Spinning of Highly Stretchable, Electrically Conductive Filament Yarns. *Polymers (Basel)* **2021**, *13* (4), 590–601.
- (176) Xiao, J.; Xiong, Y.; Chen, J.; Zhao, S.; Chen, S.; Xu, B.; Sheng, B. Ultrasensitive and Highly Stretchable Fibers with Dual Conductive Microstructural Sheaths for Human Motion and Micro Vibration Sensing. *Nanoscale* **2022**, *14* (5), 1962–1970.
- (177) Gao, Y.; Guo, F.; Cao, P.; Liu, J.; Li, D.; Wu, J.; Wang, N.; Su, Y.; Zhao, Y. Winding-Locked Carbon Nanotubes/Polymer Nanofibers Helical Yarn for Ultrastretchable Conductor and Strain Sensor. *ACS Nano* **2020**, *14* (3), 3442–3450.
- (178) Cruz-Silva, R.; Morelos-Gomez, A.; Kim, H. I.; Jang, H. K.; Tristan, F.; Vega-Diaz, S.; Rajukumar, L. P.; Elias, A. L.; Perea-Lopez, N.; Suhr, J.; Endo, M.; Terrones, M. Super-Stretchable Graphene Oxide Macroscopic Fibers with Outstanding Knotability Fabricated by Dry Film Scrolling. *ACS Nano* **2014**, *8* (6), 5959–5967.
- (179) Yuk, H.; Zhang, T.; Lin, S.; Parada, G. A.; Zhao, X. Tough Bonding of Hydrogels to Diverse Non-Porous Surfaces. *Nat. Mater.* **2016**, *15* (2), 190–196.
- (180) Sun, J. Y.; Zhao, X.; Illeperuma, W. R.; Chaudhuri, O.; Oh, K. H.; Mooney, D. J.; Vlassak, J. J.; Suo, Z. Highly Stretchable and Tough Hydrogels. *Nature* **2012**, *489* (7414), 133–136.
- (181) Guan, Q. F.; Han, Z. M.; Zhu, Y.; Xu, W. L.; Yang, H. B.; Ling, Z. C.; Yan, B. B.; Yang, K. P.; Yin, C. H.; Wu, H.; Yu, S. H. Bio-Inspired Lotus-Fiber-Like Spiral Hydrogel Bacterial Cellulose Fibers. *Nano Lett.* **2021**, *21* (2), 952–958.
- (182) Muhamaruesa, N. H. M.; Isa, M. I. N. M. Biopolymer Membranes for Battery Applications. In *Biopolymer Membranes and Films*; de Moraes, M. A., da Silva, C. F., Vieira, R. S., Eds.; Elsevier, 2020; pp 477–502.
- (183) Li, M.; Chen, X.; Li, X.; Dong, J.; Zhao, X.; Zhang, Q. Wearable and Robust Polyimide Hydrogel Fiber Textiles for Strain Sensors. *ACS Appl. Mater. Interfaces* **2021**, *13* (36), 43323–43332.
- (184) Shuai, L. Y. Z.; Guo, Z. H.; Zhang, P. P.; Wan, J. M.; Pu, X.; Wang, Z. L. Stretchable, Self-Healing, Conductive Hydrogel Fibers for Strain Sensing and Triboelectric Energy-Harvesting Smart Textiles. *Nano Energy* **2020**, *78*, 105389–105397.
- (185) Ye, Y. H.; Zhang, Y. F.; Chen, Y.; Han, X. S.; Jiang, F. Cellulose Nanofibrils Enhanced, Strong, Stretchable, Freezing-Tolerant Ionic Conductive Organohydrogel for Multi-Functional Sensors. *Adv. Funct. Mater.* **2020**, *30* (35), 2003430–2003441.
- (186) Zhang, Q.; Roach, D. J.; Geng, L. C.; Chen, H. S.; Qi, H. J.; Fang, D. N. Highly Stretchable and Conductive Fibers Enabled by Liquid Metal Dip-Coating. *Smart Mater. Struct.* **2018**, *27* (3), 035019–035034.
- (187) Yi, P.; Zou, H.; Yu, Y.; Li, X.; Li, Z.; Deng, G.; Chen, C.; Fang, M.; He, J.; Sun, X.; Liu, X.; Shui, J.; Yu, R. Mxene-Reinforced Liquid Metal/Polymer Fibers Via Interface Engineering for Wearable Multifunctional Textiles. *ACS Nano* **2022**, *16* (9), 14490–14502.
- (188) Zhou, J.; Hsieh, Y.-L. Nanocellulose Aerogel-Based Porous Coaxial Fibers for Thermal Insulation. *Nano Energy* **2020**, *68*, 104305–104313.
- (189) Fan, J.; Li, H.; Tang, S.; Li, B.; Xin, Y.; Hsieh, Y.-L.; Zhou, J. Compensation Strategy for Constructing High-Performance Aerogels Using Acrylamide-Assisted Vacuum Drying and Their Use as Water-Induced Electrical Generators. *Chem. Eng. J.* **2023**, *452*, 139685–139696.
- (190) Tang, S.; Ma, M.; Zhang, X.; Zhao, X.; Fan, J.; Zhu, P.; Shi, K.; Zhou, J. Covalent Cross-Links Enable the Formation of Ambient-Dried Biomass Aerogels through the Activation of a Triazine Derivative for Energy Storage and Generation. *Adv. Funct. Mater.* **2022**, *32* (36), 2205417–2205427.
- (191) Liu, Z.; Lyu, J.; Fang, D.; Zhang, X. Nanofibrous Kevlar Aerogel Threads for Thermal Insulation in Harsh Environments. *ACS Nano* **2019**, *13* (5), 5703–5711.
- (192) Du, Y.; Zhang, X.; Wang, J.; Liu, Z.; Zhang, K.; Ji, X.; You, Y.; Zhang, X. Reaction-Spun Transparent Silica Aerogel Fibers. *ACS Nano* **2020**, *14* (9), 11919–11928.
- (193) Li, G.; Hong, G.; Dong, D.; Song, W.; Zhang, X. Multiresponsive Graphene-Aerogel-Directed Phase-Change Smart Fibers. *Adv. Mater.* **2018**, *30* (30), 1801754–1801761.
- (194) Xu, Z.; Zhang, Y.; Li, P.; Gao, C. Strong, Conductive, Lightweight, Neat Graphene Aerogel Fibers with Aligned Pores. *ACS Nano* **2012**, *6* (8), 7103–7113.
- (195) Huang, J.; Li, J.; Xu, X.; Hua, L.; Lu, Z. In Situ Loading of Polypyrrole onto Aramid Nanofiber and Carbon Nanotube Aerogel Fibers as Physiology and Motion Sensors. *ACS Nano* **2022**, *16*, 8161–8171.
- (196) Li, Y. Z.; Zhang, X. T. Electrically Conductive, Optically Responsive, and Highly Orientated Ti_3C_2Tx Mxene Aerogel Fibers. *Adv. Funct. Mater.* **2022**, *32* (4), 2107767–2107776.
- (197) Bai, C. R.; Wang, Y. Q.; Fan, Z. Y.; Yan, L.; Jiao, H. One-Step Preparation of Gel-Electrolyte-Friendly Fiber-Shaped Aerogel Current Collector for Solid-State Fiber-Shaped Supercapacitors with Large Capacity. *J. Power Sources* **2022**, *521*, 230971–230977.
- (198) Zhou, J.; Fan, J.; Yi, M. Aerogel Fiber, Preparation Method and Application. CN 111620667 A, 2020.
- (199) Liu, Y.; Yan, Z.; Lin, Q.; Guo, X.; Han, M.; Nan, K.; Hwang, K. C.; Huang, Y.; Zhang, Y.; Rogers, J. A. Guided Formation of 3D Helical Mesostructures by Mechanical Buckling: Analytical Modeling and Experimental Validation. *Adv. Funct. Mater.* **2016**, *26* (17), 2909–2918.
- (200) Jang, K. I.; Li, K.; Chung, H. U.; Xu, S.; Jung, H. N.; Yang, Y.; Kwak, J. W.; Jung, H. H.; Song, J.; Yang, C.; Wang, A.; Liu, Z.; Lee, J. Y.; Kim, B. H.; Kim, J. H.; Lee, J.; Yu, Y.; Kim, B. J.; Jang, H.; Yu, K. J.; et al. Self-Assembled Three Dimensional Network Designs for Soft Electronics. *Nat. Commun.* **2017**, *8*, 15894.
- (201) Sun, Y. G.; Rogers, J. A. Structural Forms of Single Crystal Semiconductor Nanoribbons for High-Performance Stretchable Electronics. *J. Mater. Chem.* **2007**, *17* (9), 832–840.
- (202) Yang, Z.; Zhai, Z.; Song, Z.; Wu, Y.; Liang, J.; Shan, Y.; Zheng, J.; Liang, H.; Jiang, H. Conductive and Elastic 3D Helical Fibers for Use in Washable and Wearable Electronics. *Adv. Mater.* **2020**, *32* (10), 1907495–1907501.
- (203) Wakuda, D.; Suganuma, K. Stretchable Fine Fiber with High Conductivity Fabricated by Injection Forming. *Appl. Phys. Lett.* **2011**, *98* (7), 073304.
- (204) Yamada, T.; Hayamizu, Y.; Yamamoto, Y.; Yomogida, Y.; Izadi-Najafabadi, A.; Futaba, D. N.; Hata, K. A Stretchable Carbon Nanotube Strain Sensor for Human-Motion Detection. *Nat. Nanotechnol.* **2011**, *6* (5), 296–301.
- (205) Park, J.; You, I.; Shin, S.; Jeong, U. Material Approaches to Stretchable Strain Sensors. *ChemPhysChem* **2015**, *16* (6), 1155–1163.
- (206) Zhang, J.; Liu, J.; Zhuang, R.; Mader, E.; Heinrich, G.; Gao, S. Single MwnT-Glass Fiber as Strain Sensor and Switch. *Adv. Mater.* **2011**, *23* (30), 3392–3397.
- (207) Zhong, J. W.; Zhong, Q. Z.; Hu, Q. Y.; Wu, N.; Li, W. B.; Wang, B.; Hu, B.; Zhou, J. Stretchable Self-Powered Fiber-Based Strain Sensor. *Adv. Funct. Mater.* **2015**, *25* (12), 1798–1803.

(208) Cullinan, M. A.; Culpepper, M. L. Carbon Nanotubes as Piezoresistive Microelectromechanical Sensors: Theory and Experiment. *Phys. Rev. B* **2010**, *82* (11), 115428–115433.

(209) Obitayo, W.; Liu, T. A Review: Carbon Nanotube-Based Piezoresistive Strain Sensors. *J. Sens.* **2012**, *2012*, 1–15.

(210) Lipomi, D. J.; Vosgueritchian, M.; Tee, B. C.; Hellstrom, S. L.; Lee, J. A.; Fox, C. H.; Bao, Z. Skin-Like Pressure and Strain Sensors Based on Transparent Elastic Films of Carbon Nanotubes. *Nat. Nanotechnol* **2011**, *6* (12), 788–792.

(211) Amjadi, M.; Pichitpajongkit, A.; Lee, S.; Ryu, S.; Park, I. Highly Stretchable and Sensitive Strain Sensor Based on Silver Nanowire-Elastomer Nanocomposite. *ACS Nano* **2014**, *8* (5), 5154–5163.

(212) Amjadi, M.; Kyung, K. U.; Park, I.; Sitti, M. Stretchable, Skin-Mountable, and Wearable Strain Sensors and Their Potential Applications: A Review. *Adv. Funct. Mater.* **2016**, *26* (11), 1678–1698.

(213) Xin, Y.; Zhou, J.; Xu, X.; Lubineau, G. Laser-Engraved Carbon Nanotube Paper for Instilling High Sensitivity, High Stretchability, and High Linearity in Strain Sensors. *Nanoscale* **2017**, *9* (30), 10897–10905.

(214) Tee, B. C.; Wang, C.; Allen, R.; Bao, Z. An Electrically and Mechanically Self-Healing Composite with Pressure- and Flexion-Sensitive Properties for Electronic Skin Applications. *Nat. Nanotechnol* **2012**, *7* (12), 825–832.

(215) Benight, S. J.; Wang, C.; Tok, J. B. H.; Bao, Z. A Stretchable and Self-Healing Polymers and Devices for Electronic Skin. *Prog. Polym. Sci.* **2013**, *38* (12), 1961–1977.

(216) Chortos, A.; Liu, J.; Bao, Z. Pursuing Prosthetic Electronic Skin. *Nat. Mater.* **2016**, *15* (9), 937–950.

(217) Cao, Q.; Rogers, J. A. Ultrathin Films of Single-Walled Carbon Nanotubes for Electronics and Sensors: A Review of Fundamental and Applied Aspects. *Adv. Mater.* **2009**, *21* (1), 29–53.

(218) Zhou, J.; Zhang, Y.; Mülle, M.; Lubineau, G. Temperature Sensing of Micron Scale Polymer Fibers Using Fiber Bragg Gratings. *Meas. Sci. Technol.* **2015**, *26* (8), 085003–085011.

(219) Stuart, M. A.; Huck, W. T.; Genzer, J.; Muller, M.; Ober, C.; Stamm, M.; Sukhorukov, G. B.; Szleifer, I.; Tsukruk, V. V.; Urban, M.; Winnik, F.; Zauscher, S.; Luzinov, I.; Minko, S. Emerging Applications of Stimuli-Responsive Polymer Materials. *Nat. Mater.* **2010**, *9* (2), 101–113.

(220) Michel, S.; Chu, B. T. T.; Grimm, S.; Nuesch, F. A.; Borgschulte, A.; Opris, D. M. Self-Healing Electrodes for Dielectric Elastomer Actuators. *J. Mater. Chem.* **2012**, *22* (38), 20736–20741.

(221) Dzahir, M.; Yamamoto, S. Recent Trends in Lower-Limb Robotic Rehabilitation Orthosis: Control Scheme and Strategy for Pneumatic Muscle Actuated Gait Trainers. *Robotics* **2014**, *3* (2), 120–148.

(222) Dong, T.; Zhang, X.; Liu, T. Artificial Muscles for Wearable Assistance and Rehabilitation. *Frontiers of Information Technology & Electronic Engineering* **2018**, *19* (11), 1303–1315.

(223) Zhou, J.; Gao, Q.; Fukawa, T.; Shirai, H.; Kimura, M. Macroporous Conductive Polymer Films Fabricated by Electrospun Nanofiber Templates and Their Electromechanical Properties. *Nanotechnology* **2011**, *22* (27), 275501–275510.

(224) Hu, Z. Q.; Zhou, J.; Fu, Q. Design and Construction of Deformable Heaters: Materials, Structure, and Applications. *Adv. Electron Mater.* **2021**, *7* (11), 2100452–2100477.

(225) Shi, X.; Zuo, Y.; Zhai, P.; Shen, J.; Yang, Y.; Gao, Z.; Liao, M.; Wu, J.; Wang, J.; Xu, X.; Tong, Q.; Zhang, B.; Wang, B.; Sun, X.; Zhang, L.; Pei, Q.; Jin, D.; Chen, P.; Peng, H. Large-Area Display Textiles Integrated with Functional Systems. *Nature* **2021**, *591* (7849), 240–245.

(226) Choi, H. W.; Shin, D. W.; Yang, J.; Lee, S.; Figueiredo, C.; Sinopoli, S.; Ullrich, K.; Jovancic, P.; Marrani, A.; Momente, R.; Gomes, J.; Branquinho, R.; Emanuele, U.; Lee, H.; Bang, S. Y.; Jung, S. M.; Han, S. D.; Zhan, S.; Harden-Chatters, W.; Suh, Y. H.; et al. Smart Textile Lighting/Display System with Multifunctional Fibre

Devices for Large Scale Smart Home and Iot Applications. *Nat. Commun.* **2022**, *13* (1), 814.

(227) Sundaram, S.; Kellnhofer, P.; Li, Y.; Zhu, J. Y.; Torralba, A.; Matusik, W. Learning the Signatures of the Human Grasp Using a Scalable Tactile Glove. *Nature* **2019**, *569* (7758), 698–702.

(228) Almusallam, A.; Luo, Z. H.; Komolafe, A.; Yang, K.; Robinson, A.; Torah, R.; Beeby, S. Flexible Piezoelectric Nano-Composite Films for Kinetic Energy Harvesting from Textiles. *Nano Energy* **2017**, *33*, 146–156.

(229) Choi, S.; Kwon, S.; Kim, H.; Kim, W.; Kwon, J. H.; Lim, M. S.; Lee, H. S.; Choi, K. C. Highly Flexible and Efficient Fabric-Based Organic Light-Emitting Devices for Clothing-Shaped Wearable Displays. *Sci. Rep* **2017**, *7* (1), 6424–6431.

(230) Zhang, Z. T.; Guo, K. P.; Li, Y. M.; Li, X. Y.; Guan, G. Z.; Li, H. P.; Luo, Y. F.; Zhao, F. Y.; Zhang, Q.; Wei, B.; Pei, Q. B.; Peng, H. S. A Colour-Tunable, Weavable Fibre-Shaped Polymer Light-Emitting Electrochemical Cell. *Nat. Photonics* **2015**, *9* (4), 233–238.

(231) Davis, V. A.; Parra-Vasquez, A. N.; Green, M. J.; Rai, P. K.; Behabtu, N.; Prieto, V.; Booker, R. D.; Schmidt, J.; Kesselman, E.; Zhou, W.; Fan, H.; Adams, W. W.; Hauge, R. H.; Fischer, J. E.; Cohen, Y.; Talmon, Y.; Smalley, R. E.; Pasquali, M. True Solutions of Single-Walled Carbon Nanotubes for Assembly into Macroscopic Materials. *Nat. Nanotechnol* **2009**, *4* (12), 830–834.

(232) Parra-Vasquez, A. N.; Behabtu, N.; Green, M. J.; Pint, C. L.; Young, C. C.; Schmidt, J.; Kesselman, E.; Goyal, A.; Ajayan, P. M.; Cohen, Y.; Talmon, Y.; Hauge, R. H.; Pasquali, M. Spontaneous Dissolution of Ultralong Single- and Multiwalled Carbon Nanotubes. *ACS Nano* **2010**, *4* (7), 3969–3978.

Recommended by ACS

High-Quality Microprintable and Stretchable Conductors for High-Performance 5G Wireless Communication

Jongyoun Kim, Youngu Lee, *et al.*

NOVEMBER 16, 2022
ACS APPLIED MATERIALS & INTERFACES

READ 

Stretchable Conductive Tubular Composites Based on Braided Carbon Nanotube Yarns with an Elastomer Matrix

Avia J. Bar, Samuel Kenig, *et al.*

NOVEMBER 07, 2022
ACS OMEGA

READ 

An Ultralight Self-Powered Fire Alarm e-Textile Based on Conductive Aerogel Fiber with Repeatable Temperature Monitoring Performance Used in Firefighting Clothing

Hualing He, Jinfeng Wang, *et al.*

JANUARY 27, 2022
ACS NANO

READ 

MXene/Silver Nanowire-Based Spring Frameworks for Highly Flexible Waterproof Supercapacitors and Piezoelectrochemical-Type Pressure-Sensitive Sensor Devices

Leini Wang, Jin Yang, *et al.*

JUNE 03, 2022
LANGMUIR

READ 

Get More Suggestions >